



UNIVERSITÀ DI PARMA

ARCHIVIO DELLA RICERCA

University of Parma Research Repository

A Sequential Algorithm for Jerk Limited Speed Planning

This is the peer reviewed version of the following article:

Original

A Sequential Algorithm for Jerk Limited Speed Planning / Consolini, L.; Locatelli, M.; Minari, A.. - In: IEEE TRANSACTIONS ON AUTOMATION SCIENCE AND ENGINEERING. - ISSN 1545-5955. - (2021), pp. 1-18. [10.1109/TASE.2021.3111758]

Availability:

This version is available at: 11381/2905629 since: 2021-12-16T12:45:02Z

Publisher:

Institute of Electrical and Electronics Engineers Inc.

Published

DOI:10.1109/TASE.2021.3111758

Terms of use:

Anyone can freely access the full text of works made available as "Open Access". Works made available

Publisher copyright

note finali coverpage

(Article begins on next page)

31 December 2024

AUTHOR QUERIES

AUTHOR PLEASE ANSWER ALL QUERIES

PLEASE NOTE: We cannot accept new source files as corrections for your article. If possible, please annotate the PDF proof we have sent you with your corrections and upload it via the Author Gateway. Alternatively, you may send us your corrections in list format. You may also upload revised graphics via the Author Gateway.

Carefully check the page proofs (and coordinate with all authors); additional changes or updates **WILL NOT** be accepted after the article is published online/print in its final form. Please check author names and affiliations, funding, as well as the overall article for any errors prior to sending in your author proof corrections.

AQ:1 = Please confirm or add details for any funding or financial support for the research of this article.

AQ:2 = Please confirm the postal code for Università di Parma.

AQ:3 = Please specify the section numbers for the phrase “next sections.”

A Sequential Algorithm for Jerk Limited Speed Planning

Luca Consolini¹, Member, IEEE, Marco Locatelli¹, and Andrea Minari¹

Abstract—In this article, we discuss a sequential algorithm for the computation of a minimum-time speed profile over a given path, under velocity, acceleration, and jerk constraints. Such a problem arises in industrial contexts, such as automated warehouses, where LGVs need to perform assigned tasks as fast as possible in order to increase productivity. It can be reformulated as an optimization problem with a convex objective function, linear velocity and acceleration constraints, and non-convex jerk constraints, which, thus, represents the main source of the difficulty. While existing nonlinear programming (NLP) solvers can be employed for the solution of this problem, it turns out that the performance and robustness of such solvers can be enhanced by the sequential line-search algorithm proposed in this article. At each iteration, a feasible direction, with respect to the current feasible solution, is computed, and a step along such direction is taken in order to compute the next iterate. The computation of the feasible direction is based on the solution of a linearized version of the problem, and the solution of the linearized problem, through an approach that strongly exploits its special structure, represents the main contribution of this work. The efficiency of the proposed approach with respect to existing NLP solvers is proven through different computational experiments.

Note to Practitioners—This article was motivated by the needs of LGV manufacturers. In particular, it presents an algorithm for computing the minimum-time speed law for an LGV along a pre-assigned path, respecting assigned velocity, acceleration, and jerk constraints. The solution algorithm should be: 1) *fast*, since speed planning is made continuously throughout the workday, not only when an LGV receives a new task but also during the execution of the task itself, since conditions may change, e.g., if the LGV has to be halted for security reasons and 2) *reliable*, i.e., it should return solutions of high quality, because a better speed profile allows to save time and even small percentage improvements, say a 5% improvement, has a considerable impact on the productivity of the warehouse, and, thus, determines a significant economic gain. The algorithm that we propose meets these two requirements, and we believe that it can be a useful tool for LGV manufacturers and users. It is obvious that the proposed method also applies to the speed planning problem for vehicles other than LGVs, e.g., road vehicles.

Index Terms—Optimization, sequential line-search method, speed planning.

I. INTRODUCTION

AN IMPORTANT problem in motion planning is the computation of the minimum-time motion of a car-like vehicle from a start configuration to a target one while avoiding collisions (obstacle avoidance) and satisfying kinematic, dynamic, and mechanical constraints (for instance, on velocities, accelerations, and maximal steering angle). This problem can be approached in two ways.

- 1) As a minimum-time trajectory planning, where both the path to be followed by the vehicle and the timing law on this path (i.e., the vehicle's velocity) are simultaneously designed. For instance, one could use the RRT* algorithm (see [1]).
- 2) As a (geometric) path planning followed by a minimum-time speed planning on the planned path (see [2]).

In this article, following the second paradigm, we assume that the path that joins the initial and the final configuration is assigned, and we aim at finding the time-optimal speed law that satisfies some kinematic and dynamic constraints. The problem can be reformulated as an optimization problem, and it is quite relevant from the practical point of view. In particular, in automated warehouses, the speed of LGVs needs to be planned under acceleration and jerk constraints. As previously mentioned, the solution algorithm should be both *fast* and *reliable*. In our previous work [3], we proposed an optimal time-complexity algorithm for finding the time-optimal speed law that satisfies constraints on maximum velocity and tangential and normal acceleration. In the subsequent work [4], we included a bound on the derivative of the acceleration with respect to the arc length. In this article, we consider the presence of jerk constraints (constraints on the time derivative of the acceleration). The resulting optimization problem is nonconvex and, for this reason, is significantly more complex than the ones that we discussed in [3] and [4]. The main contribution of this work is the development of a line-search algorithm for this problem based on the sequential solution of convex problems. The proposed algorithm meets both requirements of being fast and reliable. The former is met by heavily exploiting the special structure of the optimization problem, the latter by the theoretical guarantee that the returned solution is a first-order stationary point (in practice, a local minimizer) of the optimization problem.

Manuscript received June 29, 2021; accepted August 24, 2021. This article was recommended for publication by Associate Editor M. Robba and Editor C. Seatzu upon evaluation of the reviewers' comments. This work was supported in part by the Programme "FIL-Quota Incentivante" of the University of Parma and in part by the Fondazione Cariparma. (Corresponding author: Marco Locatelli.)

The authors are with the Dipartimento di Ingegneria e Architettura, Università di Parma, 43121 Parma, Italy (e-mail: luca.consolini@unipr.it; marco.locatelli@unipr.it; andrea.minari2@studenti.unipr.it).

This article has supplementary material provided by the authors and color versions of one or more figures available at <https://doi.org/10.1109/TASE.2021.3111758>.

Digital Object Identifier 10.1109/TASE.2021.3111758

86 A. Problem Statement

87 Here, we introduce the problem at hand more formally.
 88 Let $\boldsymbol{\gamma}: [0, s_f] \rightarrow \mathbb{R}^2$ be a smooth function. The image set
 89 $\boldsymbol{\gamma}([0, s_f])$ is the path to be followed, $\boldsymbol{\gamma}(0)$ the initial configu-
 90 ration, and $\boldsymbol{\gamma}(s_f)$ the final one. Function $\boldsymbol{\gamma}$ has arc-length para-
 91 meterization, such that $(\forall \lambda \in [0, s_f]), \|\boldsymbol{\gamma}'(\lambda)\| = 1$. In this
 92 way, s_f is the path length. We want to compute the speed-law
 93 that minimizes the overall transfer time (i.e., the time needed to
 94 go from $\boldsymbol{\gamma}(0)$ to $\boldsymbol{\gamma}(s_f)$). To this end, let $\lambda: [0, t_f] \rightarrow [0, s_f]$ be
 95 a differentiable monotone increasing function that represents
 96 the vehicle's arc-length position along the curve as a function
 97 of time, and let $v: [0, s_f] \rightarrow [0, +\infty[$ be such that $(\forall t \in$
 98 $[0, t_f]) \dot{\lambda}(t) = v(\lambda(t))$. In this way, $v(s)$ is the derivative of the
 99 vehicle arc-length position, which corresponds to the norm of
 100 its velocity vector at position s . The position of the vehicle as
 101 a function of time is given by $\mathbf{x}: [0, t_f] \rightarrow \mathbb{R}^2$, $\mathbf{x}(t) = \boldsymbol{\gamma}(\lambda(t))$.
 102 The velocity and acceleration are given, respectively, by

$$103 \quad \dot{\mathbf{x}}(t) = \boldsymbol{\gamma}'(\lambda(t))v(\lambda(t))$$

$$104 \quad \ddot{\mathbf{x}}(t) = a_T(t)\boldsymbol{\gamma}'(\lambda(t)) + a_N(t)\boldsymbol{\gamma}'^\perp(\lambda(t))$$

105 where $a_T(t) = v'(\lambda(t))v(\lambda(t))$ and $a_N(t) = k(\lambda(t))v(\lambda(t))^2$
 106 are, respectively, the tangential and normal components of the
 107 acceleration (i.e., the projections of the acceleration vector
 108 $\ddot{\mathbf{x}}$ on the tangent and the normal to the curve). Moreover
 109 $\boldsymbol{\gamma}'^\perp(\lambda)$ is the normal to vector $\boldsymbol{\gamma}'(\lambda)$ and the tangent of $\boldsymbol{\gamma}'$
 110 at λ . Here, $k: [0, s_f] \rightarrow \mathbb{R}$ is the scalar curvature, defined as
 111 $k(s) = \langle \boldsymbol{\gamma}''(s), \boldsymbol{\gamma}'(s)^\perp \rangle$. Note that $|k(s)| = \|\boldsymbol{\gamma}''(s)\|$. In the
 112 following, we assume that $k(s) \in C^1([0, s_f], \mathbb{R})$. The total
 113 maneuver time, for a given velocity profile $v \in C^1([0, s_f], \mathbb{R})$,
 114 is returned by the functional

$$115 \quad \mathcal{F}: C^1([0, s_f], \mathbb{R}) \rightarrow \mathbb{R}, \quad \mathcal{F}(v) = \int_0^{s_f} v^{-1}(s) ds. \quad (1)$$

116 In our previous work [3], we considered the problem

$$117 \quad \min_{v \in \mathcal{V}} \mathcal{F}(v) \quad (2)$$

118 where the feasible region $\mathcal{V} \subset C^1([0, s_f], \mathbb{R})$ is defined by the
 119 following set of constraints:

$$120 \quad v(0) = 0, \quad v(s_f) = 0 \quad (3a)$$

$$121 \quad 0 \leq v(s) \leq v_{\max}, \quad s \in [0, s_f] \quad (3b)$$

$$122 \quad |v'(s)v(s)| \leq A, \quad s \in [0, s_f] \quad (3c)$$

$$123 \quad |k(s)|v(s)^2 \leq A_N, \quad s \in [0, s_f] \quad (3d)$$

124 where v_{\max} , A , and A_N are upper bounds for the velocity, the
 125 tangential acceleration, and the normal acceleration, respec-
 126 tively. Constraints (3a) are the initial and final interpolation
 127 conditions, while constraints (3b)–(3d) limit velocity and the
 128 tangential and normal components of acceleration. In [3],
 129 we presented an algorithm, with linear-time computational
 130 complexity with respect to the number of variables, which
 131 provides an optimal solution of (2) after spatial discretiza-
 132 tion. One limitation of this algorithm is that the obtained
 133 velocity profile is Lipschitz¹ but not differentiable so that
 134 the vehicle's acceleration is discontinuous. With the aim

¹A function $f: \mathbb{R} \rightarrow \mathbb{R}$ is *Lipschitz* if there exists a real positive constant L such that $(\forall x, y \in \mathbb{R}) |f(x) - f(y)| \leq L|x - y|$.

of obtaining a smoother velocity profile, in the subsequent
 work [4], we required that the velocity be differentiable, and
 we imposed a Lipschitz condition (with constant J) on its
 derivative. In this way, after setting $w = v^2$, the feasible region
 of the problem $\mathcal{W} \subset C^1([0, s_f], \mathbb{R})$ is defined by the set of
 functions $w \in C^1([0, s_f], \mathbb{R})$ that satisfy the following set of
 constraints:

$$135 \quad w(0) = 0, \quad w(s_f) = 0 \quad (4a) \quad 142$$

$$136 \quad 0 \leq w(s) \leq v_{\max}^2, \quad s \in [0, s_f] \quad (4b) \quad 143$$

$$137 \quad \frac{1}{2}|w'(s)| \leq A, \quad s \in [0, s_f] \quad (4c) \quad 144$$

$$138 \quad |k(s)|w(s) \leq A_N, \quad s \in [0, s_f] \quad (4d) \quad 145$$

$$139 \quad |w'(s_1) - w'(s_2)| \leq J|s_1 - s_2|, \quad s_1, s_2 \in [0, s_f]. \quad (4e) \quad 146$$

147 Then, we end up with the problem

$$148 \quad \min_{w \in \mathcal{W}} G(w) \quad (5) \quad 148$$

149 where the objective function is

$$150 \quad G: C^1([0, s_f], \mathbb{R}) \rightarrow \mathbb{R}, \quad G(w) = \int_0^{s_f} w^{-1/2}(s) ds. \quad (6)$$

151 The objective function (6) and constraints (4a)–(4d) cor-
 152 respond to the ones in problem (2) after the substitution
 153 $w = v^2$. Note that this change of variable is well known in
 154 the literature. It has been first proposed in [5], while, in [6],
 155 it is observed that Problem (2) becomes convex after this
 156 change of variable. The added set of constraints (4e) is a
 157 Lipschitz condition on the derivative of the squared velocity w .
 158 It is used to enforce a smoother velocity profile by bounding
 159 the second derivative of the squared velocity with respect
 160 to arc length. Note that constraints (4) are linear, and the
 161 objective function (6) is convex. In [4], we proposed an
 162 algorithm for solving a finite-dimensional approximation of
 163 Problem (4). The algorithm exploited the particular structure
 164 of the resulting convex finite-dimensional problem. This article
 165 extends the results of [4]. It considers a nonconvex varia-
 166 tion of Problem (4), in which constraint (4e) is substituted
 167 with a constraint on the time derivative of the acceleration
 168 $|\dot{a}(t)| \leq J$, where $a(t) = (d/dt)v(\lambda(t)) = v'(\lambda(t))v(\lambda(t)) =$
 169 $(1/2)w'(\lambda(t))$. Then, we set

$$170 \quad j_L(t) = \dot{a}(t) = \frac{1}{2}w''(s(t))\sqrt{w(s(t))}.$$

171 This quantity is commonly called “jerk.” Bounding the
 172 absolute value of jerk allows to avoid sudden changes of
 173 acceleration and obtain a smoother motion. Then, we end up
 174 with the following minimum-time problem.

175 *Problem 1 (Smooth Minimum-Time Velocity Planning*
 176 *Problem: Continuous Version):*

$$177 \quad \min_{w \in C^2} \int_0^{s_f} w(s)^{-1/2} ds$$

$$178 \quad w(0) = 0, \quad w(s_f) = 0 \quad 178$$

$$179 \quad 0 \leq w(s) \leq \mu^+(s), \quad s \in [0, s_f] \quad 179$$

$$180 \quad \frac{1}{2}|w'(s)| \leq A, \quad s \in [0, s_f] \quad (7) \quad 180$$

$$181 \quad \frac{1}{2}|w''(s)\sqrt{w(s)}| \leq J \quad s \in [0, s_f] \quad (8) \quad 181$$

where μ^+ is the square velocity upper bound depending on the shape of the path, i.e.,

$$\mu^+(s) = \min \left\{ v_{\max}^2, \frac{A_N}{|k(s)|} \right\}$$

where v_{\max} , A_N , and k are the maximum vehicle velocity, the maximum normal acceleration, and the path curvature, respectively. Parameters A and J are the bounds representing the limitations on the (tangential) acceleration and the jerk, respectively. For the sake of simplicity, we consider constraints (7) and (8) symmetric and constant. However, the following development could be easily extended to the non-symmetric and nonconstant case. Note that the jerk constraint (8) is nonconvex. The continuous problem is discretized as follows. We subdivide the path into $n - 1$ intervals of equal length, i.e., we evaluate function w at points $s_i = ((i - 1)s_f)/(n - 1)$, $i = 1, \dots, n$, so that we have the following n -dimensional vector of variables:

$$\mathbf{w} = (w_1, w_2, \dots, w_n) = (w(s_1), w(s_2), \dots, w(s_n)).$$

Then, the finite dimensional version of the problem is given as follows.

Problem 2 (Smooth Minimum-Time Velocity Planning Problem: Discretized Version):

$$\min_{\mathbf{w} \in \mathbb{R}^n} \sum_{i=1}^{n-1} \frac{2h}{\sqrt{w_{i+1}} + \sqrt{w_i}} \quad (9)$$

$$0 \leq \mathbf{w} \leq \mathbf{u} \quad (10)$$

$$w_{i+1} - w_i \leq 2hA, \quad i = 1, \dots, n-1 \quad (11)$$

$$w_i - w_{i+1} \leq 2hA, \quad i = 1, \dots, n-1 \quad (12)$$

$$(w_{i-1} - 2w_i + w_{i+1})\sqrt{\frac{\ell_i(\mathbf{w})}{4}} \leq 2h^2J \quad (13)$$

$$i = 2, \dots, n-1$$

$$-(w_{i-1} - 2w_i + w_{i+1})\sqrt{\frac{\ell_i(\mathbf{w})}{4}} \leq 2h^2J \quad (14)$$

$$i = 2, \dots, n-1$$

where

$$\ell_i(\mathbf{w}) = w_{i+1} + w_{i-1} + 2w_i \quad (15)$$

while $u_i = \mu^+(s_i)$, for $i = 1, \dots, n$, and, in particular, $u_1 = 0$ and $u_n = 0$ since we are assuming that the initial and final velocities are equal to 0. The objective function (9) is an approximation of (6) given by the Riemann sum of the intervals obtained by dividing each interval $[s_i, s_{i+1}]$, for $i = 1, \dots, n - 1$, in two subintervals of the same size. Constraints (11) and (12) are obtained by a finite difference approximation of w' . Constraints (13) and (14) are obtained by using a second-order central finite difference to approximate w'' , while w is approximated by a weighted arithmetic mean of three consecutive samples. Due to jerk constraints (13) and (14), Problem 2 is nonconvex and cannot be solved with the algorithm presented in [4].

B. Main Result

The main contribution of this article is the development of a new solution algorithm for finding a local minimum of the

nonconvex Problem 2. As detailed in next sections, we propose to solve Problem 2 by a line-search algorithm based on the sequential solution of convex problems. The algorithm is an iterative one where the following operations are performed at each iteration.

1) *Constraint Linearization:* We first define a convex problem by linearizing constraints (13) and (14) through a first-order Taylor approximation around the current point $\mathbf{w}^{(k)}$. Different from other sequential algorithms for nonlinear programming (NLP) problems, we keep the original convex objective function. The linearized problem is introduced in Section II.

2) *Computation of a Feasible Descent Direction:* The convex problem (actually, a relaxation of such problem) is solved in order to compute a feasible descent direction $\delta\mathbf{w}^{(k)}$. The main contribution of this article lies in this part. The computation requires the minimization of a suitably defined objective function through a further iterative algorithm. At each iteration of this algorithm, the following operations are performed:

C. Objective Function Evaluation

Such evaluation requires the solution of a problem with the same objective function but subject to a subset of the constraints. The special structure of the resulting subproblem is heavily exploited in order to solve it efficiently. This is the topic of Section III.

D. Computation of a Descent Step

Some Lagrange multipliers of the subproblem define a subgradient for the objective function. This can be employed to define a linear programming (LP) problem that returns a descent step for the objective function. This is the topic of Section IV.

Line Search: Finally, a standard line search along the half-line $\mathbf{w}^{(k)} + \alpha\delta\mathbf{w}^{(k)}$, $\alpha \geq 0$, is performed.

Sections II–IV detail all what we discussed above. Next, in Section V, we present different computational experiments.

E. Comparison With Existing Literature

Although many works consider the problem of minimum-time speed planning with acceleration constraints (see [7]–[9]), relatively few consider jerk constraints. Perhaps, this is also due to the fact that the jerk constraint is nonconvex so that its presence significantly increases the complexity of the optimization task. One can use a general-purpose NLP solver (such as SNOPT or IPOPT) for finding a local solution of Problem 2, but the required time is, in general, too large for the speed planning application. As outlined in Section I-D, in this work, we tackle this problem through an approach based on the solution of a sequence of convex subproblems. There are different approaches in the literature based on the sequential solution of convex subproblems. In [10], it is first observed that the problem with acceleration constraints but no jerk constraints for robotic manipulators can be reformulated as a convex one with linear constraints, and it is solved by a sequence of LP problems obtained by linearizing the

AQ:3
230
231
232
233
234
235
236
237
238
239
240
241
242
243
244
245
246
247
248
249
250
251
252
253
254
255
256
257
258
259
260
261
262
263
264
265
266
267
268
269
270
271
272
273
274
275
276
277
278
279
280
281

282 objective function at the current point, i.e., the objective
 283 function is replaced by its supporting hyperplane at the
 284 current point, and by introducing a trust region centered at the
 285 current point. In [11] and [12], it is further observed that this
 286 problem can be solved very efficiently through the solution
 287 of a sequence of 2-D LP problems. In [13], an interior point
 288 barrier method is used to solve the same problem based on
 289 Newton's method. Each Newton step requires the solution of
 290 a KKT system, and an efficient way to solve such systems
 291 is proposed in that work. Moving to approaches also dealing
 292 with jerk constraints, we mention [14]. In this work, it is
 293 observed that jerk constraints are nonconvex but can be
 294 written as the difference between two convex functions.
 295 Based on this observation, the authors solve the problem by
 296 a sequence of convex subproblems obtained by linearizing
 297 at the current point the concave part of the jerk constraints
 298 and by adding a proximal term in the objective function that
 299 plays the same role as a trust region, preventing from taking
 300 too large steps. In [15] a slightly different objective function
 301 is considered. Rather than minimizing the traveling time
 302 along the given path, the integral of the squared difference
 303 between the maximum velocity profile and the computed
 304 velocity profile is minimized. After representing time-varying
 305 control inputs as products of parametric exponential and
 306 polynomial functions, the authors reformulate the problem in
 307 such a way that its objective function is convex quadratic,
 308 while nonconvexity lies in difference-of-convex functions.
 309 The resulting problem is tackled through the solution of a
 310 sequence of convex subproblems obtained by linearizing
 311 the concave part of the nonconvex constraints. In [16], the
 312 problem of speed planning for robotic manipulators with jerk
 313 constraints is reformulated in such a way that nonconvexity
 314 lies in simple bilinear terms. Such bilinear terms are replaced
 315 by the corresponding convex and concave envelopes, obtaining
 316 the so-called McCormick relaxation, which is the tightest
 317 possible convex relaxation of the nonconvex problem. Other
 318 approaches dealing with jerk constraints do not rely on
 319 the solution of convex subproblems. For instance, in [17],
 320 a concatenation of fifth-order polynomials is employed to
 321 provide smooth trajectories, which results in quadratic jerk
 322 profiles, while, in [18], cubic polynomials are employed,
 323 resulting in piecewise constant jerk profiles. The decision
 324 process involves the choice of the phase durations, i.e.,
 325 of the intervals over which a given polynomial applies. A
 326 very recent and interesting approach to the problem with
 327 jerk constraints is [19]. In this work, an approach based
 328 on numerical integration is discussed. Numerical integration
 329 has been first applied under acceleration constraints in [20]
 330 and [21]. In [19], jerk constraints are taken into account. The
 331 algorithm detects a position s along the trajectory where the
 332 jerk constraint is singular, that is, the jerk term disappears
 333 from one of the constraints. Then, it computes the speed
 334 profile up to s by computing two maximum jerk profiles and
 335 then connecting them by a minimum jerk profile, found by a
 336 shooting method. In general, the overall solution is composed
 337 of a sequence of various maximum and minimum jerk
 338 profiles. This approach does not guarantee reaching a local
 339 minimum of the traversal time. Moreover, since Problem 4

340 has velocity and acceleration constraints, the jerk constraint
 341 is singular for all values of s so that the algorithm presented
 342 in [19] cannot be directly applied to Problem 4.

343 Some algorithms use heuristics to quickly find sub-
 344 optimal solutions of acceptable quality. For instance,
 345 Villagra *et al.* [22] propose an algorithm that applies to curves
 346 composed of clothoids, circles, and straight lines. The algo-
 347 rithm does not guarantee the local optimality of the solution.
 348 Raineri and Guarino Lo Bianco [23] present an efficient
 349 heuristic algorithm. Also, this method does not guarantee
 350 global nor local optimality. Various works in the literature
 351 consider jerk bounds in the speed optimization problem for
 352 robotic manipulators instead of mobile vehicles. This is a
 353 slightly different problem but mathematically equivalent to
 354 Problem (1). In particular, paper [24] presents a method based
 355 on the solution of a large number of nonlinear and nonconvex
 356 subproblems. The resulting algorithm is slow due to a large
 357 number of subproblems; moreover, the authors do not prove its
 358 convergence. Zhang *et al.* [25] propose a similar method that
 359 gives a continuous-time solution. Again, the method is com-
 360 putationally slow since it is based on the numerical solution of
 361 a large number of differential equations; moreover, this article
 362 does not contain proof of convergence or local optimality.
 363 Some other works replace the jerk constraint with *pseudo-*
 364 *jerk*, that is, the derivative of the acceleration with respect
 365 to arc length, obtaining a constraint analogous to (4e) and
 366 ending up with a convex optimization problem. For instance,
 367 Zhang *et al.* [26] add to the objective function a pseudo-jerk
 368 penalizing term. This approach is computationally convenient,
 369 but substituting (8) with (4e) may be overly restrictive at low
 370 speeds.

371 F. Statement of Contribution

372 The method presented in this article is a sequential convex
 373 one that aims at finding a local optimizer of Problem 2.
 374 To be more precise, as usual with nonconvex problems, only
 375 convergence to a stationary point can usually be proved.
 376 However, the fact that the sequence of generated feasible
 377 points is decreasing with respect to the objective function
 378 values usually guarantees that the stationary point is a local
 379 minimizer, except in rather pathological cases (see [27, p. 19]).
 380 Moreover, in our experiments, even after running a local solver
 381 from different starting points, we have never been able to
 382 detect local minimizers better than the one returned by the
 383 method we propose. Thus, a possible, nontrivial, topic for
 384 future research could be that of proving the global optimality
 385 of the solution. To the best of our knowledge and as detailed
 386 in the following, this algorithm is more efficient than the ones
 387 existing in the literature since it leverages the special struc-
 388 ture of the subproblems obtained as local approximations of
 389 Problem 2. We discussed this class of problems in our previous
 390 work [28]. This structure allows computing very efficiently a
 391 feasible descent direction for the main line-search algorithm;
 392 it is one of the key elements that allow us to outperform
 393 generic NLP solvers. In summary, the main contributions of
 394 this work are: 1) on the theoretical side, the development of an
 395 approach for which a rigorous mathematical analysis has been

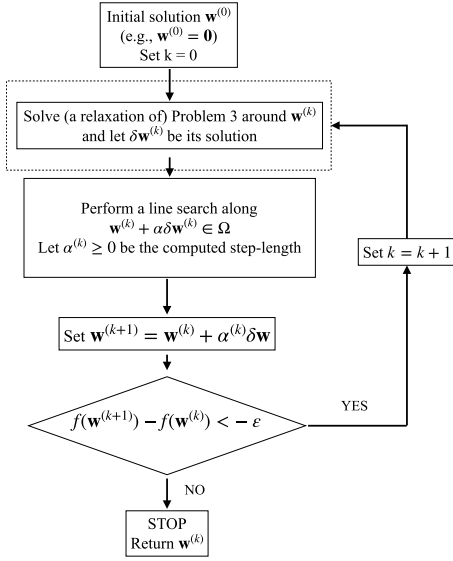


Fig. 1. Flowchart of algorithm SCA. The dashed block corresponds to a call of the procedure `ComputeUpdate`, proposed to solve Problem 3, which represents the main contribution of this article.

performed, proving a convergence result to a stationary point (see Section II) and 2) on the computational side, to exploit heavily the structure of the problem in order to implement the approach in a fairly efficient way (see Sections III and IV) so that its computing times outperform those of nonlinear solvers and are competitive with heuristic approaches that are only able to return suboptimal solutions of lower quality (see Section V).

II. SEQUENTIAL ALGORITHM BASED ON CONSTRAINT LINEARIZATION

To account for the nonconvexity of Problem 2, we propose a line-search method based on the solution of a sequence of special structured convex problems. Throughout this article, we call this algorithm Sequential Convex Algorithm (SCA), and its flowchart is shown in Fig. 1. It belongs to the class of Sequential Convex Programming algorithms, where, at each iteration, a convex subproblem is solved. In what follows, we denote by Ω the feasible region of Problem 2. At each iteration k , we replace the current point $\mathbf{w}^{(k)} \in \Omega$ with a new point $\mathbf{w}^{(k)} + \alpha^{(k)} \delta \mathbf{w}^{(k)} \in \Omega$, where the step size $\alpha^{(k)} \in [0, 1]$ is obtained by a *line search* along the descent direction $\delta \mathbf{w}^{(k)}$, which, in turn, is obtained through the solution of a convex problem. The constraints of the convex problem are linear approximations of (10)–(14) around $\mathbf{w}^{(k)}$, while the objective function is the original one. Then, the problem that we consider to compute the direction $\delta \mathbf{w}^{(k)}$ is given in the following (superscript k of $\mathbf{w}^{(k)}$ is omitted):

Problem 3:

$$\min_{\delta \mathbf{w} \in \mathbb{R}^n} \sum_{i=1}^{n-1} \frac{2h}{\sqrt{w_{i+1} + \delta w_{i+1}} + \sqrt{w_i + \delta w_i}} \quad (16)$$

$$\mathbf{l}_B \leq \delta \mathbf{w} \leq \mathbf{u}_B \quad (17)$$

$$\delta w_{i+1} - \delta w_i \leq b_{A_i}, \quad i = 1, \dots, n-1 \quad (18)$$

$$\delta w_i - \delta w_{i+1} \leq b_{D_i}, \quad i = 1, \dots, n-1 \quad (19)$$

$$\delta w_i - \eta_i \delta w_{i-1} - \eta_i \delta w_{i+1} \leq b_{N_i}, \quad i = 2, \dots, n-1 \quad (20)$$

$$\eta_i \delta w_{i-1} + \eta_i \delta w_{i+1} - \delta w_i \leq b_{P_i}, \quad i = 2, \dots, n-1 \quad (21)$$

where $\mathbf{l}_B = -\mathbf{w}$ and $\mathbf{u}_B = \mathbf{u} - \mathbf{w}$ (recall that \mathbf{u} has been introduced in (10), and its components have been defined immediately in Problem 2), while parameters η , \mathbf{b}_A , \mathbf{b}_D , \mathbf{b}_N , and \mathbf{b}_P depend on the point \mathbf{w} around which the constraints (10)–(14) are linearized. More precisely, we have

$$\begin{aligned} b_{A_i} &= 2hA - w_{i+1} + w_i & (22) \\ b_{D_i} &= 2hA - w_i + w_{i+1} \\ \eta_i &= \frac{3w_{i+1} + 3w_{i-1} + 2w_i}{2(w_{i+1} + w_{i-1} + 6w_i)} \\ b_{P_i} &= \frac{\sqrt{\ell_i(\mathbf{w})} 8h^2 J + (w_{i-1} - 2w_i + w_{i+1}) \sqrt{\ell_i(\mathbf{w})}}{2(w_{i+1} + w_{i-1} + 6w_i)} \\ b_{N_i} &= \frac{\sqrt{\ell_i(\mathbf{w})} 8h^2 J - (w_{i-1} - 2w_i + w_{i+1}) \sqrt{\ell_i(\mathbf{w})}}{2(w_{i+1} + w_{i-1} + 6w_i)} \end{aligned}$$

where ℓ_i is defined in (15). The following proposition is an immediate consequence of the feasibility of \mathbf{w} .

Proposition 1: All parameters η , \mathbf{b}_A , \mathbf{b}_D , \mathbf{b}_N , and \mathbf{b}_P are nonnegative.

The proposed approach follows some standard ideas of sequential quadratic approaches employed in the literature about nonlinearly constrained problems. However, a quite relevant difference is that the true objective function (9) is employed in the problem to compute the direction, rather than a quadratic approximation of such function. This choice comes from the fact that the objective function (9) has some features (in particular, convexity and being decreasing), which, combined with the structure of the linearized constraints, allows for an efficient solution of Problem 3. Problem 3 is a convex problem with a nonempty feasible region ($\delta \mathbf{w} = \mathbf{0}$ is always a feasible solution) and, consequently, can be solved by existing NLP solvers. However, such solvers tend to increase computing times since they need to be called many times within the iterative algorithm SCA. The main contribution of this article lies in the routine `computeUpdate` (see dashed block in Fig. 1), which is able to solve Problem 3 and efficiently returns a descent direction $\delta \mathbf{w}^{(k)}$. To be more precise, we solve a *relaxation* of Problem 3. Such relaxation, as well as the routine to solve it, is detailed in Sections III and IV. In Section III, we present efficient approaches to solve some subproblems, including proper subsets of the constraints. Then, in Section IV, we address the solution of the relaxation of Problem 3.

Remark 1: It is possible to see that, if one of the constraints (13) and (14) is active at $\mathbf{w}^{(k)}$, then, along the direction $\delta \mathbf{w}^{(k)}$ computed through the solution of the linearized Problem 3, it holds that $\mathbf{w}^{(k)} + \alpha \delta \mathbf{w}^{(k)} \in \Omega$ for any sufficiently small $\alpha > 0$. In other words, small perturbations of the current solution $\mathbf{w}^{(k)}$ along direction $\delta \mathbf{w}^{(k)}$ do not lead outside the feasible region Ω . This fact is illustrated in Fig. 2. Let us

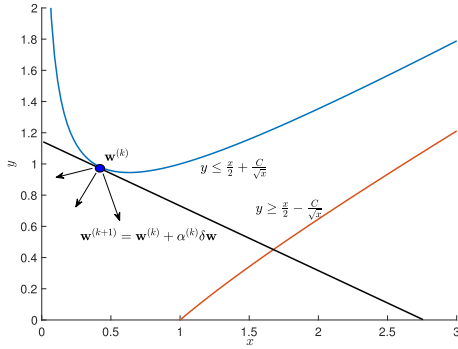


Fig. 2. Constraints (13) and (14) and their linearization ($C = 4h^2J$).

477 rewrite constraints (13) and (14) as follows:

$$478 \quad |(x - 2y)\sqrt{x}| \leq C \quad (23)$$

479 where $x = \ell_i(\mathbf{w})$, $y = 2w_i$, and $C = 4h^2J$ is a constant. The
 480 feasible region associated with constraint (23) is reported in
 481 Fig. 2. In particular, it is the region between the blue and red
 482 curves. Suppose that constraint $y \leq (x/2) + (C/2\sqrt{x})$ is active
 483 at $\mathbf{w}^{(k)}$ (the case when $y \geq (x/2) - (C/2\sqrt{x})$ is active can
 484 be dealt with in a completely analogous way). If we linearize
 485 such constraint around $\mathbf{w}^{(k)}$, then we obtain a linear constraint
 486 (black line in Fig. 2), which defines a region completely
 487 contained into the one defined by the nonlinear constraint
 488 $y \leq (x/2) + (C/2\sqrt{x})$. Hence, for each direction $\delta\mathbf{w}^{(k)}$ feasible
 489 with respect to the linearized constraint, we are always able to
 490 perform sufficiently small steps, without violating the original
 491 nonlinear constraints, i.e., for $\alpha > 0$ small enough, it holds
 492 that $\mathbf{w}^{(k)} + \alpha\delta\mathbf{w}^{(k)} \in \Omega$.

493 Constraints (13) and (14) can also be rewritten as follows:

$$494 \quad w_{i-1} + w_{i+1} - 2w_i - 4h^2J(\ell_i(\mathbf{w}))^{-\frac{1}{2}} \leq 0 \quad (24)$$

$$495 \quad 2w_i - w_{i-1} - w_{i+1} - 4h^2J(\ell_i(\mathbf{w}))^{-\frac{1}{2}} \leq 0. \quad (25)$$

496 Note that the functions on the left-hand side of these
 497 constraints are concave. Now, we can define a variant of
 498 Problem 3 where constraints (20) and (21) are replaced by
 499 the following linearizations of constraints (24) and (25):

$$500 \quad -\beta_i\delta w_{i-1} - \beta_i\delta w_{i+1} + \delta w_i \leq b'_{N_i} \quad (26)$$

$$501 \quad \theta_i\delta w_{i-1} + \theta_i\delta w_{i+1} - \delta w_i \leq b'_{P_i} \quad (27)$$

502 where

$$503 \quad \theta_i = \frac{1 + 2h^2J(\ell_i(\mathbf{w}))^{-\frac{3}{2}}}{2 - 4h^2J(\ell_i(\mathbf{w}))^{-\frac{3}{2}}}$$

$$504 \quad \beta_i = \frac{1 - 2h^2J(\ell_i(\mathbf{w}))^{-\frac{3}{2}}}{2 + 4h^2J(\ell_i(\mathbf{w}))^{-\frac{3}{2}}}$$

$$505 \quad b'_{N_i} = \frac{6h^2J(\ell_i(\mathbf{w}))^{-\frac{1}{2}}}{2 + 4h^2J(\ell_i(\mathbf{w}))^{-\frac{3}{2}}}$$

$$506 \quad b'_{P_i} = \frac{6h^2J(\ell_i(\mathbf{w}))^{-\frac{1}{2}}}{2 - 4h^2J(\ell_i(\mathbf{w}))^{-\frac{3}{2}}}. \quad (28)$$

507 The following proposition states that constraints (26)
 508 and (27) are tighter than constraints (20) and (21).

509 *Proposition 2:* For all $i = 2, \dots, n - 1$, it holds that $\beta_i \leq$
 510 $\eta_i \leq \theta_i$. Equality $\eta_i = \theta_i$ holds if the corresponding nonlinear
 511 constraint (24) is active at the current point \mathbf{w} . Similarly, $\eta_i =$
 512 β_i holds if the corresponding nonlinear constraint (25) is active
 513 at the current point \mathbf{w} .

514 *Proof:* We only prove the results about θ_i and η_i . Those
 515 about β_i and η_i are proved in a completely analogous way.
 516 By definition of η_i and θ_i , we need to prove that

$$517 \quad \frac{3w_{i+1} + 3w_{i-1} + 2w_i}{w_{i+1} + 6w_i + w_{i-1}} \leq \frac{1 + 2h^2J(\ell_i(\mathbf{w}))^{-\frac{3}{2}}}{2 - 4h^2J(\ell_i(\mathbf{w}))^{-\frac{3}{2}}}.$$

518 After few simple computations, this inequality can be
 519 rewritten as

$$520 \quad 4h^2J(\ell_i(\mathbf{w}))^{-\frac{1}{2}} \geq (w_{i-1} - 2w_i + w_{i+1})$$

521 which holds in view of feasibility of \mathbf{w} and, moreover, holds
 522 as an equality if constraint (24) is active at the current point
 523 \mathbf{w} , as we wanted to prove. \square

524 In view of this result, by replacing constraints (20) and (21)
 525 with (26) and (27), we reduce the search space of the new
 526 displacement $\delta\mathbf{w}$. On the other hand, the following proposition
 527 states that, with constraints (26) and (27), no line search is
 528 needed along the direction $\delta\mathbf{w}$, i.e., we can always choose the
 529 step length $\alpha = 1$.

530 *Proposition 3:* If constraints (26) and (27) are employed as
 531 a replacement of constraints (20) and (21) in the definition of
 532 Problem 3, then, for each feasible solution $\delta\mathbf{w}$ of this problem,
 533 it holds that $\mathbf{w} + \delta\mathbf{w} \in \Omega$.

534 *Proof:* For the sake of convenience, let us rewrite
 535 Problem 2 in the following more compact form:

$$536 \quad \min f(\mathbf{w} + \delta\mathbf{w})$$

$$537 \quad \mathbf{c}(\mathbf{w} + \delta\mathbf{w}) \leq 0 \quad (29)$$

538 where the vector function \mathbf{c} contains all constraints
 539 of Problem 2 and the nonlinear ones are given as
 540 in (24) and (25) (recall that, in that case, vector \mathbf{c} is a vector of
 541 concave functions). Then, Problem 3 can be written as follows:

$$542 \quad \min f(\mathbf{w} + \delta\mathbf{w}) \quad \mathbf{c}(\mathbf{w}) + \nabla\mathbf{c}(\mathbf{w})\delta\mathbf{w} \leq 0. \quad (30)$$

543 Now, it is enough to observe that, by concavity,

$$544 \quad \mathbf{c}(\mathbf{w} + \delta\mathbf{w}) \leq \mathbf{c}(\mathbf{w}) + \nabla\mathbf{c}(\mathbf{w})\delta\mathbf{w}$$

545 so that each feasible solution of (30) is also feasible for (29).
 546 \square

547 The above proposition states that the feasible region of
 548 Problem 3, when constraints (26) and (27) are employed
 549 in its definition, is a subset of the feasible region Ω of
 550 the original Problem 2. As a final result of this section,
 551 we state the following theorem, which establishes convergence
 552 of algorithm SCA to a stationary (KKT) point of Problem 2.

553 *Theorem 1:* If algorithm SCA is run for an infinite number
 554 of iterations and there exists some positive integer value K
 555 such that for all iterations $k \geq K$, constraints (26) and (27) are
 556 always employed in the definition of Problem 3, and then, the
 557 sequence of points $\{\mathbf{w}^{(k)}\}$ generated by the algorithm converges
 558 to a KKT point of Problem 2.

In order to prove the theorem, we first need to prove some lemmas.

Lemma 1: The sequence $\{f(\mathbf{w}^{(k)})\}$ of the function values at points generated by algorithm SCA converges to a finite value.

Proof: The sequence is nonincreasing and bounded from below, e.g., by the value $f(\mathbf{u}_B)$, in view of the fact that the objective function f is monotonic decreasing. Thus, it converges to a finite value. \square

Next, we need the following result based on strict convexity of the objective function f .

Lemma 2: For each $\delta > 0$ sufficiently small, it holds that

$$\min \left\{ \max\{f(\mathbf{x}), f(\mathbf{y})\} - f\left(\frac{\mathbf{x} + \mathbf{y}}{2}\right) : \mathbf{x}, \mathbf{y} \in \Omega, \|\mathbf{x} - \mathbf{y}\| \geq \delta \right\} \geq \varepsilon_\delta > 0. \quad (31)$$

Proof: Due to strict convexity, it holds that, $\forall \mathbf{x} \neq \mathbf{y}$,

$$\max\{f(\mathbf{x}), f(\mathbf{y})\} - f\left(\frac{\mathbf{x} + \mathbf{y}}{2}\right) > 0.$$

Moreover, the function is a continuous one. Next, we observe that the region

$$\{\mathbf{x}, \mathbf{y} \in \Omega : \|\mathbf{x} - \mathbf{y}\| \geq \delta\}$$

is a compact set. Thus, by the Weierstrass theorem, the minimum in (31) is attained, and it must be strictly positive, as we wanted to prove. \square

Finally, we prove that also the sequence of points generated by algorithm SCA converges to some point, feasible for Problem 2.

Lemma 3: It holds that

$$\|\delta \mathbf{w}^{(k)}\| \rightarrow 0.$$

Proof: Let us assume, by contradiction, that, over some infinite subsequence with index set \mathcal{K} , it holds that $\|\delta \mathbf{w}^{(k)}\| \geq 2\rho > 0$ for all $k \in \mathcal{K}$, i.e.,

$$\|\mathbf{w}^{(k+1)} - \mathbf{w}^{(k)}\| \geq 2\rho > 0 \quad (32)$$

where $\mathbf{w}^{(k+1)} = \mathbf{w}^{(k)} + \delta \mathbf{w}^{(k)}$. Over this subsequence, it holds, by strict convexity, that

$$f(\mathbf{w}^{(k+1)}) \leq f(\mathbf{w}^{(k)}) - \zeta \quad \forall k \in \mathcal{K} \quad (33)$$

for some $\zeta > 0$. Indeed, it follows by optimality of $\mathbf{w}^{(k)} + \delta \mathbf{w}^{(k)}$ for Problem 3 and convexity of f that

$$f(\mathbf{w}^{(k+1)}) \leq f\left(\frac{\mathbf{w}^{(k+1)} + \mathbf{w}^{(k)}}{2}\right) \leq f(\mathbf{w}^{(k)})$$

so that

$$\max\{f(\mathbf{w}^{(k)}), f(\mathbf{w}^{(k+1)})\} = f(\mathbf{w}^{(k)}).$$

Then, it follows from (32) and Lemma 2 that we can choose $\zeta = \varepsilon_\rho > 0$. Thus, since (33) holds infinitely often, we should have $f(\mathbf{w}^{(k)}) \rightarrow -\infty$, which, however, is not possible in view of Lemma 1. \square

Now, we are ready to prove Theorem 1.

Proof: As a consequence of Lemma 3, it also holds that

$$\mathbf{w}^{(k)} \rightarrow \bar{\mathbf{w}} \in \Omega. \quad (34)$$

Indeed, all points $\mathbf{w}^{(k)}$ belong to the compact feasible region Ω so that the sequence $\{\mathbf{w}^{(k)}\}$ admits accumulation points. However, due to Lemma 3, the sequence cannot have distinct accumulation points.

Now, let us consider the compact reformulation (29) of Problem 2 and the related linearization (30), equivalent to Problem 3 with the linearized constraints (26) and (27). Since the latter is a convex problem with linear constraints, its local minimizer $\delta \mathbf{w}^{(k)}$ (unique in view of strict convexity of the objective function) fulfills the following KKT conditions:

$$\begin{aligned} \nabla f(\mathbf{w}^{(k)} + \delta \mathbf{w}^{(k)}) + \boldsymbol{\mu}_k^\top \nabla \mathbf{c}(\mathbf{w}^{(k)}) &= \mathbf{0} \\ \mathbf{c}(\mathbf{w}^{(k)}) + \nabla \mathbf{c}(\mathbf{w}^{(k)}) \delta \mathbf{w}^{(k)} &\leq \mathbf{0} \\ \boldsymbol{\mu}_k^\top (\mathbf{c}(\mathbf{w}^{(k)}) + \nabla \mathbf{c}(\mathbf{w}^{(k)}) \delta \mathbf{w}^{(k)}) &= 0 \\ \boldsymbol{\mu}_k &\geq \mathbf{0} \end{aligned} \quad (35)$$

where $\boldsymbol{\mu}_k$ is the vector of Lagrange multipliers. Now, by taking the limit of system (35), possibly over a subsequence, in order to guarantee convergence of the multiplier vectors $\boldsymbol{\mu}_k$ to a vector $\bar{\boldsymbol{\mu}}$, in view of Lemma 3 and (34), we have that

$$\begin{aligned} \nabla f(\bar{\mathbf{w}}) + \bar{\boldsymbol{\mu}}^\top \nabla \mathbf{c}(\bar{\mathbf{w}}) &= \mathbf{0} \\ \mathbf{c}(\bar{\mathbf{w}}) &\leq \mathbf{0} \\ \bar{\boldsymbol{\mu}}^\top \mathbf{c}(\bar{\mathbf{w}}) &= 0 \\ \bar{\boldsymbol{\mu}} &\geq \mathbf{0} \end{aligned}$$

or, equivalently, the limit point $\bar{\mathbf{w}}$ is a KKT point of Problem 2, as we wanted to prove. \square

Remark 2: In algorithm SCA at each iteration, we solve to optimality Problem 3. This is indeed necessary for the final iterations to prove the convergence result stated in Theorem 1. However, during the first iterations, it is not necessary to solve the problem to optimality: finding a feasible descent direction is enough. This does not alter the theoretical properties of the algorithm and allows to reduce the computing times.

In the rest of this article, we refer to constraints (18) and (19) as acceleration constraints, while constraints (20) and (21) [or (26) and (27)] are called (linearized) negative acceleration rate (NAR) and positive acceleration rate (PAR) constraints, respectively. Also, note that, in the different subproblems discussed in the following, we always refer to the linearization with constraints (20) and (21) and, thus, with parameters η_i , but the same results also hold for the linearization with constraints (26) and (27) and, thus, with parameters θ_i and β_i .

III. SUBPROBLEM WITH ACCELERATION AND NAR CONSTRAINTS

In this section, we propose an efficient method to solve Problem 3 when PAR constraints are removed. The solution of this subproblem becomes part of an approach to solve a suitable relaxation of Problem 3 and, in fact, under very mild assumptions, to solve Problem 3 itself. This is clarified in Section IV. We discuss: 1) the subproblem including only (17) and the acceleration constraints (18) and (19); 2) the subproblem including only (17) and the NAR constraints (20);

and 2) the subproblem including all constraints (17)–(20). Throughout the section, we need the results stated in the following two propositions. Let us consider problems with the following form, where $N = \{1, \dots, n\}$ and $M_j = \{1, \dots, m_j\}$, $j \in N$:

$$\begin{aligned} \min \quad & g(x_1, \dots, x_n) \\ & x_j \leq a_{i,j}x_{j-1} + b_{i,j}x_{j+1} + c_{i,j}, \quad i \in M_j, \quad j \in N \\ & \ell_j \leq x_j \leq u_j, \quad j \in N \end{aligned} \quad (36)$$

where g is a monotonic decreasing function; $a_{i,j}, b_{i,j}, c_{i,j} \geq 0$, for $i \in M_j$ and $j \in N$; $a_{i,1} = 0$ for $i \in M_1$; and $b_{i,n} = 0$ for $i \in M_n$. The following result is proven in [28]. Here, we report the proof in order to make this article self-contained. We denote by P the feasible polytope of problem (36). Moreover, we denote by \mathbf{z} the componentwise maximum of all feasible solutions in P , i.e., for each $j \in N$, $z_j = \max_{\mathbf{x} \in P} x_j$ (note that the above maximum value is attained since P is a polytope).

Proposition 4: The unique optimal solution of (36) is the componentwise maximum \mathbf{z} of all its feasible solutions.

Proof: If we are able to prove that the componentwise maximum \mathbf{z} of all feasible solutions is itself a feasible solution, by monotonicity of g , it must also be the unique optimal solution. In order to prove that \mathbf{z} is feasible, we proceed as follows. For $j \in N$, let \mathbf{x}^{*j} be the optimal solution of $\max_{\mathbf{x} \in P} x_j$ so that $z_j = x_j^{*j}$. Since $\mathbf{x}^{*j} \in P$, then it must hold that $\ell_j \leq z_j \leq u_j$. Moreover, let us consider the generic constraint

$$x_j \leq a_{i,j}x_{j-1} + b_{i,j}x_{j+1} + c_{i,j}$$

for $i \in M_j$. It holds that

$$\begin{aligned} z_j = x_j^{*j} &\leq a_{i,j}x_{j-1}^{*j} + b_{i,j}x_{j+1}^{*j} + c_{i,j} \\ &\leq a_{i,j}z_{j-1} + b_{i,j}z_{j+1} + c_{i,j} \end{aligned}$$

where the first inequality follows from feasibility of \mathbf{x}^{*j} , while the second follows from nonnegativity of a_{ij} and b_{ij} and the definition of \mathbf{z} . Since this holds for all $j \in N$, the result is proven. \square

Now, consider the problem obtained from (36) by removing some constraints, i.e., by taking $M'_j \subseteq M_j$ for each $j \in N$

$$\begin{aligned} \min \quad & g(x_1, \dots, x_n) \\ & x_j \leq a_{i,j}x_{j-1} + b_{i,j}x_{j+1} + c_{i,j}, \quad i \in M'_j, \quad j \in N \\ & \ell_j \leq x_j \leq u_j, \quad j \in N. \end{aligned} \quad (37)$$

Later, we also need the result stated in the following proposition.

Proposition 5: The optimal solution $\bar{\mathbf{x}}^*$ of problem (37) is an upper bound for the optimal solution \mathbf{x}^* of problem (36), i.e., $\bar{\mathbf{x}}^* \geq \mathbf{x}^*$.

Proof: It holds that \mathbf{x}^* is a feasible solution of problem (37) so that, in view of Proposition 4, $\bar{\mathbf{x}}^* \geq \mathbf{x}^*$ holds. \square

A. Acceleration Constraints

The simplest case is the one where we only consider the acceleration constraints (18) and (19), besides constraints (17)

with a generic upper bound vector $\mathbf{y} \geq \mathbf{0}$. The problem to be solved is

Problem 4:

$$\begin{aligned} \min_{\delta \mathbf{w} \in \mathbb{R}^n} \quad & \sum_{i=1}^{n-1} \frac{2h}{\sqrt{w_{i+1} + \delta w_{i+1}} + \sqrt{w_i + \delta w_i}} \\ & \mathbf{l}_B \leq \delta \mathbf{w} \leq \mathbf{y} \\ & \delta w_{i+1} - \delta w_i \leq b_{A_i}, \quad i = 1, \dots, n-1 \\ & \delta w_i - \delta w_{i+1} \leq b_{D_i}, \quad i = 1, \dots, n-1. \end{aligned}$$

It can be seen that such a problem belongs to the class of problems (36). Therefore, in view of Proposition 4, the optimal solution of Problem 4 is the componentwise maximum of its feasible region. Moreover, in [3], it has been proven that Algorithm 1, based on a forward and a backward iteration and with $O(n)$ computational complexity, returns an optimal solution of Problem 4.

Algorithm 1 Routine SOLVEACC for the Solution of the Problem With Acceleration Constraints

input : Upper bound \mathbf{y}
output: $\delta \mathbf{w}$
1 $\delta w_1 = 0, \delta w_n = 0$;
2 **for** $i = 1$ **to** $n - 1$ **do**
3 $\lfloor \delta w_{i+1} = \min\{\delta w_i + b_{A_i}, y_{i+1}\}$
4 **for** $i = n - 1$ **to** 1 **do**
5 $\lfloor \delta w_i = \min\{\delta w_{i+1} + b_{A_i}, y_i\}$
6 **return** $\delta \mathbf{w}$

B. NAR Constraints

Now, we consider the problem only including NAR constraints (20) and constraints (17) with upper bound vector \mathbf{y}

Problem 5:

$$\begin{aligned} \min_{\delta \mathbf{w} \in \mathbb{R}^n} \quad & \sum_{i=1}^{n-1} \frac{2h}{\sqrt{w_{i+1} + \delta w_{i+1}} + \sqrt{w_i + \delta w_i}} \\ & \mathbf{0} \leq \delta \mathbf{w} \leq \mathbf{y} \\ & \delta w_i \leq \eta_i(\delta w_{i-1} + \delta w_{i+1}) + b_{N_i}, \quad i = 2, \dots, n-1 \end{aligned} \quad (38)$$

where $y_1 = y_n = 0$ because of the boundary conditions. Also, this problem belongs to the class of problems (36) so that Proposition 4 states that its optimal solution is the componentwise maximum of its feasible region. Problem 5 can be solved by using the graph-based approach presented in [4] and [28]. However, Cabassi *et al.* [4] show that, by exploiting the structure of a simpler version of the NAR constraints, it is possible to develop an algorithm more efficient than the graph-based one. Our purpose is to extend the results presented in [4] to a case with different and more challenging NAR constraints in order to develop an efficient algorithm outperforming the graph-based one.

Now, let us consider the restriction of Problem 5 between two generic indexes s and t such that $1 \leq s < t \leq n$, obtained by fixing $\delta w_s = y_s$ and $\delta w_t = y_t$ and by considering only the

743 NAR and upper bound constraints at $s + 1, \dots, t - 1$. Let $\delta \mathbf{w}^*$
 744 be the optimal solution of the restriction. We first prove the
 745 following lemma.

746 *Lemma 4:* The optimal solution $\delta \mathbf{w}^*$ of the restriction of
 747 Problem 5 between two indexes s and t , $1 \leq s < t \leq n$,
 748 is such that, for each $j \in \{s + 1, \dots, t - 1\}$, either $\delta w_j^* \leq y_j$
 749 or $\delta w_j^* \leq \eta_j(\delta w_{j+1}^* + \delta w_{j-1}^*) + b_{N_j}$ holds as an equality.

750 *Proof:* It is enough to observe that, in case both inequali-
 751 ties were strict for some j , then, in view of the monotonicity of
 752 the objective function, we could decrease the objective func-
 753 tion value by increasing the value of δw_j^* , thus contradicting
 754 optimality of $\delta \mathbf{w}^*$. \square

755 Note that the above result also applies to the full Problem 5,
 756 which corresponds to the special case $s = 1, t = n$ with
 757 $y_1 = y_n = 0$. In view of Lemma 4, we have that there exists
 758 an index j , with $s < j \leq t$, such that: 1) $\delta w_j^* = y_j$; 2) the
 759 upper bound constraint is not active at $s + 1, \dots, j - 1$; and
 760 3) all NAR constraints $s + 1, \dots, j - 1$ are active. Then, j is
 761 the lowest index in $\{s + 1, \dots, t - 1\}$ where the upper bound
 762 constraint is active. If index j were known, then the following
 763 observation allows returning the components of the optimal
 764 solution between s and j . Let us first introduce the following
 765 definitions of matrix \mathbf{A} and vector \mathbf{q} :

$$766 \quad \mathbf{A} = \begin{bmatrix} 1 & -\eta_{s+1} & 0 & \cdots & 0 \\ -\eta_{s+2} & 1 & -\eta_{s+2} & \ddots & \vdots \\ 0 & \ddots & \ddots & \ddots & 0 \\ 0 & \cdots & 0 & -\eta_{j-1} & 1 \end{bmatrix}$$

$$767 \quad \mathbf{q} = \begin{bmatrix} b_{N_{s+1}} + \eta_{s+1}y_s \\ b_{N_{s+2}} \\ \vdots \\ b_{N_{j-2}} \\ b_{N_{j-1}} + \eta_{j-1}y_j \end{bmatrix}. \quad (40)$$

768 Note that \mathbf{A} is the square submatrix of the NAR constraints
 769 restricted to rows $s + 1$ up to $j - 1$ and the related columns.

770 *Observation 1:* Let $\delta \mathbf{w}^*$ be the optimal solution of the
 771 restriction of Problem 5 between s and t and let $s < j$.
 772 If constraints $\delta w_s^* \leq y_s$, $\delta w_j^* \leq y_j$, and $\delta w_i^* \leq \eta_i(\delta w_{i+1}^* +$
 773 $\delta w_{i-1}^*) + b_{N_i}$, for $i = s + 1, \dots, j - 1$, are all active, then
 774 $\delta w_{s+1}^*, \dots, \delta w_{j-1}^*$ are obtained by the solution of the following
 775 tridiagonal system:

$$776 \quad \delta w_s = y_s$$

$$777 \quad \delta w_r - \eta_r \delta w_{r+1} - \eta_r \delta w_{r-1} = b_{N_r}, \quad r = s + 1, \dots, j - 1$$

$$778 \quad \delta w_j = y_j$$

779 or, equivalently, as

$$780 \quad \delta w_{s+1} - \eta_{s+1} \bar{x}_{s+2}$$

$$781 \quad = b_{N_{s+1}} + \eta_{s+1} y_s$$

$$782 \quad \delta w_r - \eta_r \delta w_{r+1} - \eta_r \delta w_{r-1} = b_{N_r}, \quad r = s + 2, \dots, j - 2$$

$$783 \quad \delta w_{s+1} - \eta_{s+1} \bar{x}_{s+2} = b_{N_{s+1}} + \eta_{s+1} y_s. \quad (41)$$

784 In the matrix form, the above tridiagonal linear system can
 785 be written as

$$786 \quad \mathbf{A} \delta \mathbf{w}_{s+1, j-1}^* = \mathbf{q} \quad (42)$$

787 where matrix \mathbf{A} and vector \mathbf{q} are defined in (40) and $\delta \mathbf{w}_{s+1, j-1}^*$
 788 is the restriction of vector $\delta \mathbf{w}$ to its components between $s + 1$
 789 and $j - 1$. 789

790 Tridiagonal systems 790

$$791 \quad a_i x_{i-1} + b_i x_i + c_i x_{i+1} = d_i, \quad i = 1, \dots, m$$

792 with $a_1 = c_m = 0$ can be solved through so-called Thomas
 793 algorithm [29] with $O(m)$ operations. In order to detect the
 794 lowest index $j \in \{s + 1, \dots, t - 1\}$ such that the upper bound
 795 constraint is active at j , we propose Algorithm 2, also called
 796 SOLVEnAR and described in what follows. We initially set
 797 $j = t$. Then, at each iteration, we solve the linear system (42).
 798 Let $\bar{\mathbf{x}} = (\bar{x}_{s+1}, \dots, \bar{x}_{j-1})$ be its solution. We check whether
 799 it is feasible and optimal or not. Namely, if there exists $k \in$
 800 $\{s + 1, \dots, j - 1\}$ such that either $\bar{x}_k < 0$ or $\bar{x}_k > y_k$, then
 801 $\bar{\mathbf{x}}$ is unfeasible, and consequently, we need to reduce j by 1.
 802 If $\bar{x}_k = y_k$ for some $k \in \{s + 1, \dots, j - 1\}$, then we also
 803 reduce j by 1 since j is not in any case the lowest index
 804 of the optimal solution where the upper bound constraint is
 805 active. Finally, if $0 \leq \bar{x}_k < y_k$, for $k = s + 1, \dots, j - 1$, then
 806 we need to verify if $\bar{\mathbf{x}}$ is the best possible solution over the
 807 interval $\{s + 1, \dots, j - 1\}$. We are able to check that after
 808 proving the following result. 808

809 *Proposition 6:* Let matrix \mathbf{A} and vector \mathbf{q} be defined as
 810 in (40). The optimal solution $\delta \mathbf{w}^*$ of the restriction of
 811 Problem 5 between s and t satisfies 811

$$812 \quad \delta w_s^* = y_s, \quad \delta w_r^* = \bar{x}_r, \quad r = s + 1, \dots, j - 1, \quad \delta w_j^* = y_j \quad (43)$$

813 if and only if the optimal value of the LP problem 813

$$814 \quad \max_{\boldsymbol{\epsilon}} \mathbf{1}^T \boldsymbol{\epsilon}$$

$$815 \quad \mathbf{A} \boldsymbol{\epsilon} \leq \mathbf{0}$$

$$816 \quad \boldsymbol{\epsilon} \leq \bar{\mathbf{y}} - \bar{\mathbf{x}} \quad (44)$$

817 is strictly positive or, equivalently, if the following system 817
 818 admits no solution: 818

$$819 \quad \mathbf{A}^T \boldsymbol{\lambda} = \mathbf{1}, \quad \boldsymbol{\lambda} \geq \mathbf{0}. \quad (45)$$

820 *Proof:* Let us first assume that $\delta \mathbf{w}^*$ does not fulfill (43).
 821 Then, in view of Lemma 4, j is not the lowest index such
 822 that the upper bound is active at the optimal solution, and
 823 consequently, $\delta w_k^* = y_k > \bar{x}_k$ for some $k \in \{s + 1, \dots, j - 1\}$.
 824 Such optimal solution must be feasible, and in particular,
 825 it must satisfy all NAR constraints between $s + 1$ and $j - 1$
 826 and the upper bound constraints between $s + 1$ and j , i.e., 826

$$827 \quad \delta w_{s+1}^* - \eta_{s+1} \delta w_{s+2}^*$$

$$828 \quad \leq b_{N_{s+1}} + \eta_{s+1} y_s$$

$$829 \quad \delta w_r^* - \eta_r \delta w_{r+1}^* - \eta_r \delta w_{r-1}^* \leq b_{N_r}, \quad r = s + 2, \dots, j - 2$$

$$830 \quad \delta w_{j-1}^* - \eta_{j-1} \delta w_{j-2}^* - \eta_{j-1} \delta w_j^* \leq b_{N_{j-1}}$$

$$831 \quad \delta w_r^* \leq y_r, \quad r = s + 1, \dots, j.$$

832 In view of $\delta w_j^* \leq y_j$ and $\eta_{j-1} \geq 0$, $\delta \mathbf{w}^*$ also satisfies the
 833 following system of inequalities: 833

$$834 \quad \delta w_{s+1}^* - \eta_{s+1} \delta w_{s+2}^*$$

$$835 \quad \leq b_{N_{s+1}} + \eta_{s+1} y_s$$

$$836 \quad \delta w_r^* - \eta_r \delta w_{r+1}^* - \eta_r \delta w_{r-1}^* \leq b_{N_r}, \quad r = s + 2, \dots, j - 2$$

$$\begin{aligned} \delta w_{j-1}^* - \eta_{j-1} \delta w_{j-2}^* &\leq b_{Nj-1} + \eta_{j-1} y_j \\ \delta w_r^* &\leq y_r, \quad r = s+1, \dots, j-1. \end{aligned}$$

After making the change of variables $\delta w_r^* = \bar{x}_r + \epsilon_r$ for $r = s+1, \dots, j-1$, and recalling that $\bar{\mathbf{x}}$ solves system (41), the system of inequalities can be further rewritten as

$$\begin{aligned} \epsilon_{s+1} - \eta_{s+1} \epsilon_{s+2} &\leq 0 \\ \epsilon_r - \eta_r \epsilon_{r+1} - \eta_r \epsilon_{r-1} &\leq 0, \quad r = s+2, \dots, j-2 \\ \epsilon_{j-1} - \eta_{j-1} \epsilon_{j-2} &\leq 0 \\ \epsilon_r &\leq y_r - \bar{x}_r, \quad r = s+1, \dots, j-1. \end{aligned}$$

Finally, recalling the definition of matrix \mathbf{A} and vector \mathbf{q} given in (40), this can also be written in a more compact form as

$$\begin{aligned} \mathbf{A}\boldsymbol{\epsilon} &\leq \mathbf{0} \\ \boldsymbol{\epsilon} &\leq \bar{\mathbf{y}} - \bar{\mathbf{x}}. \end{aligned}$$

If $\delta w_k^* = y_k > \bar{x}_k$ for some $k \in \{s+1, \dots, j-1\}$, then the system must admit a solution with $\epsilon_k > 0$. This is equivalent to prove that problem (44) has an optimal solution with at least one strictly positive component, and the optimal value is strictly positive. Indeed, in view of the definition of matrix \mathbf{A} , problem (44) has the structure of the problems discussed in Proposition 4. More precisely, to see that, we need to remark that maximizing $\mathbf{1}^T \boldsymbol{\epsilon}$ is equivalent to minimizing the decreasing function $-\mathbf{1}^T \boldsymbol{\epsilon}$. Then, observing that $\boldsymbol{\epsilon} = \mathbf{0}$ is a feasible solution of problem (44), by Proposition 4, the optimal solution $\boldsymbol{\epsilon}^*$ must be a nonnegative vector, and since at least one component, namely, component k , is strictly positive, then the optimal value must also be strictly positive.

Conversely, let us assume that the optimal value is strictly positive, and $\boldsymbol{\epsilon}^*$ is an optimal solution with at least one strictly positive component. Then, there are two possible alternatives. Either the optimal solution $\delta \mathbf{w}^*$ of the restriction of Problem 5 between s and t is such that $\delta w_j^* < y_j$, in which case (43) obviously does not hold, or $\delta w_j^* = y_j$. In the latter case, let us assume by contradiction that (43) holds. We observe that the solution that is defined as follows:

$$\begin{aligned} x'_s &= y_s \\ x'_r &= \bar{x}_r + \epsilon_r^* = \delta w_r^* + \epsilon_r^*, \quad r = s+1, \dots, j-1 \\ x'_j &= y_j = \delta w_j^* \\ x'_r &= \delta w_r^*, \quad r = j+1, \dots, t \end{aligned}$$

is feasible for the restriction of Problem 5 between s and t . Indeed, by feasibility of $\boldsymbol{\epsilon}^*$ in problem (44), all upper bound and NAR constraints between s and $j-1$ are fulfilled. Those between $j+1$ and t , are also fulfilled by the feasibility of $\delta \mathbf{w}^*$. Then, we only need to prove that the NAR constraint at j is satisfied. By feasibility of $\delta \mathbf{w}^*$ and in view of $\epsilon_{j-1}^*, \eta_j \geq 0$, we have that

$$\begin{aligned} x'_j &= \delta w_j^* \leq \eta_j \delta w_{j-1}^* + \eta_j \delta w_{j+1}^* + b_{Nj} \\ &\leq \eta_j (\delta w_{j-1}^* + \epsilon_{j-1}) + \eta_j \delta w_{j+1}^* + b_{Nj} \\ &= \eta_j x'_{j-1} + \eta_j x'_{j+1} + b_{Nj}. \end{aligned}$$

Thus, \mathbf{x}' is feasible such that $\mathbf{x}' \geq \delta \mathbf{w}^*$ with at least one strict inequality (recall that at least one component of $\boldsymbol{\epsilon}^*$ is strictly positive), which contradicts the optimality of $\delta \mathbf{w}^*$ (recall that the optimal solution must be the componentwise maximum of all feasible solutions).

In order to prove the last part, i.e., problem (44) has a positive optimal value if and only if (45) admits no solution, and we notice that the optimal value is positive if and only if the feasible point $\boldsymbol{\epsilon} = \mathbf{0}$ is not an optimal solution, or equivalently, the null vector is not a KKT point. Since, at $\boldsymbol{\epsilon} = \mathbf{0}$, constraints $\boldsymbol{\epsilon} \leq \bar{\mathbf{y}} - \bar{\mathbf{x}}$ cannot be active, then the KKT conditions for problem (44) at this point are exactly those established in (45), where vector $\boldsymbol{\lambda}$ is the vector of Lagrange multipliers for constraints $\mathbf{A}\boldsymbol{\epsilon} \leq \mathbf{0}$. This concludes the proof. \square

Then, if (45) admits no solution, (43) does not hold, and again, we need to reduce j by 1. Otherwise, we can fix the optimal solution between s and j according to (43). After that, we recursively call the routine `SolveNAR` on the remaining subinterval $\{j, \dots, t\}$ in order to obtain the solution over the full interval.

Remark 3: In Algorithm 2, routine `isFeasible` is the routine used to verify if, for $k = s+1, \dots, j-1$, $0 \leq \bar{x}_k < y_k$, while `isOptimal` is the procedure to check optimality of $\bar{\mathbf{x}}$ over the interval $\{s+1, \dots, j-1\}$, i.e., (43) holds.

Now, we are ready to prove that Algorithm 2 solves Problem 5.

Proposition 7: The call `solveNAR(y, 1, n)` of Algorithm 2 returns the optimal solution of Problem 5.

Proof: After the call `solveNAR(y, 1, n)`, we are able to identify the portion of the optimal solution between 1 and some index j_1 , $1 < j_1 \leq n$. If $j_1 = n$, then we are done. Otherwise, we make the recursive call `solveNAR(y, j_1, n)`, which enables to identify also the portion of the optimal solution between j_1 and some index j_2 , $j_1 < j_2 \leq n$. If $j_2 = n$, then we are done. Otherwise, we make the recursive call `solveNAR(y, j_2, n)` and so on. After at most n recursive calls, we are able to return the full optimal solution. \square

Algorithm 2 `SolveNAR(y, s, t)`

input : Upper bound \mathbf{y} and two indices s and t with $1 \leq s < t \leq n$
output: $\delta \mathbf{w}^*$

- 1 Set $j = t$;
- 2 $\delta \mathbf{w}^* = \mathbf{y}$;
- 3 **while** $j \geq s+1$ **do**
- 4 Compute the solution $\bar{\mathbf{x}}$ of the linear system (42);
- 5 **if** `isFeasible`($\bar{\mathbf{x}}$) and `isOptimal`($\bar{\mathbf{x}}$) **then**
- 6 **Break**;
- 7 **else**
- 8 Set $j = j-1$;
- 9 **for** $i = s+1, \dots, j-1$ **do**
- 10 Set $\delta w_i^* = \bar{x}_i$;
- 11 **return** $\delta \mathbf{w}^* = \min\{\delta \mathbf{w}^*, \text{SolveNAR}(\delta \mathbf{w}^*, j, t)\}$;

Remark 4: Note that Algorithm 2 involves solving a significant amount of linear systems, both to compute $\bar{\mathbf{x}}$ and verify its optimality [see (42) and (45)]. Some tricks can be employed to reduce the number of operations. Some of these are discussed in [30].

The following proposition states the worst case complexity of `solveNAR`($\mathbf{y}, 1, n$).

Proposition 8: Problem 5 can be solved with $O(n^3)$ operations by running the procedure `SolveNAR`($\mathbf{y}, 1, n$) and by using the Thomas algorithm for the solution of each linear system.

Proof: In the worst case, at the first call, we have $j_1 = 2$ since we need to go all the way from $j = n$ down to $j = 2$. Since, for each j , we need to solve a tridiagonal system, which requires at most $O(n)$ operations, the first call of `SolveNAR` requires $O(n^2)$ operations. This is similar for all successive calls, and since the number of recursive calls is at most $O(n)$, the overall effort is at most of $O(n^3)$ operations. \square

In fact, what we observed is that the practical complexity of the algorithm is much better, namely, $\Theta(n^2)$.

C. Acceleration and NAR Constraints

Now, we discuss the problem with acceleration and NAR constraints, with upper bound vector \mathbf{y} , i.e.,

Problem 6:

$$\min_{\delta \mathbf{w} \in \mathbb{R}^n} \sum_{i=1}^{n-1} \frac{2h}{\sqrt{w_{i+1} + \delta w_{i+1}} + \sqrt{w_i + \delta w_i}}$$

$$\mathbf{l}_B \leq \delta \mathbf{w} \leq \mathbf{y}$$

$$\delta w_{i+1} - \delta w_i \leq b_{A_i}, \quad i = 1, \dots, n-1$$

$$\delta w_i - \delta w_{i+1} \leq b_{D_i}, \quad i = 1, \dots, n-1$$

$$\delta w_i - \eta_i \delta w_{i-1} - \eta_i \delta w_{i+1} \leq b_{N_i}, \quad i = 2, \dots, n-1.$$

We first remark that Problem 6 has the structure of problem (36) so that, by Proposition 4, its unique optimal solution is the componentwise maximum of its feasible region. As for Problem 5, we can solve Problem 6 by using the graph-based approach proposed in [28]. However, Cabassi *et al.* [4] show that, if we adopt a very efficient procedure to solve Problems 4 and 5, then it is worth splitting the full problem into two separated ones and use an iterative approach (see Algorithm 3). Indeed, Problems 4–6 share the common property that their optimal solution is also the componentwise maximum of the corresponding feasible region. Moreover, according to Proposition 5, the optimal solutions of Problems 4 and 5 are valid upper bounds for the optimal solution (actually, also for any feasible solution) of the full Problem 6. In Algorithm 3, we first call the procedure `SolveACC` with input the upper bound vector \mathbf{y} . Then, the output of this procedure, which, according to what we have just stated, is an upper bound for the solution of the full Problem 6, satisfies $\delta \mathbf{w}_{\text{Acc}} \leq \mathbf{y}$, and becomes the input for a call of the procedure `SolveNAR`. The output $\delta \mathbf{w}_{\text{NAR}}$ of this call is again an upper bound for the solution of the full Problem 6, and it satisfies $\delta \mathbf{w}_{\text{NAR}} \leq \delta \mathbf{w}_{\text{Acc}}$. This output becomes the input of a further call to the procedure `SolveACC`, and we proceed in this way until the distance between two consecutive output vectors falls below a

prescribed tolerance value ε . The following proposition states that the sequence of output vectors generated by the alternate calls to the procedures `SolveACC` and `SolveNAR` converges to the optimal solution of the full Problem 6.

Proposition 9: Algorithm 3 converges to the the optimal solution of Problem 6 when $\varepsilon = 0$ and stops after a finite number of iterations if $\varepsilon > 0$.

Proof: We have observed that the sequence of alternate solutions of Problems 4 and 5, here denoted by $\{\mathbf{y}_i\}$, is: 1) a sequence of valid upper bounds for the optimal solution of Problem 6; 2) componentwise monotonic nonincreasing; and 3) componentwise bounded from below by the null vector. Thus, if $\varepsilon = 0$, an infinite sequence is generated, which converges to some point $\bar{\mathbf{y}}$, which is also an upper bound for the optimal solution of Problem 6 but, more precisely, by continuity, is also a feasible point of the problem and, is thus, also the optimal solution of the problem. If $\varepsilon > 0$, due to the convergence to some point $\bar{\mathbf{y}}$, at some finite iteration, the exit condition of the while loop must be satisfied. \square

Algorithm 3 Algorithm `SolveACC` for the Solution of Problem 6

input : The upper bound \mathbf{y} and the tolerance ε
output: The optimal solution $\delta \mathbf{w}^*$ and the optimal value f^*

- 1 $\delta \mathbf{w}_{\text{Acc}} = \text{SolveACC}(\mathbf{y});$
- 2 $\delta \mathbf{w}_{\text{NAR}} = \text{SolveNAR}(\delta \mathbf{w}_{\text{Acc}}, 1, n);$
- 3 **while** $\|\delta \mathbf{w}_{\text{NAR}} - \delta \mathbf{w}_{\text{Acc}}\| > \varepsilon$ **do**
- 4 $\delta \mathbf{w}_{\text{Acc}} = \text{SolveACC}(\delta \mathbf{w}^*);$
- 5 $\delta \mathbf{w}_{\text{NAR}} = \text{SolveNAR}(\delta \mathbf{w}_{\text{Acc}}, 1, n);$
- 6 $\delta \mathbf{w}^* = \delta \mathbf{w}_{\text{NAR}};$
- 7 **return** $\delta \mathbf{w}^*$, `evaluateObj`($\delta \mathbf{w}^*$)

IV. DESCENT METHOD FOR THE CASE OF ACCELERATION, PAR, AND NAR CONSTRAINTS

Unfortunately, PAR constraints (21) do not satisfy the assumptions requested in Proposition 4 in order to guarantee that the componentwise maximum of the feasible region is the optimal solution of Problem 3. However, in Section III, we have shown that Problem 6, i.e., Problem 3 without the PAR constraints, can be efficiently solved by Algorithm 3. Our purpose then is to separate the acceleration and NAR constraints from the PAR constraints.

Definition 1: Let $f: \mathbb{R}^n \rightarrow \mathbb{R}$ be the objective function of Problem 3, and let \mathcal{D} be the region defined by the acceleration and NAR constraints (the feasible region of Problem 6). We define the function $F: \mathbb{R}^n \rightarrow \mathbb{R}$ as follows:

$$F(\mathbf{y}) = \min\{f(\mathbf{x}) \mid \mathbf{x} \in \mathcal{D}, \mathbf{x} \leq \mathbf{y}\}.$$

Namely, F is the optimal value function of Problem 6 when the upper bound vector is \mathbf{y} .

Proposition 10: Function F is a convex function.

Proof: Since Problem 6 is convex, then the optimal value function F is convex (see [31, Sec. 5.6.1]). \square

Now, let us introduce the following problem:

1017 *Problem 7:*

$$1018 \quad \min_{\mathbf{y} \in \mathbb{R}^n} F(\mathbf{y}) \quad (46)$$

$$1019 \quad \eta_i(y_{i-1} + y_{i+1}) - y_i \leq b_{P_i}, \quad i = 2, \dots, n-1 \quad (47)$$

$$1020 \quad \mathbf{l}_B \leq \mathbf{y} \leq \mathbf{u}_B. \quad (48)$$

1021 Such a problem is a relaxation of Problem 3. Indeed, each
1022 feasible solution of Problem 3 is also feasible for Problem 7,
1023 and the value of F at such solution is equal to the value
1024 of the objective function of Problem 3 at the same solution.
1025 We solve Problem 7 rather than Problem 3 to compute the
1026 new displacement $\delta \mathbf{w}$. More precisely, if \mathbf{y}^* is the optimal
1027 solution of Problem 7, then we set

$$1028 \quad \delta \mathbf{w} = \arg \min_{\mathbf{x} \in \mathcal{D}, \mathbf{x} \leq \mathbf{y}^*} f(\mathbf{x}). \quad (49)$$

1029 In the following proposition, we prove that, under a very
1030 mild condition, the optimal solution of Problem 7 computed
1031 in (49) is feasible and, thus, optimal for Problem 3 so that,
1032 although we solve a relaxation of the latter problem, we return
1033 an optimal solution for it.

1034 *Proposition 11:* Let $\mathbf{w}^{(k)}$ be the current point. If

$$1035 \quad \ell_j(\delta \mathbf{w}) \leq \ell_j(\mathbf{w}^{(k)})(3 + \min\{0, \zeta(\mathbf{w}^{(k)})\}), \quad j = 2, \dots, n-1 \quad (50)$$

1037 where $\delta \mathbf{w}$ is computed through (49) and

$$1038 \quad \zeta(\mathbf{w}^{(k)}) = \frac{\sqrt{\ell_j(\mathbf{w}^{(k)})} (w_{j-1}^{(k)} + w_{j+1}^{(k)} - 2w_j^{(k)})}{2h^2 J} \geq -2$$

1039 (the inequality follows from feasibility of $\mathbf{w}^{(k)}$), then $\delta \mathbf{w}$ is
1040 feasible for Problem 3, both if the nonlinear constraints are
1041 linearized as in (20) and (21), and if they are linearized as
1042 in (26) and (27).

1043 *Proof:* First, we notice that, if we prove the result for
1044 the tighter constraints (26) and (27), then it must also hold
1045 for constraints (20) and (21). Thus, we prove the result only
1046 for the former. By definition (49), $\delta \mathbf{w}$ satisfies the acceleration
1047 and NAR constraints so that

$$1048 \quad \delta w_j \leq \delta w_{j+1} + b_{D_j}$$

$$1049 \quad \delta w_j \leq \delta w_{j-1} + b_{A_{j-1}}$$

$$1050 \quad \delta w_j \leq \beta_j(\delta w_{j+1} + \delta w_{j-1}) + b'_{N_j}$$

$$1051 \quad \delta w_j \leq y_j^*.$$

1052 At least one of these constraints must be active; otherwise,
1053 δw_j could be increased, thus contradicting optimality. If the
1054 active constraint is $\delta w_j \leq \beta_j(\delta w_{j+1} + \delta w_{j-1}) + b'_{N_j}$, then
1055 constraint (27) can be rewritten as follows:

$$1056 \quad 4h^2 J (\ell_j(\mathbf{w}^{(k)}))^{-\frac{3}{2}} (\delta w_{j+1} + 2\delta w_j + \delta w_{j-1}) \\ 1057 \quad \leq 12h^2 J (\ell_j(\mathbf{w}^{(k)}))^{-\frac{1}{2}}$$

1058 or, equivalently,

$$1059 \quad \ell_j(\delta \mathbf{w}) \leq 3\ell_j(\mathbf{w}^{(k)})$$

1060 implied by (50), and thus, the constraint is satisfied under the
1061 given assumption. If $\delta w_j = y_j^*$, then

$$1062 \quad \theta_j(\delta w_{j-1} + \delta w_{j+1}) \leq \theta_j(y_{j-1}^* + y_{j+1}^*) \leq y_j^* + b'_{P_j} = \delta w_j + b'_{P_j}$$

1063 where the second inequality follows from the fact that \mathbf{y}^*
1064 satisfies the PAR constraints. Now, let $\delta w_j = \delta w_{j+1} + b_{D_j}$
1065 (the case when $\delta w_j \leq \delta w_{j-1} + b_{A_{j-1}}$ is active can be dealt
1066 with in a completely analogous way). First, we observe that
1067 $\delta w_j \geq \delta w_{j-1} - b_{D_{j-1}}$. Then,

$$1068 \quad 2\delta w_j \geq \delta w_{j+1} + \delta w_{j-1} + b_{D_j} - b_{D_{j-1}}.$$

1069 In view of the definitions of b_{D_j} and $b_{D_{j-1}}$, this can also be
1070 written as

$$1071 \quad 2\delta w_j \geq \delta w_{j+1} + \delta w_{j-1} + w_{j+1}^{(k)} - 2w_j^{(k)} + w_{j-1}^{(k)}. \quad (51)$$

1072 Now, after recalling the definitions of θ_j and b'_{P_j} given
1073 in (28), and setting $\Delta = h^2 J$, (27) can be rewritten as

$$1074 \quad 2\delta w_j \geq \delta w_{j+1} + \delta w_{j-1} + 2\Delta (\ell_j(\mathbf{w}^{(k)}))^{-\frac{3}{2}} \ell_j(\delta \mathbf{w}) \\ 1075 \quad - 6\Delta (\ell_j(\mathbf{w}^{(k)}))^{-\frac{1}{2}}.$$

1076 Taking into account (51), such inequality certainly holds if

$$1077 \quad w_{j+1}^{(k)} - 2w_j^{(k)} + w_{j-1}^{(k)} \geq 2\Delta (\ell_j(\mathbf{w}^{(k)}))^{-\frac{3}{2}} \ell_j(\delta \mathbf{w}) \\ 1078 \quad - 6\Delta (\ell_j(\mathbf{w}^{(k)}))^{-\frac{1}{2}}$$

1079 which is equivalent to

$$1080 \quad \ell_j(\delta \mathbf{w}) \leq \ell_j(\mathbf{w}^{(k)})(3 + \zeta(\mathbf{w}^{(k)})).$$

1081 This is also implied by (50). \square

1082 Assumption (50) is mild. In order to fulfill it, one can
1083 impose restrictions on δw_{j-1} , δw_j and δw_{j+1} . In fact, in the
1084 computational experiments, we did not impose such restric-
1085 tions unless a positive step-length along the computed direc-
1086 tion $\delta \mathbf{w}$ could not be taken (which, however, never occurred
1087 in our experiments).

1088 Now, let us turn our attention toward the solution of
1089 Problem 7. In order to solve it, we propose a descent method.
1090 We can exploit the information provided by the dual optimal
1091 solution $\mathbf{v} \in \mathbb{R}_+^n$ associated with the upper bound constraints
1092 of Problem 6. Indeed, from the sensitivity theory, we know
1093 that the dual solution is related to the gradient of the optimal
1094 value function F (see Definition 1) and provides information
1095 about how it changes its value for small perturbations of the
1096 upper bound values (for further details, see [31, Secs. 5.6.2 and
1097 5.6.5]). Let $\mathbf{y}^{(t)}$ be a feasible solution of Problem 7 and $\mathbf{v} \in \mathbb{R}_+^n$
1098 be the Lagrange multipliers of the upper bound constraints of
1099 Problem 6 when the upper bound is $\mathbf{y}^{(t)}$. Let

$$1100 \quad \varphi_i = b_{P_i} - \eta_i(y_{i-1}^{(t)} + y_{i+1}^{(t)}) + y_i^{(t)}, \quad i = 2, \dots, n-1.$$

1101 Then, a *feasible descent direction* $\mathbf{d}^{(t)}$ can be obtained by
1102 solving the following LP problem:

1103 *Problem 8:*

$$1104 \quad \min_{\mathbf{d} \in \mathbb{R}^n} -\mathbf{v}^T \mathbf{d} \quad (52)$$

$$1105 \quad \eta_i(d_{i-1} + d_{i+1}) - d_i \leq \varphi_i, \quad i = 2, \dots, n-1 \quad (53)$$

$$1106 \quad \mathbf{l}_B \leq \mathbf{y}^{(t)} + \mathbf{d} \leq \mathbf{u}_B \quad (54)$$

1107 where the objective function (52) imposes that $\mathbf{d}^{(t)}$ is a
1108 descent direction, while constraints (53) and (54) guarantee
1109 feasibility with respect to Problem 7. Problem 8 is an LP
1109

1110 problem, and consequently, it can easily be solved through a
 1111 standard LP solver. In particular, we employed GUROBI [32].
 1112 Unfortunately, since the information provided by the dual
 1113 optimal solution \mathbf{v} is local and related to small perturbations of
 1114 the upper bounds, it might happen that $F(\mathbf{y}^{(t)} + \mathbf{d}^{(t)}) \geq F(\mathbf{y}^{(t)})$.
 1115 To overcome this issue, we introduce a trust-region constraint
 1116 in Problem 8. Thus, let $\sigma^{(t)} \in \mathbb{R}_+$ be the radius of the trust
 1117 region at iteration t ; then, we have

1118 *Problem 9:*

$$1119 \quad \min_{\mathbf{d} \in \mathbb{R}^n} -\mathbf{v}^T \mathbf{d} \quad (55)$$

$$1120 \quad \eta_i (d_{i-1} + d_{i+1}) - d_i \leq \varphi_i, \quad i = 2, \dots, n-1 \quad (56)$$

$$1121 \quad \bar{\mathbf{l}}_{\mathbf{B}} \leq \mathbf{d} \leq \bar{\mathbf{u}}_{\mathbf{B}} \quad (57)$$

1122 where $\bar{l}_{B_i} = \max\{l_{B_i} - y_i^{(t)}, -\sigma^{(t)}\}$ and $\bar{u}_{B_i} = \min\{u_{B_i} -$
 1123 $y_i^{(t)}, \sigma^{(t)}\}$ for $i = 1, \dots, n$. After each iteration of the descent
 1124 algorithm, we change the radius $\sigma^{(t)}$ according to the following
 1125 rules.

- 1126 1) If $F(\mathbf{y}^{(t)} + \mathbf{d}^{(t)}) \geq F(\mathbf{y}^{(t)})$, then we set $\mathbf{y}^{(t+1)} = \mathbf{y}^{(t)}$, and
 1127 we tight the trust region by decreasing $\sigma^{(t)}$ by a factor
 1128 $\tau \in (0, 1)$.
- 1129 2) If $F(\mathbf{y}^{(t)} + \mathbf{d}^{(t)}) < F(\mathbf{y}^{(t)})$, then we set $\mathbf{y}^{(t+1)} = \mathbf{y}^{(t)} + \mathbf{d}^{(t)}$
 1130 and enlarge the radius $\sigma^{(t)}$ by a factor $\rho > 1$.

1131 The proposed descent algorithm is sketched in Fig. 3, which
 1132 reports the flowchart of the procedure `ComputeUpdate` used
 1133 in algorithm SCA. We initially set $\mathbf{y}^{(0)} = \mathbf{0}$. At each iteration t ,
 1134 we evaluate the objective function $F(\mathbf{y}^t)$ by solving Problem 6
 1135 with upper bound vector $\mathbf{y}^{(t)}$ through a call of the routine
 1136 `solveACCNAR` (see Algorithm 3). Then, we compute the
 1137 Lagrange multipliers $\mathbf{v}^{(t)}$ associated with the upper bound con-
 1138 straints. After that, we compute a candidate descent direction
 1139 $\mathbf{d}^{(t)}$ by solving Problem 9. If $\mathbf{d}^{(t)}$ is a descent step, then we set
 1140 $\mathbf{y}^{(t+1)} = \mathbf{y}^{(t)} + \mathbf{d}^{(t)}$ and enlarge the radius of the trust region;
 1141 otherwise, we do not move to a new point, and we tight the
 1142 trust region and solve again Problem 9. The descent algorithm
 1143 stops as soon as the radius of the trust region becomes smaller
 1144 than a fixed tolerance ε_1 .

1145 *Remark 5:* Note that we initially set $\mathbf{y}^{(0)} = \mathbf{0}$. However, any
 1146 feasible solution of Problem 9 does the job, and actually, start-
 1147 ing with a good initial solution may enhance the performance
 1148 of the algorithm.

1149 *Remark 6:* Problem 9 is an LP and can be solved by
 1150 any existing LP solver. However, a suboptimal solution to
 1151 Problem 9, obtained by a heuristic approach, is also accept-
 1152 able. Indeed, we observe that: 1) an *optimal* descent direction
 1153 is not strictly required and 2) a heuristic approach allows to
 1154 reduce the time needed to get a descent direction. In this
 1155 article, we employed a possible heuristic, whose description
 1156 can be found in [30], but the development of further heuristic
 1157 approaches is a possible topic for future research.

1158 V. COMPUTATIONAL EXPERIMENTS

1159 In this section, we present various computational experi-
 1160 ments performed in order to evaluate the approaches proposed
 1161 in Sections III and IV.

1162 In particular, we compared solutions of Problem 2 computed
 1163 by algorithm SCA to solutions obtained with commercial NLP

solvers. Note that, with a single exception, we did not carry out
 a direct comparison with other methods specifically tailored to
 Problem 2 for the following reasons.

- 1164 1) Some algorithms (such as [22] and [23]) use heuristics to
 1165 quickly find suboptimal solutions of acceptable quality
 1166 but do not achieve local optimality. Hence, comparing
 1167 their solution times with SCA would not be fair. How-
 1168 ever, in one of our experiments (see Experiment 4),
 1169 we made a comparison between the most recent heuristic
 1170 proposed in [23] and algorithm SCA, both in terms
 1171 of computing times and in terms of the quality of the
 1172 returned solution.
- 1173 2) The method presented in [26] does not consider the
 1174 (nonconvex) jerk constraint but solves a convex problem
 1175 whose objective function has a penalization term that
 1176 includes pseudojerk. Due to this difference, a direct
 1177 comparison with SCA is not possible.
- 1178 3) The method presented in [24] is based on the numerical
 1179 solution of a large number of nonlinear and nonconvex
 1180 subproblems and is, therefore, structurally slower than
 1181 SCA, whose main iteration is based on the efficient
 1182 solution of the convex Problem 3.

1183 In the first two experiments, we compare the computational
 1184 time of IPOPT, a general-purpose NLP solver [33], with that
 1185 of algorithm SCA over some randomly generated instances of
 1186 Problem 2. In particular, we tested two different versions of
 1187 the algorithm SCA. The first version, called SCA-H in what
 1188 follows, employs the heuristic mentioned in Remark 6. Since
 1189 the heuristic procedure may fail in some cases, in such cases,
 1190 we also need an LP solver. In particular, in our experiments,
 1191 we used GUROBI whenever the heuristic did not produce
 1192 either a feasible solution to Problem 9 or a descent direc-
 1193 tion. In the second version, called SCA-G in what follows,
 1194 we always employed GUROBI to solve Problem 9. For what
 1195 concerns the choice of the NLP solver IPOPT, we remark
 1196 that we chose it after a comparison with two further general-
 1197 purpose NLP solvers, SNOPT and MINOS, which, however,
 1198 turned out to perform worse than IPOPT on this class of
 1199 problems.

1200 In the third experiment, we compare the performance of
 1201 the two implemented versions of algorithm SCA applied to
 1202 two specific paths and see their behavior as the number n of
 1203 discretized points increases.

1204 In the fourth experiment, we compare the solutions returned
 1205 by algorithm SCA with those returned by the heuristic recently
 1206 proposed in [23].

1207 Finally, in the fifth experiment, we present a real-life speed
 1208 planning task for an LGV operating in an industrial setting,
 1209 using real problem bounds and paths layouts, provided by an
 1210 automation company based in Parma, Italy.

1211 We remark that, according to our experiments, the spe-
 1212 cial purpose routine `solveACCNAR` (Algorithm 3) strongly
 1213 outperforms general-purpose approaches, such as the graph-
 1214 based approach proposed in [28], and GUROBI, when solving
 1215 Problem 6 (which can be converted into an LP as discussed
 1216 in [28]).

1217 Finally, we remark that we also tried to solve the con-
 1218 vex Problem 3 arising at each iteration of the proposed
 1219

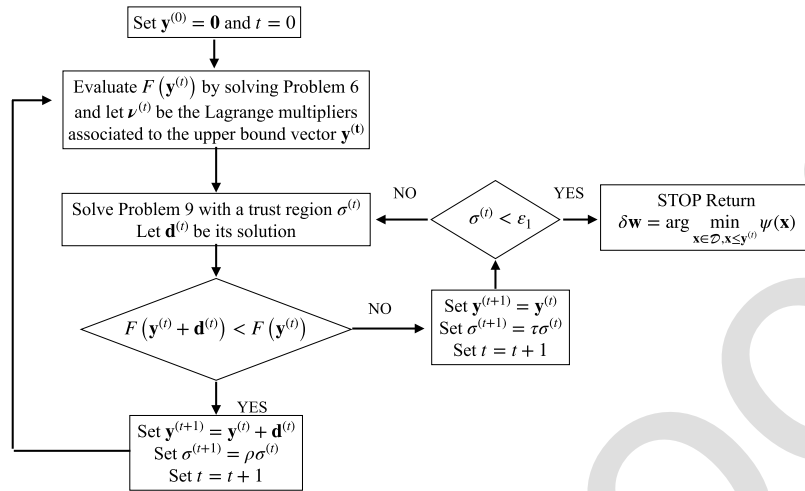


Fig. 3. Flowchart of the routine ComputeUpdate.

1222 method with an NLP solver in place of the procedure
1223 ComputeUpdate, presented in this article. However, the
1224 experiments revealed that, in doing this, the computing times
1225 become much larger even with respect to the single call to the
1226 NLP solver for solving the nonconvex Problem 2.

1227 All tests have been performed on an IntelCore i7-8550U
1228 CPU at 1.8 GHz. Both for IPOPT and algorithm SCA, the
1229 null vector was chosen as a starting point. The parameters
1230 used within algorithm SCA were $\varepsilon = 1e^{-8}$, $\varepsilon_1 = 1e^{-6}$
1231 (tolerance parameters), $\rho = 4$, and $\tau = 0.25$ (trust-region
1232 update parameters). The initial trust region radius $\sigma^{(0)}$ was
1233 initialized to 1 in the first iteration $k = 0$ but adaptively
1234 set equal to the size of the last update $\|w^{(k)} - w^{(k-1)}\|_\infty$
1235 in all subsequent iterations (this adaptive choice allowed to
1236 reduce computing times by more than a half). We remark that
1237 algorithm SCA has been implemented in MATLAB, so we
1238 expect better performance after a C/C++ implementation.

1239 A. Experiments 1 and 2

1240 In Experiment 1, we generated a set of 50 different paths,
1241 each of which was discretized setting $n = 100$, $n = 500$,
1242 and $n = 1000$ sample points. The instances were generated
1243 by assuming that the traversed path was divided into seven
1244 intervals over which the curvature of the path was assumed
1245 to be constant. Thus, the n -dimensional upper bound vector
1246 \mathbf{u} was generated as follows. First, we fixed $u_1 = u_n = 0$,
1247 i.e., the initial and final speeds must be equal to 0. Next,
1248 we partitioned the set $\{2, \dots, n-1\}$ into seven subintervals
1249 I_j , $j \in \{1, \dots, 7\}$, which corresponds to intervals with
1250 constant curvature. Then, for each subinterval, we randomly
1251 generated a value $u_j \in (0, \tilde{u}]$, where \tilde{u} is the maximum upper
1252 bound (which was set equal to $100 \text{ m}^2\text{s}^{-2}$). Finally, for each
1253 $j \in \{1, \dots, 7\}$, we set $u_k = \tilde{u}_j \forall k \in I_j$. The maximum
1254 acceleration parameter A is set equal to 2.78 ms^{-2} and the
1255 maximum jerk J to 0.5 ms^{-3} , while the path length is $s_f =$
1256 60 m . The values for A and J allow a comfortable motion for
1257 a ground transportation vehicle (see [34]).

1258 In Experiment 2, we generated a further set of 50 different
1259 paths, each of which was discretized using $n = 100$, $n = 500$,
1260 and $n = 1000$ variables. These new instances were randomly
1261 generated such that the traversed path was divided into up to
1262 five intervals over which the curvature could be zero, linear
1263 with respect to the arc length or constant. We chose this kind
1264 of path since they are able to represent the curvature of a
1265 road trip (see [35]). The maximum squared speed along the
1266 path was fixed equal to $192.93 \text{ m}^2\text{s}^{-2}$ (corresponding to a
1267 maximum speed of 50 kmh^{-1} , a typical value for an urban
1268 driving scenario). The total length of the paths was fixed to
1269 $s_f = 1000 \text{ m}$, while parameter A was set equal to 0.25 ms^{-2} ,
1270 J to 0.025 ms^{-3} , and A_N to 4.9 ms^{-2} .

1271 The results are reported in Table I, in which we show
1272 the average (minimum and maximum) computational times
1273 for SCA-H, SCA-G, and IPOPT. They show that algorithm
1274 SCA-H is the fastest one, while SCA-G is slightly faster than
1275 IPOPT at $n = 100$ but clearly faster for a larger number of
1276 sample points n . In general, we observe that both SCA-H and
1277 SCA-G tend to outperform IPOPT as n increases. Moreover,
1278 while the computing times for IPOPT at $n = 100$ are not much
1279 worse than those of SCA-H and SCA-G, we should point out
1280 that, at this dimension, IPOPT is sometimes unable to converge
1281 and return solutions whose objective function value differs
1282 from the best one by more than 100%. Also, the objective
1283 function values returned by SCA-H and SCA-G are sometimes
1284 slightly different, due to numerical issues related to the choice
1285 of the tolerance parameters, but such differences are mild ones
1286 and never exceed 1%. Therefore, these approaches appear to
1287 be fast and robust. It is also worthwhile to remark that SCA
1288 approaches are compatible with online planning requirements
1289 within the context of the LGV application. According to
1290 Haschke *et al.* [18] (see also [36]), in “highly unstructured,
1291 unpredictable, and dynamic environments,” there is a need to
1292 replan in order to adapt the motion in reaction to unforeseen
1293 events or obstacles. How often to replan depends strictly on the
1294 application. Within the context of the LGV application (where
1295 the environment is structured), replanning every 100–150 ms

TABLE I

AVERAGE (MINIMUM AND MAXIMUM) COMPUTING TIMES (IN SECONDS) FOR SCA-H, SCA-G, AND IPOPT OVER EXPERIMENTS 1 AND 2

| Exp. | n | | SCA-H | SCA-G | IPOPT |
|------|------|------|-------|-------|-------|
| 1 | 100 | min | 0.012 | 0.042 | 0.03 |
| | | mean | 0.016 | 0.072 | 0.132 |
| | | max | 0.026 | 0.138 | 0.305 |
| 1 | 500 | min | 0.042 | 0.21 | 0.352 |
| | | mean | 0.064 | 0.276 | 1.01 |
| | | max | 0.104 | 0.456 | 1.828 |
| 1 | 1000 | min | 0.1 | 0.426 | 1.432 |
| | | mean | 0.149 | 0.626 | 3.289 |
| | | max | 0.237 | 0.828 | 7.137 |
| 2 | 100 | min | 0.012 | 0.036 | 0.052 |
| | | mean | 0.02 | 0.047 | 0.113 |
| | | max | 0.038 | 0.073 | 0.263 |
| 2 | 500 | min | 0.049 | 0.102 | 0.534 |
| | | mean | 0.093 | 0.172 | 0.886 |
| | | max | 0.212 | 0.237 | 1.457 |
| 2 | 1000 | min | 0.083 | 0.228 | 1.733 |
| | | mean | 0.242 | 0.386 | 2.487 |
| | | max | 0.709 | 0.539 | 3.74 |

1296 is acceptable, and thus, the computing times of the SCA
 1297 approaches at $n = 100$ are suitable. Of course, computing
 1298 times increase with n , but we notice that the computing times
 1299 of SCA-H still meet the requirement at $n = 500$. Moreover,
 1300 a relevant feature of SCA-H and SCA-G is that, at each
 1301 iteration, a feasible solution is available. Thus, we could stop
 1302 them as soon as a time limit is reached. At $n = 500$, if we
 1303 impose a time limit of 150 ms, which is still quite reasonable
 1304 for the application, SCA-G returns slightly worse feasible
 1305 solutions, but these do not differ from the best ones by more
 1306 than 2%.

1307 **B. Experiment 3**

1308 In our third experiment, we compared the performance
 1309 of the two proposed approaches (SCA-H and SCA-G), over
 1310 two possible automated driving scenarios, as the number
 1311 n of samples increases. As a first example, we considered
 1312 a continuous curvature path composed of a line segment,
 1313 a clothoid, a circle arc, a clothoid, and a final line segment
 1314 (see Fig. 4). The minimum-time velocity planning on this
 1315 path, whose total length is $s_f = 90$ m, is addressed with the
 1316 following data. The problem constants are compatible with a
 1317 typical urban driving scenario. The maximum squared velocity
 1318 is $225 \text{ m}^2\text{s}^{-2}$ (corresponding to 54 km h^{-1}), the longitudinal
 1319 acceleration limit is $A = 1.5 \text{ ms}^{-2}$, and the maximal normal
 1320 acceleration is $A_N = 1 \text{ ms}^{-2}$, while, for the jerk constraints,
 1321 we set $J = 1 \text{ ms}^{-3}$. Next, we considered a path of length
 1322 $s_f = 60$ m (see Fig. 5) whose curvature was defined according
 1323 to the following function:

$$k(s) = \frac{1}{5} \sin\left(\frac{s}{10}\right), \quad s \in [0, s_f]$$

1324 and parameter A , A_N , and J were set equal to 1.39 ms^{-2} ,
 1325 4.9 ms^{-2} , and 0.5 ms^{-3} , respectively. The maximum squared
 1326 velocity is still equal to $225 \text{ m}^2\text{s}^{-2}$. The computational results
 1327 are reported in Figs. 6 and 7 for values of n that grows
 1328 from 100 to 1000. They show that the performance of SCA-H
 1329 and SCA-G depends on the path. In particular, it seems that
 1330 the heuristic performs in a poorer way when the number of
 1331

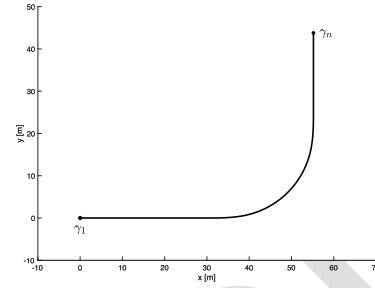


Fig. 4. Experiment 3—first path.

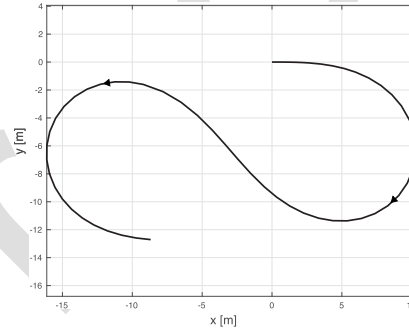


Fig. 5. Experiment 3—second path.

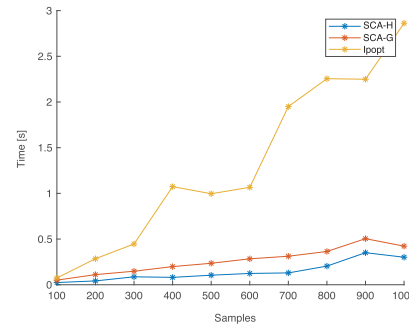


Fig. 6. Computing times (in seconds) for the path in Fig. 4.

1332 points of the upper bound vector at which PAR constraints are
 1333 violated tends to be large, which is the case for the second
 1334 instance. We can give two possible motivations: 1) the direc-
 1335 tions computed by the heuristic procedure are not necessarily
 1336 good descent directions, so routine `computeUpdate` slowly
 1337 converges to a solution and 2) the heuristic procedure often
 1338 fails, and it is in any case necessary to call GUROBI. Note
 1339 that the computing times of IPOPT on these two paths are
 1340 larger than those of SCA-H and SCA-G, and, as usual, the gap
 1341 increases with n . Moreover, for the second path, IPOPT was
 1342 unable to converge for $n = 100$ and returned a solution, which
 1343 differed by more than 35% with respect to those returned by
 1344 SCA-H and SCA-G.

1345 As a final remark, we notice that the computed traveling
 1346 times along the paths only slightly vary with n . For the first
 1347 path, they vary between 14.44 and 14.45 s while, for the
 1348 second path, between 20.65 and 20.66 s. The differences are
 1349 very mild, but we should point out that this is not always
 1350

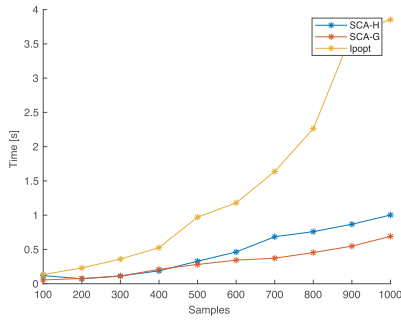


Fig. 7. Computing times (in seconds) for the path in Fig. 5.

TABLE II

MINIMUM, AVERAGE, AND MAXIMUM COMPUTING TIMES (IN SECONDS) AND RELATIVE PERCENTAGE DIFFERENCE BETWEEN THE TRAVELING TIMES COMPUTED BY THE HEURISTIC PRESENTED IN [23] AND THE SCA APPROACHES WITH $n = 100$ FOR THE INSTANCES OF EXPERIMENT 1

| Heuristic from [23] | min | mean | max |
|--------------------------------|-------|-------|--------|
| Time | 0.016 | 0.048 | 0.2049 |
| Relative percentage difference | 5.5% | 12.1% | 31.2% |

1350 the case. We further comment on this point when presenting
1351 Experiment 5.

1352 C. Experiment 4

1353 In this experiment, we compared the performance of our
1354 approach with the heuristic procedure recently proposed
1355 in [23]. In Table II, we report the computing times and the
1356 relative percentage difference $[(f_{\text{HEUR}} - f_{\text{SCA}})/f_{\text{SCA}}] * 100\%$
1357 between the traveling times computed by the heuristic and
1358 the SCA approaches for the instances of Experiment 1 with
1359 $n = 100$. Algorithms SCA-H and SCA-G have comparable
1360 computing times (actually, better for what concerns SCA-H)
1361 with respect to that heuristic, and the quality of the final
1362 solutions is, on average, larger than 10% (these observations
1363 also extend to other experiments). Such difference between
1364 the quality of the solutions returned by algorithm SCA and
1365 those returned by the heuristic is best explained through the
1366 discussion of a representative instance, taken from Experiment
1367 1 with $n = 100$. In this instance, we set $A = 2.78 \text{ ms}^{-2}$,
1368 while, for the jerk constraints, we set $J = 2 \text{ ms}^{-3}$. The total
1369 length of the path is $s_f = 60 \text{ m}$. The maximum velocity
1370 profile is the piecewise constant black line in Fig. 8. In the
1371 same figure, we report in red the velocity profile returned
1372 by the heuristic and in blue the one returned by algorithm
1373 SCA. The computing time for the heuristic is 45 ms, while,
1374 for algorithm SCA-H, it is 39 ms. The final objective function
1375 value (i.e., the traveling time along the given path) is 15.4 s
1376 for the velocity profile returned by the heuristic and 14.02 s
1377 for the velocity profile returned by algorithm SCA. From the
1378 qualitative point of view, it can be observed in this instance
1379 (and similar observations hold for the other instances that we
1380 tested) that the heuristic produces velocity profiles whose local
1381 minima coincide with those of the maximum velocity profile.
1382 For instance, in the interval between 10 and 20 m, we notice
1383 that the velocity profile returned by the heuristic coincides

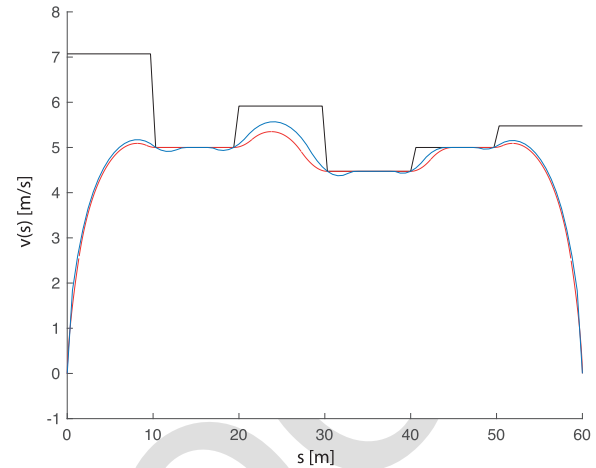


Fig. 8. Velocity profile returned by the heuristic proposed in [23] (red line) and by algorithm SCA (blue line). The black line is the maximum velocity profile.

1384 with the maximum velocity profile in that interval. Instead, the
1385 velocity profile generated by algorithm SCA generates velocity
1386 profiles that fall below the local minima of the maximum
1387 velocity profile, but, this way, they are able to keep the
1388 velocity higher in the regions preceding and following the local
1389 minima of the maximum velocity profile. Again, referring to
1390 the interval between 10 and 20 m, we notice that the velocity
1391 profile computed by algorithm SCA falls below the maximum
1392 velocity profile in that region and, thus, below the velocities
1393 returned by the heuristic, but, this way, velocities in the region
1394 before 10 m and in the one after 20 m are larger with respect
1395 to those computed by the heuristic.

1396 D. Experiment 5

1397 As a final experiment, we planned the speed law of an
1398 autonomous guided vehicle operating in a real-life auto-
1399 mated warehouse. Paths and problem data have been provided
1400 by packaging company Ocme S.r.l., based in Parma, Italy.
1401 We generated 50 random paths from a general layout. Fig. 9
1402 shows the warehouse layout and a possible path. In all paths,
1403 we set maximum velocity to 2 m s^{-1} , maximum longitudinal
1404 acceleration to $A = 0.28 \text{ m/s}^2$, maximum normal acceleration
1405 to 0.2 m/s^2 , and maximum jerk to $J = 0.025 \text{ m/s}^3$. Table III
1406 shows computation times for algorithms SCA-H, SCA-G, and
1407 IPOPT for a number of sampling points $n \in \{100, 500, 1000\}$.
1408 SCA-H is quite fast although it sometimes returns slightly
1409 worse solutions (the largest percentage error, at a single
1410 instance with $n = 1000$, is 8%). IPOPT is clearly slower than
1411 SCA-H and SCA-G for $n = 500$ and 1000, while, for $n = 100$,
1412 it is slower than SCA-H but quite similar to SCA-G. However,
1413 for these paths, the difference in terms of traveling times as
1414 n increases is much more significant with respect to the other
1415 experiments (see also the discussion at the end of Experiment
1416 3). More precisely, the percentage difference between the
1417 traveling times of solutions at $n = 100$ and $n = 1000$ is
1418 0.5% on average for Experiment 1 with a maximum of 2.1%,
1419 while, for Experiment 2, the average difference is 0.3% with
1420 a maximum of 0.4%. Instead, for the current experiment,

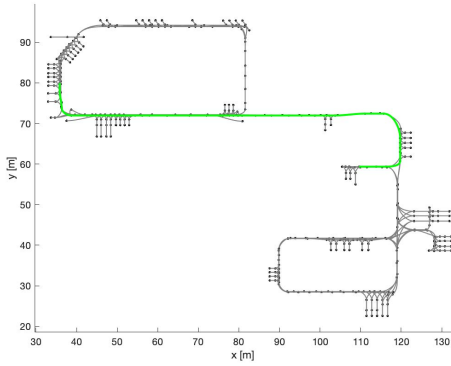


Fig. 9. Warehouse layout considered in Example 5 and a possible path.

TABLE III

AVERAGE, MINIMUM, AND MAXIMUM COMPUTING TIMES (IN SECONDS) FOR SCA-H, SCA-G, AND IPOPT OVER EXPERIMENT 5

| n | | SCA-H | SCA-G | IPOPT |
|------|------|-------|-------|-------|
| 100 | min | 0.009 | 0.033 | 0.029 |
| | mean | 0.013 | 0.043 | 0.037 |
| | max | 0.026 | 0.062 | 0.052 |
| 500 | min | 0.032 | 0.104 | 0.222 |
| | mean | 0.068 | 0.146 | 0.289 |
| | max | 0.174 | 0.224 | 0.423 |
| 1000 | min | 0.078 | 0.249 | 0.744 |
| | mean | 0.201 | 0.385 | 1.25 |
| | max | 0.501 | 0.65 | 3.359 |

1421 the average difference is 2.7% with a maximum of 7.9%.
 1422 However, the average falls to 0.2% and the maximum to 0.6%
 1423 if we consider the percentage difference between the traveling
 1424 times of solutions at $n = 500$ and $n = 1000$. Thus, for this
 1425 experiment, it is advisable to use a finer discretization or,
 1426 equivalently, a larger number of sampling points. A tentative
 1427 explanation for such different behavior is related to the lower
 1428 velocity limits of Experiment 5 with respect to the other
 1429 experiments. Indeed, the objective function is much more
 1430 sensitive to small changes at low speeds so that a finer grid of
 1431 sampling points is able to reduce the impact of approximation
 1432 errors. However, this is just a possible explanation. A further
 1433 possible explanation is that, in Experiments 1–4, curves are
 1434 composed of segments with constant and linear curvature,
 1435 whereas curves on industrial LGV layouts typically have
 1436 curvatures that are highly nonlinear with respect to arc length.

1437 VI. CONCLUSION

1438 In this article, we considered a speed planning problem
 1439 under jerk constraints. The problem is a nonconvex one,
 1440 and we proposed a sequential convex approach, where we
 1441 exploited the special structure of the convex subproblems
 1442 to solve them very efficiently. The approach is fast and is
 1443 theoretically guaranteed to converge to a stationary point of the
 1444 nonconvex problem. As a possible topic for future research, we
 1445 would like to investigate ways to solve Problem 9, currently
 1446 the bottleneck of the proposed approach, alternative to the
 1447 solver GUROBI, and the heuristic mentioned in Remark 6.
 1448 Moreover, we suspect that the stationary point to which the
 1449 proposed approach converges is, in fact, a global minimizer

of the nonconvex problem, and proving this fact is a further
 interesting topic for future research.

ACKNOWLEDGMENT

The authors are really grateful to the Associate Editor and
 the three anonymous reviewers for their careful reading and
 very useful suggestions.

REFERENCES

[1] P. Pharpatara, B. Hérisse, and Y. Bestaoui, “3-D trajectory planning of aerial vehicles using RRT*,” *IEEE Trans. Control Syst. Technol.*, vol. 25, no. 3, pp. 1116–1123, May 2017.

[2] K. Kant and S. W. Zucker, “Toward efficient trajectory planning: The path-velocity decomposition,” *Int. J. Robot. Res.*, vol. 5, no. 3, pp. 72–89, Sep. 1986.

[3] L. Consolini, M. Locatelli, A. Minari, and A. Piazzini, “An optimal complexity algorithm for minimum-time velocity planning,” *Syst. Control Lett.*, vol. 103, pp. 50–57, May 2017.

[4] F. Cabassi, L. Consolini, and M. Locatelli, “Time-optimal velocity planning by a bound-tightening technique,” *Comput. Optim. Appl.*, vol. 70, no. 1, pp. 61–90, May 2018.

[5] F. Pfeiffer and R. Johanni, “A concept for manipulator trajectory planning,” *IEEE J. Robot. Autom.*, vol. RA-3, no. 2, pp. 115–123, Apr. 1987.

[6] D. Verscheure, B. Demeulenaere, J. Swevers, J. De Schutter, and M. Diehl, “Time-optimal path tracking for robots: A convex optimization approach,” *IEEE Trans. Autom. Control*, vol. 54, no. 10, pp. 2318–2327, Oct. 2009.

[7] M. Yuan, Z. Chen, B. Yao, and X. Zhu, “Time optimal contouring control of industrial biaxial gantry: A highly efficient analytical solution of trajectory planning,” *IEEE/ASME Trans. Mechatronics*, vol. 22, no. 1, pp. 247–257, Feb. 2017.

[8] E. Velenis and P. Tsotras, “Minimum-time travel for a vehicle with acceleration limits: Theoretical analysis and receding-horizon implementation,” *J. Optim. Theory Appl.*, vol. 138, no. 2, pp. 275–296, 2008.

[9] M. Frego, E. Bertolazzi, F. Biral, D. Fontanelli, and L. Palopoli, “Semi-analytical minimum time solutions with velocity constraints for trajectory following of vehicles,” *Automatica*, vol. 86, pp. 18–28, Dec. 2017.

[10] K. Hauser, “Fast interpolation and time-optimization with contact,” *Int. J. Robot. Res.*, vol. 33, no. 9, pp. 1231–1250, 2014.

[11] H. Pham and Q.-C. Pham, “A new approach to time-optimal path parameterization based on reachability analysis,” *IEEE Trans. Robot.*, vol. 34, no. 3, pp. 645–659, Jun. 2018.

[12] L. Consolini, M. Locatelli, A. Minari, A. Nagy, and I. Vajk, “Optimal time-complexity speed planning for robot manipulators,” *IEEE Trans. Robot.*, vol. 35, no. 3, pp. 790–797, Jun. 2019.

[13] T. Lipp and S. Boyd, “Minimum-time speed optimisation over a fixed path,” *Int. J. Control*, vol. 87, no. 6, pp. 1297–1311, 2014.

[14] F. Debrouwere *et al.*, “Time-optimal path following for robots with convex-concave constraints using sequential convex programming,” *IEEE Trans. Robot.*, vol. 29, no. 6, pp. 1485–1495, Dec. 2013.

[15] A. K. Singh and K. M. Krishna, “A class of non-linear time scaling functions for smooth time optimal control along specified paths,” in *Proc. IEEE/RSJ Int. Conf. Intell. Robots Syst. (IROS)*, Sep. 2015, pp. 5809–5816.

[16] A. Palleschi, M. Garabini, D. Caporale, and L. Pallottino, “Time-optimal path tracking for jerk controlled robots,” *IEEE Robot. Autom. Lett.*, vol. 4, no. 4, pp. 3932–3939, Oct. 2019.

[17] S. Macfarlane and E. A. Croft, “Jerk-bounded manipulator trajectory planning: Design for real-time applications,” *IEEE Trans. Robotics Autom.*, vol. 19, no. 1, pp. 42–52, Feb. 2003.

[18] R. Haschke, E. Weitnauer, and H. Ritter, “On-line planning of time-optimal, jerk-limited trajectories,” in *Proc. IEEE/RSJ Int. Conf. Intell. Robots Syst.*, Sep. 2008, pp. 3248–3253.

[19] H. Pham and Q.-C. Pham, “On the structure of the time-optimal path parameterization problem with third-order constraints,” in *Proc. IEEE Int. Conf. Robot. Automat. (ICRA)*, May 2017, pp. 679–686.

[20] J. E. Bobrow, S. Dubowsky, and J. S. Gibson, “Time-optimal control of robotic manipulators along specified paths,” *Int. J. Robot. Res.*, vol. 4, no. 3, pp. 3–17, Sep. 1985.

[21] K. G. Shin and N. D. McKay, “Minimum-time control of robotic manipulators with geometric path constraints,” *IEEE Trans. Autom. Control*, vol. AC-30, no. 6, pp. 531–541, Jun. 1985.

- 1520 [22] J. Villagra, V. Milanés, J. Pérez, and J. Godoy, "Smooth path and speed
1521 planning for an automated public transport vehicle," *Robot. Auton. Syst.*,
1522 vol. 60, no. 2, pp. 252–265, 2012.
- 1523 [23] M. Raineri and C. G. L. Bianco, "Jerk limited planner for real-time
1524 applications requiring variable velocity bounds," in *Proc. IEEE Int. Conf.*
1525 *Automat. Sci. Eng. (CASE)*, Aug. 2019, pp. 1611–1617.
- 1526 [24] J. Dong, P. M. Ferreira, and J. A. Stori, "Feed-rate optimization with
1527 jerk constraints for generating minimum-time trajectories," *Int. J. Mach.*
1528 *Tools Manuf.*, vol. 47, nos. 12–13, pp. 1941–1955, Oct. 2007.
- 1529 [25] K. Zhang, X. S. Gao, H. B. Li, and C. M. Yuan, "A greedy algorithm for
1530 feedrate planning of CNC machines along curved tool paths with con-
1531 fined jerk," *Robot. Comput.-Integr. Manuf.*, vol. 28, no. 4, pp. 472–483,
1532 Aug. 2012.
- 1533 [26] Y. Zhang *et al.*, "Speed planning for autonomous driving via convex
1534 optimization," in *Proc. 21st Int. Conf. Intell. Transp. Syst. (ITSC)*,
1535 Nov. 2018, pp. 1089–1094.
- 1536 [27] R. Fletcher, *Practical Methods of Optimization*, 2nd ed. Singapore:
1537 Wiley, 2000.
- 1538 [28] L. Consolini, M. Laurini, and M. Locatelli, "Graph-based algorithms for
1539 the efficient solution of optimization problems involving monotone func-
1540 tions," *Comput. Optim. Appl.*, vol. 73, no. 1, pp. 101–128, May 2019.
- 1541 [29] N. J. Higham, *Accuracy and Stability of Numerical Algorithms*, vol. 80.
1542 Philadelphia, PA, USA: SIAM, 2002.
- 1543 [30] L. Consolini, M. Locatelli, and A. Minari, "A sequential approach
1544 for speed planning under jerk constraints," 2021, *arXiv:2105.15095*.
1545 [Online]. Available: <http://arxiv.org/abs/2105.15095>
- 1546 [31] S. Boyd and L. Vandenberghe, *Convex Optimization*. Cambridge, U.K.:
1547 Cambridge Univ. Press, 2004.
- 1548 [32] Gurobi Optimization Inc. (2016). *Gurobi Optimizer Reference Manual*.
1549 [Online]. Available: <http://www.gurobi.com>
- 1550 [33] A. Wächter and L. T. Biegler, "On the implementation of an interior-
1551 point filter line-search algorithm for large-scale nonlinear programming,"
1552 *Math. Program.*, vol. 106, no. 1, pp. 25–57, May 2006.
- 1553 [34] L. L. Hoberock, "A survey of longitudinal acceleration comfort studies
1554 in ground transportation vehicles," *J. Dyn. Syst., Meas., Control*, vol. 99,
1555 no. 2, pp. 76–84, Jun. 1977.
- 1556 [35] T. Fraichard and A. Scheuer, "From Reeds and Shepp's to continuous-
1557 curvature paths," *IEEE Trans. Robot.*, vol. 20, no. 6, pp. 1025–1035,
1558 Dec. 2004.
- 1559 [36] D. Verscheure, M. Diehl, J. De Schutter, and J. Swevers, "Recursive log-
1560 barrier method for on-line time-optimal robot path tracking," in *Proc.*
1561 *Amer. Control Conf.*, St. Louis, MO, USA, Apr. 2009, pp. 4134–4140.



Luca Consolini (Member, IEEE) received the Laurea degree (*cum laude*) in electronic engineering and the Ph.D. degree from the University of Parma, Parma, Italy, in 2000 and 2005, respectively.

From 2005 to 2009, he held a post-doctoral position at the University of Parma, where he was an Assistant Professor from 2009 to 2014. Since 2014, he has been an Associate Professor with the University of Parma. His main current research interests are nonlinear control, motion planning, and control of mechanical systems.



Marco Locatelli is currently a Full Professor of Operations Research with the University of Parma, Parma, Italy. He published more than 90 articles in international journals and coauthored, with F. Schoen, the book *Global Optimization: Theory, Algorithms, and Applications* [Society for Industrial and Applied Mathematics (SIAM)]. His main research interests are the theoretical, practical, and applicative aspects of optimization.

Dr. Locatelli has been nominated as a EUROPT Fellow in 2018. He is also on the Editorial Board of the journals *Computational Optimization and Applications*, *Journal of Global Optimization*, and *Operations Research Forum*.



Andrea Minari received the B.S. and M.S. degrees (*cum laude*) in computer engineering and the Ph.D. degree from the University of Parma, Parma, Italy, in 2013, 2016, and 2020, respectively. He presented a dissertation about optimization-based algorithms applied to the speed planning problem for mobile robots and industrial manipulators.

AUTHOR QUERIES

AUTHOR PLEASE ANSWER ALL QUERIES

PLEASE NOTE: We cannot accept new source files as corrections for your article. If possible, please annotate the PDF proof we have sent you with your corrections and upload it via the Author Gateway. Alternatively, you may send us your corrections in list format. You may also upload revised graphics via the Author Gateway.

Carefully check the page proofs (and coordinate with all authors); additional changes or updates **WILL NOT** be accepted after the article is published online/print in its final form. Please check author names and affiliations, funding, as well as the overall article for any errors prior to sending in your author proof corrections.

AQ:1 = Please confirm or add details for any funding or financial support for the research of this article.

AQ:2 = Please confirm the postal code for Università di Parma.

AQ:3 = Please specify the section numbers for the phrase “next sections.”

A Sequential Algorithm for Jerk Limited Speed Planning

Luca Consolini¹, Member, IEEE, Marco Locatelli¹, and Andrea Minari¹

Abstract—In this article, we discuss a sequential algorithm for the computation of a minimum-time speed profile over a given path, under velocity, acceleration, and jerk constraints. Such a problem arises in industrial contexts, such as automated warehouses, where LGVs need to perform assigned tasks as fast as possible in order to increase productivity. It can be reformulated as an optimization problem with a convex objective function, linear velocity and acceleration constraints, and non-convex jerk constraints, which, thus, represents the main source of the difficulty. While existing nonlinear programming (NLP) solvers can be employed for the solution of this problem, it turns out that the performance and robustness of such solvers can be enhanced by the sequential line-search algorithm proposed in this article. At each iteration, a feasible direction, with respect to the current feasible solution, is computed, and a step along such direction is taken in order to compute the next iterate. The computation of the feasible direction is based on the solution of a linearized version of the problem, and the solution of the linearized problem, through an approach that strongly exploits its special structure, represents the main contribution of this work. The efficiency of the proposed approach with respect to existing NLP solvers is proven through different computational experiments.

Note to Practitioners—This article was motivated by the needs of LGV manufacturers. In particular, it presents an algorithm for computing the minimum-time speed law for an LGV along a pre-assigned path, respecting assigned velocity, acceleration, and jerk constraints. The solution algorithm should be: 1) *fast*, since speed planning is made continuously throughout the workday, not only when an LGV receives a new task but also during the execution of the task itself, since conditions may change, e.g., if the LGV has to be halted for security reasons and 2) *reliable*, i.e., it should return solutions of high quality, because a better speed profile allows to save time and even small percentage improvements, say a 5% improvement, has a considerable impact on the productivity of the warehouse, and, thus, determines a significant economic gain. The algorithm that we propose meets these two requirements, and we believe that it can be a useful tool for LGV manufacturers and users. It is obvious that the proposed method also applies to the speed planning problem for vehicles other than LGVs, e.g., road vehicles.

Index Terms—Optimization, sequential line-search method, speed planning.

I. INTRODUCTION

AN IMPORTANT problem in motion planning is the computation of the minimum-time motion of a car-like vehicle from a start configuration to a target one while avoiding collisions (obstacle avoidance) and satisfying kinematic, dynamic, and mechanical constraints (for instance, on velocities, accelerations, and maximal steering angle). This problem can be approached in two ways.

- 1) As a minimum-time trajectory planning, where both the path to be followed by the vehicle and the timing law on this path (i.e., the vehicle's velocity) are simultaneously designed. For instance, one could use the RRT* algorithm (see [1]).
- 2) As a (geometric) path planning followed by a minimum-time speed planning on the planned path (see [2]).

In this article, following the second paradigm, we assume that the path that joins the initial and the final configuration is assigned, and we aim at finding the time-optimal speed law that satisfies some kinematic and dynamic constraints. The problem can be reformulated as an optimization problem, and it is quite relevant from the practical point of view. In particular, in automated warehouses, the speed of LGVs needs to be planned under acceleration and jerk constraints. As previously mentioned, the solution algorithm should be both *fast* and *reliable*. In our previous work [3], we proposed an optimal time-complexity algorithm for finding the time-optimal speed law that satisfies constraints on maximum velocity and tangential and normal acceleration. In the subsequent work [4], we included a bound on the derivative of the acceleration with respect to the arc length. In this article, we consider the presence of jerk constraints (constraints on the time derivative of the acceleration). The resulting optimization problem is nonconvex and, for this reason, is significantly more complex than the ones that we discussed in [3] and [4]. The main contribution of this work is the development of a line-search algorithm for this problem based on the sequential solution of convex problems. The proposed algorithm meets both requirements of being fast and reliable. The former is met by heavily exploiting the special structure of the optimization problem, the latter by the theoretical guarantee that the returned solution is a first-order stationary point (in practice, a local minimizer) of the optimization problem.

Manuscript received June 29, 2021; accepted August 24, 2021. This article was recommended for publication by Associate Editor M. Robba and Editor C. Seatzu upon evaluation of the reviewers' comments. This work was supported in part by the Programme "FIL-Quota Incentivante" of the University of Parma and in part by the Fondazione Cariparma. (Corresponding author: Marco Locatelli.)

The authors are with the Dipartimento di Ingegneria e Architettura, Università di Parma, 43121 Parma, Italy (e-mail: luca.consolini@unipr.it; marco.locatelli@unipr.it; andrea.minari2@studenti.unipr.it).

This article has supplementary material provided by the authors and color versions of one or more figures available at <https://doi.org/10.1109/TASE.2021.3111758>.

Digital Object Identifier 10.1109/TASE.2021.3111758

86 A. Problem Statement

87 Here, we introduce the problem at hand more formally.
 88 Let $\boldsymbol{\gamma}: [0, s_f] \rightarrow \mathbb{R}^2$ be a smooth function. The image set
 89 $\boldsymbol{\gamma}([0, s_f])$ is the path to be followed, $\boldsymbol{\gamma}(0)$ the initial configura-
 90 tion, and $\boldsymbol{\gamma}(s_f)$ the final one. Function $\boldsymbol{\gamma}$ has arc-length para-
 91 meterization, such that $(\forall \lambda \in [0, s_f], \|\boldsymbol{\gamma}'(\lambda)\| = 1)$. In this
 92 way, s_f is the path length. We want to compute the speed-law
 93 that minimizes the overall transfer time (i.e., the time needed to
 94 go from $\boldsymbol{\gamma}(0)$ to $\boldsymbol{\gamma}(s_f)$). To this end, let $\lambda: [0, t_f] \rightarrow [0, s_f]$ be
 95 a differentiable monotone increasing function that represents
 96 the vehicle's arc-length position along the curve as a function
 97 of time, and let $v: [0, s_f] \rightarrow [0, +\infty[$ be such that $(\forall t \in$
 98 $[0, t_f]) \dot{\lambda}(t) = v(\lambda(t))$. In this way, $v(s)$ is the derivative of the
 99 vehicle arc-length position, which corresponds to the norm of
 100 its velocity vector at position s . The position of the vehicle as
 101 a function of time is given by $\mathbf{x}: [0, t_f] \rightarrow \mathbb{R}^2$, $\mathbf{x}(t) = \boldsymbol{\gamma}(\lambda(t))$.
 102 The velocity and acceleration are given, respectively, by

$$\dot{\mathbf{x}}(t) = \boldsymbol{\gamma}'(\lambda(t))v(\lambda(t))$$

$$\ddot{\mathbf{x}}(t) = a_T(t)\boldsymbol{\gamma}'(\lambda(t)) + a_N(t)\boldsymbol{\gamma}'^\perp(\lambda(t))$$

105 where $a_T(t) = v'(\lambda(t))v(\lambda(t))$ and $a_N(t) = k(\lambda(t))v(\lambda(t))^2$
 106 are, respectively, the tangential and normal components of the
 107 acceleration (i.e., the projections of the acceleration vector
 108 $\ddot{\mathbf{x}}$ on the tangent and the normal to the curve). Moreover
 109 $\boldsymbol{\gamma}'^\perp(\lambda)$ is the normal to vector $\boldsymbol{\gamma}'(\lambda)$ and the tangent of $\boldsymbol{\gamma}'$
 110 at λ . Here, $k: [0, s_f] \rightarrow \mathbb{R}$ is the scalar curvature, defined as
 111 $k(s) = \langle \boldsymbol{\gamma}''(s), \boldsymbol{\gamma}'(s)^\perp \rangle$. Note that $|k(s)| = \|\boldsymbol{\gamma}''(s)\|$. In the
 112 following, we assume that $k(s) \in C^1([0, s_f], \mathbb{R})$. The total
 113 maneuver time, for a given velocity profile $v \in C^1([0, s_f], \mathbb{R})$,
 114 is returned by the functional

$$\mathcal{F}: C^1([0, s_f], \mathbb{R}) \rightarrow \mathbb{R}, \quad \mathcal{F}(v) = \int_0^{s_f} v^{-1}(s) ds. \quad (1)$$

116 In our previous work [3], we considered the problem

$$\min_{v \in \mathcal{V}} \mathcal{F}(v) \quad (2)$$

118 where the feasible region $\mathcal{V} \subset C^1([0, s_f], \mathbb{R})$ is defined by the
 119 following set of constraints:

$$v(0) = 0, \quad v(s_f) = 0 \quad (3a)$$

$$0 \leq v(s) \leq v_{\max}, \quad s \in [0, s_f] \quad (3b)$$

$$|v'(s)v(s)| \leq A, \quad s \in [0, s_f] \quad (3c)$$

$$|k(s)|v(s)^2 \leq A_N, \quad s \in [0, s_f] \quad (3d)$$

124 where v_{\max} , A , and A_N are upper bounds for the velocity, the
 125 tangential acceleration, and the normal acceleration, respec-
 126 tively. Constraints (3a) are the initial and final interpolation
 127 conditions, while constraints (3b)–(3d) limit velocity and the
 128 tangential and normal components of acceleration. In [3],
 129 we presented an algorithm, with linear-time computational
 130 complexity with respect to the number of variables, which
 131 provides an optimal solution of (2) after spatial discretiza-
 132 tion. One limitation of this algorithm is that the obtained
 133 velocity profile is Lipschitz¹ but not differentiable so that
 134 the vehicle's acceleration is discontinuous. With the aim

¹A function $f: \mathbb{R} \rightarrow \mathbb{R}$ is *Lipschitz* if there exists a real positive constant L such that $(\forall x, y \in \mathbb{R}) |f(x) - f(y)| \leq L|x - y|$.

of obtaining a smoother velocity profile, in the subsequent
 work [4], we required that the velocity be differentiable, and
 we imposed a Lipschitz condition (with constant J) on its
 derivative. In this way, after setting $w = v^2$, the feasible region
 of the problem $\mathcal{W} \subset C^1([0, s_f], \mathbb{R})$ is defined by the set of
 functions $w \in C^1([0, s_f], \mathbb{R})$ that satisfy the following set of
 constraints:

$$w(0) = 0, \quad w(s_f) = 0 \quad (4a)$$

$$0 \leq w(s) \leq v_{\max}^2, \quad s \in [0, s_f] \quad (4b)$$

$$\frac{1}{2}|w'(s)| \leq A, \quad s \in [0, s_f] \quad (4c)$$

$$|k(s)|w(s) \leq A_N, \quad s \in [0, s_f] \quad (4d)$$

$$|w'(s_1) - w'(s_2)| \leq J|s_1 - s_2|, \quad s_1, s_2 \in [0, s_f]. \quad (4e)$$

Then, we end up with the problem

$$\min_{w \in \mathcal{W}} G(w) \quad (5)$$

where the objective function is

$$G: C^1([0, s_f], \mathbb{R}) \rightarrow \mathbb{R}, \quad G(w) = \int_0^{s_f} w^{-1/2}(s) ds. \quad (6)$$

The objective function (6) and constraints (4a)–(4d) cor-
 respond to the ones in problem (2) after the substitution
 $w = v^2$. Note that this change of variable is well known in
 the literature. It has been first proposed in [5], while, in [6],
 it is observed that Problem (2) becomes convex after this
 change of variable. The added set of constraints (4e) is a
 Lipschitz condition on the derivative of the squared velocity w .
 It is used to enforce a smoother velocity profile by bounding
 the second derivative of the squared velocity with respect
 to arc length. Note that constraints (4) are linear, and the
 objective function (6) is convex. In [4], we proposed an
 algorithm for solving a finite-dimensional approximation of
 Problem (4). The algorithm exploited the particular structure
 of the resulting convex finite-dimensional problem. This article
 extends the results of [4]. It considers a nonconvex varia-
 tion of Problem (4), in which constraint (4e) is substituted
 with a constraint on the time derivative of the acceleration
 $|\dot{a}(t)| \leq J$, where $a(t) = (d/dt)v(\lambda(t)) = v'(\lambda(t))v(\lambda(t)) =$
 $(1/2)w'(\lambda(t))$. Then, we set

$$j_L(t) = \dot{a}(t) = \frac{1}{2}w''(s(t))\sqrt{w(s(t))}. \quad (7)$$

This quantity is commonly called ‘‘jerk.’’ Bounding the
 absolute value of jerk allows to avoid sudden changes of
 acceleration and obtain a smoother motion. Then, we end up
 with the following minimum-time problem.

Problem 1 (Smooth Minimum-Time Velocity Planning Problem: Continuous Version):

$$\min_{w \in C^2} \int_0^{s_f} w(s)^{-1/2} ds$$

$$w(0) = 0, \quad w(s_f) = 0$$

$$0 \leq w(s) \leq \mu^+(s), \quad s \in [0, s_f]$$

$$\frac{1}{2}|w'(s)| \leq A, \quad s \in [0, s_f] \quad (7)$$

$$\frac{1}{2}|w''(s)\sqrt{w(s)}| \leq J \quad s \in [0, s_f] \quad (8)$$

where μ^+ is the square velocity upper bound depending on the shape of the path, i.e.,

$$\mu^+(s) = \min \left\{ v_{\max}^2, \frac{A_N}{|k(s)|} \right\}$$

where v_{\max} , A_N , and k are the maximum vehicle velocity, the maximum normal acceleration, and the path curvature, respectively. Parameters A and J are the bounds representing the limitations on the (tangential) acceleration and the jerk, respectively. For the sake of simplicity, we consider constraints (7) and (8) symmetric and constant. However, the following development could be easily extended to the non-symmetric and nonconstant case. Note that the jerk constraint (8) is nonconvex. The continuous problem is discretized as follows. We subdivide the path into $n - 1$ intervals of equal length, i.e., we evaluate function w at points $s_i = ((i - 1)s_f)/(n - 1)$, $i = 1, \dots, n$, so that we have the following n -dimensional vector of variables:

$$\mathbf{w} = (w_1, w_2, \dots, w_n) = (w(s_1), w(s_2), \dots, w(s_n)).$$

Then, the finite dimensional version of the problem is given as follows.

Problem 2 (Smooth Minimum-Time Velocity Planning Problem: Discretized Version):

$$\min_{\mathbf{w} \in \mathbb{R}^n} \sum_{i=1}^{n-1} \frac{2h}{\sqrt{w_{i+1}} + \sqrt{w_i}} \quad (9)$$

$$0 \leq \mathbf{w} \leq \mathbf{u} \quad (10)$$

$$w_{i+1} - w_i \leq 2hA, \quad i = 1, \dots, n-1 \quad (11)$$

$$w_i - w_{i+1} \leq 2hA, \quad i = 1, \dots, n-1 \quad (12)$$

$$(w_{i-1} - 2w_i + w_{i+1}) \sqrt{\frac{\ell_i(\mathbf{w})}{4}} \leq 2h^2 J$$

$$i = 2, \dots, n-1 \quad (13)$$

$$-(w_{i-1} - 2w_i + w_{i+1}) \sqrt{\frac{\ell_i(\mathbf{w})}{4}} \leq 2h^2 J$$

$$i = 2, \dots, n-1 \quad (14)$$

where

$$\ell_i(\mathbf{w}) = w_{i+1} + w_{i-1} + 2w_i \quad (15)$$

while $u_i = \mu^+(s_i)$, for $i = 1, \dots, n$, and, in particular, $u_1 = 0$ and $u_n = 0$ since we are assuming that the initial and final velocities are equal to 0. The objective function (9) is an approximation of (6) given by the Riemann sum of the intervals obtained by dividing each interval $[s_i, s_{i+1}]$, for $i = 1, \dots, n-1$, in two subintervals of the same size. Constraints (11) and (12) are obtained by a finite difference approximation of w' . Constraints (13) and (14) are obtained by using a second-order central finite difference to approximate w'' , while w is approximated by a weighted arithmetic mean of three consecutive samples. Due to jerk constraints (13) and (14), Problem 2 is nonconvex and cannot be solved with the algorithm presented in [4].

B. Main Result

The main contribution of this article is the development of a new solution algorithm for finding a local minimum of the

nonconvex Problem 2. As detailed in next sections, we propose to solve Problem 2 by a line-search algorithm based on the sequential solution of convex problems. The algorithm is an iterative one where the following operations are performed at each iteration.

1) *Constraint Linearization:* We first define a convex problem by linearizing constraints (13) and (14) through a first-order Taylor approximation around the current point $\mathbf{w}^{(k)}$. Different from other sequential algorithms for nonlinear programming (NLP) problems, we keep the original convex objective function. The linearized problem is introduced in Section II.

2) *Computation of a Feasible Descent Direction:* The convex problem (actually, a relaxation of such problem) is solved in order to compute a feasible descent direction $\delta \mathbf{w}^{(k)}$. The main contribution of this article lies in this part. The computation requires the minimization of a suitably defined objective function through a further iterative algorithm. At each iteration of this algorithm, the following operations are performed:

C. Objective Function Evaluation

Such evaluation requires the solution of a problem with the same objective function but subject to a subset of the constraints. The special structure of the resulting subproblem is heavily exploited in order to solve it efficiently. This is the topic of Section III.

D. Computation of a Descent Step

Some Lagrange multipliers of the subproblem define a subgradient for the objective function. This can be employed to define a linear programming (LP) problem that returns a descent step for the objective function. This is the topic of Section IV.

Line Search: Finally, a standard line search along the half-line $\mathbf{w}^{(k)} + \alpha \delta \mathbf{w}^{(k)}$, $\alpha \geq 0$, is performed.

Sections II–IV detail all what we discussed above. Next, in Section V, we present different computational experiments.

E. Comparison With Existing Literature

Although many works consider the problem of minimum-time speed planning with acceleration constraints (see [7]–[9]), relatively few consider jerk constraints. Perhaps, this is also due to the fact that the jerk constraint is nonconvex so that its presence significantly increases the complexity of the optimization task. One can use a general-purpose NLP solver (such as SNOPT or IPOPT) for finding a local solution of Problem 2, but the required time is, in general, too large for the speed planning application. As outlined in Section I-D, in this work, we tackle this problem through an approach based on the solution of a sequence of convex subproblems. There are different approaches in the literature based on the sequential solution of convex subproblems. In [10], it is first observed that the problem with acceleration constraints but no jerk constraints for robotic manipulators can be reformulated as a convex one with linear constraints, and it is solved by a sequence of LP problems obtained by linearizing the

282 objective function at the current point, i.e., the objective
 283 function is replaced by its supporting hyperplane at the
 284 current point, and by introducing a trust region centered at the
 285 current point. In [11] and [12], it is further observed that this
 286 problem can be solved very efficiently through the solution
 287 of a sequence of 2-D LP problems. In [13], an interior point
 288 barrier method is used to solve the same problem based on
 289 Newton's method. Each Newton step requires the solution of
 290 a KKT system, and an efficient way to solve such systems
 291 is proposed in that work. Moving to approaches also dealing
 292 with jerk constraints, we mention [14]. In this work, it is
 293 observed that jerk constraints are nonconvex but can be
 294 written as the difference between two convex functions.
 295 Based on this observation, the authors solve the problem by
 296 a sequence of convex subproblems obtained by linearizing
 297 at the current point the concave part of the jerk constraints
 298 and by adding a proximal term in the objective function that
 299 plays the same role as a trust region, preventing from taking
 300 too large steps. In [15] a slightly different objective function
 301 is considered. Rather than minimizing the traveling time
 302 along the given path, the integral of the squared difference
 303 between the maximum velocity profile and the computed
 304 velocity profile is minimized. After representing time-varying
 305 control inputs as products of parametric exponential and
 306 polynomial functions, the authors reformulate the problem in
 307 such a way that its objective function is convex quadratic,
 308 while nonconvexity lies in difference-of-convex functions.
 309 The resulting problem is tackled through the solution of a
 310 sequence of convex subproblems obtained by linearizing
 311 the concave part of the nonconvex constraints. In [16], the
 312 problem of speed planning for robotic manipulators with jerk
 313 constraints is reformulated in such a way that nonconvexity
 314 lies in simple bilinear terms. Such bilinear terms are replaced
 315 by the corresponding convex and concave envelopes, obtaining
 316 the so-called McCormick relaxation, which is the tightest
 317 possible convex relaxation of the nonconvex problem. Other
 318 approaches dealing with jerk constraints do not rely on
 319 the solution of convex subproblems. For instance, in [17],
 320 a concatenation of fifth-order polynomials is employed to
 321 provide smooth trajectories, which results in quadratic jerk
 322 profiles, while, in [18], cubic polynomials are employed,
 323 resulting in piecewise constant jerk profiles. The decision
 324 process involves the choice of the phase durations, i.e.,
 325 of the intervals over which a given polynomial applies. A
 326 very recent and interesting approach to the problem with
 327 jerk constraints is [19]. In this work, an approach based
 328 on numerical integration is discussed. Numerical integration
 329 has been first applied under acceleration constraints in [20]
 330 and [21]. In [19], jerk constraints are taken into account. The
 331 algorithm detects a position s along the trajectory where the
 332 jerk constraint is singular, that is, the jerk term disappears
 333 from one of the constraints. Then, it computes the speed
 334 profile up to s by computing two maximum jerk profiles and
 335 then connecting them by a minimum jerk profile, found by a
 336 shooting method. In general, the overall solution is composed
 337 of a sequence of various maximum and minimum jerk
 338 profiles. This approach does not guarantee reaching a local
 339 minimum of the traversal time. Moreover, since Problem 4

340 has velocity and acceleration constraints, the jerk constraint
 341 is singular for all values of s so that the algorithm presented
 342 in [19] cannot be directly applied to Problem 4.

343 Some algorithms use heuristics to quickly find sub-
 344 optimal solutions of acceptable quality. For instance,
 345 Villagra *et al.* [22] propose an algorithm that applies to curves
 346 composed of clothoids, circles, and straight lines. The algo-
 347 rithm does not guarantee the local optimality of the solution.
 348 Raineri and Guarino Lo Bianco [23] present an efficient
 349 heuristic algorithm. Also, this method does not guarantee
 350 global nor local optimality. Various works in the literature
 351 consider jerk bounds in the speed optimization problem for
 352 robotic manipulators instead of mobile vehicles. This is a
 353 slightly different problem but mathematically equivalent to
 354 Problem (1). In particular, paper [24] presents a method based
 355 on the solution of a large number of nonlinear and nonconvex
 356 subproblems. The resulting algorithm is slow due to a large
 357 number of subproblems; moreover, the authors do not prove its
 358 convergence. Zhang *et al.* [25] propose a similar method that
 359 gives a continuous-time solution. Again, the method is com-
 360 putationally slow since it is based on the numerical solution of
 361 a large number of differential equations; moreover, this article
 362 does not contain proof of convergence or local optimality.
 363 Some other works replace the jerk constraint with *pseudo-*
 364 *jerk*, that is, the derivative of the acceleration with respect
 365 to arc length, obtaining a constraint analogous to (4e) and
 366 ending up with a convex optimization problem. For instance,
 367 Zhang *et al.* [26] add to the objective function a pseudo-jerk
 368 penalizing term. This approach is computationally convenient,
 369 but substituting (8) with (4e) may be overly restrictive at low
 370 speeds.

371 F. Statement of Contribution

372 The method presented in this article is a sequential convex
 373 one that aims at finding a local optimizer of Problem 2.
 374 To be more precise, as usual with nonconvex problems, only
 375 convergence to a stationary point can usually be proved.
 376 However, the fact that the sequence of generated feasible
 377 points is decreasing with respect to the objective function
 378 values usually guarantees that the stationary point is a local
 379 minimizer, except in rather pathological cases (see [27, p. 19]).
 380 Moreover, in our experiments, even after running a local solver
 381 from different starting points, we have never been able to
 382 detect local minimizers better than the one returned by the
 383 method we propose. Thus, a possible, nontrivial, topic for
 384 future research could be that of proving the global optimality
 385 of the solution. To the best of our knowledge and as detailed
 386 in the following, this algorithm is more efficient than the ones
 387 existing in the literature since it leverages the special struc-
 388 ture of the subproblems obtained as local approximations of
 389 Problem 2. We discussed this class of problems in our previous
 390 work [28]. This structure allows computing very efficiently a
 391 feasible descent direction for the main line-search algorithm;
 392 it is one of the key elements that allow us to outperform
 393 generic NLP solvers. In summary, the main contributions of
 394 this work are: 1) on the theoretical side, the development of an
 395 approach for which a rigorous mathematical analysis has been

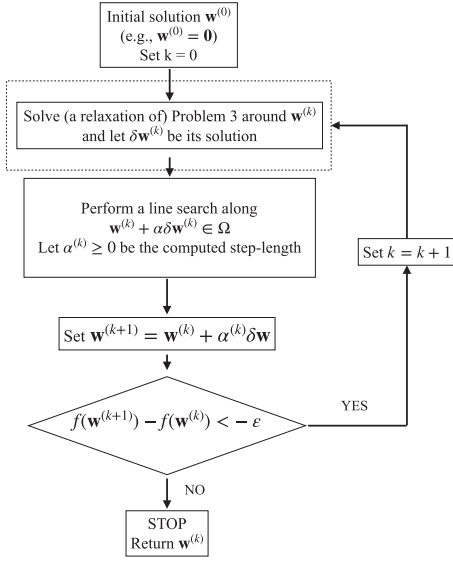


Fig. 1. Flowchart of algorithm SCA. The dashed block corresponds to a call of the procedure `ComputeUpdate`, proposed to solve Problem 3, which represents the main contribution of this article.

performed, proving a convergence result to a stationary point (see Section II) and 2) on the computational side, to exploit heavily the structure of the problem in order to implement the approach in a fairly efficient way (see Sections III and IV) so that its computing times outperform those of nonlinear solvers and are competitive with heuristic approaches that are only able to return suboptimal solutions of lower quality (see Section V).

II. SEQUENTIAL ALGORITHM BASED ON CONSTRAINT LINEARIZATION

To account for the nonconvexity of Problem 2, we propose a line-search method based on the solution of a sequence of special structured convex problems. Throughout this article, we call this algorithm Sequential Convex Algorithm (SCA), and its flowchart is shown in Fig. 1. It belongs to the class of Sequential Convex Programming algorithms, where, at each iteration, a convex subproblem is solved. In what follows, we denote by Ω the feasible region of Problem 2. At each iteration k , we replace the current point $\mathbf{w}^{(k)} \in \Omega$ with a new point $\mathbf{w}^{(k)} + \alpha^{(k)} \delta \mathbf{w}^{(k)} \in \Omega$, where the step size $\alpha^{(k)} \in [0, 1]$ is obtained by a *line search* along the descent direction $\delta \mathbf{w}^{(k)}$, which, in turn, is obtained through the solution of a convex problem. The constraints of the convex problem are linear approximations of (10)–(14) around $\mathbf{w}^{(k)}$, while the objective function is the original one. Then, the problem that we consider to compute the direction $\delta \mathbf{w}^{(k)}$ is given in the following (superscript k of $\mathbf{w}^{(k)}$ is omitted):

Problem 3:

$$\min_{\delta \mathbf{w} \in \mathbb{R}^n} \sum_{i=1}^{n-1} \frac{2h}{\sqrt{w_{i+1} + \delta w_{i+1}} + \sqrt{w_i + \delta w_i}} \quad (16)$$

$$\mathbf{l}_B \leq \delta \mathbf{w} \leq \mathbf{u}_B \quad (17)$$

$$\delta w_{i+1} - \delta w_i \leq b_{A_i}, \quad i = 1, \dots, n-1 \quad (18)$$

$$\delta w_i - \delta w_{i+1} \leq b_{D_i}, \quad i = 1, \dots, n-1 \quad (19)$$

$$\delta w_i - \eta_i \delta w_{i-1} - \eta_i \delta w_{i+1} \leq b_{N_i}, \quad i = 2, \dots, n-1 \quad (20)$$

$$\eta_i \delta w_{i-1} + \eta_i \delta w_{i+1} - \delta w_i \leq b_{P_i}, \quad i = 2, \dots, n-1 \quad (21)$$

where $\mathbf{l}_B = -\mathbf{w}$ and $\mathbf{u}_B = \mathbf{u} - \mathbf{w}$ (recall that \mathbf{u} has been introduced in (10), and its components have been defined immediately in Problem 2), while parameters η , \mathbf{b}_A , \mathbf{b}_D , \mathbf{b}_N , and \mathbf{b}_P depend on the point \mathbf{w} around which the constraints (10)–(14) are linearized. More precisely, we have

$$\begin{aligned} b_{A_i} &= 2hA - w_{i+1} + w_i & (22) \\ b_{D_i} &= 2hA - w_i + w_{i+1} \\ \eta_i &= \frac{3w_{i+1} + 3w_{i-1} + 2w_i}{2(w_{i+1} + w_{i-1} + 6w_i)} \\ b_{P_i} &= \frac{\sqrt{\ell_i(\mathbf{w})} 8h^2 J + (w_{i-1} - 2w_i + w_{i+1}) \sqrt{\ell_i(\mathbf{w})}}{2(w_{i+1} + w_{i-1} + 6w_i)} \\ b_{N_i} &= \frac{\sqrt{\ell_i(\mathbf{w})} 8h^2 J - (w_{i-1} - 2w_i + w_{i+1}) \sqrt{\ell_i(\mathbf{w})}}{2(w_{i+1} + w_{i-1} + 6w_i)} \end{aligned}$$

where ℓ_i is defined in (15). The following proposition is an immediate consequence of the feasibility of \mathbf{w} .

Proposition 1: All parameters η , \mathbf{b}_A , \mathbf{b}_D , \mathbf{b}_N , and \mathbf{b}_P are nonnegative.

The proposed approach follows some standard ideas of sequential quadratic approaches employed in the literature about nonlinearly constrained problems. However, a quite relevant difference is that the true objective function (9) is employed in the problem to compute the direction, rather than a quadratic approximation of such function. This choice comes from the fact that the objective function (9) has some features (in particular, convexity and being decreasing), which, combined with the structure of the linearized constraints, allows for an efficient solution of Problem 3. Problem 3 is a convex problem with a nonempty feasible region ($\delta \mathbf{w} = \mathbf{0}$ is always a feasible solution) and, consequently, can be solved by existing NLP solvers. However, such solvers tend to increase computing times since they need to be called many times within the iterative algorithm SCA. The main contribution of this article lies in the routine `computeUpdate` (see dashed block in Fig. 1), which is able to solve Problem 3 and efficiently returns a descent direction $\delta \mathbf{w}^{(k)}$. To be more precise, we solve a *relaxation* of Problem 3. Such relaxation, as well as the routine to solve it, is detailed in Sections III and IV. In Section III, we present efficient approaches to solve some subproblems, including proper subsets of the constraints. Then, in Section IV, we address the solution of the relaxation of Problem 3.

Remark 1: It is possible to see that, if one of the constraints (13) and (14) is active at $\mathbf{w}^{(k)}$, then, along the direction $\delta \mathbf{w}^{(k)}$ computed through the solution of the linearized Problem 3, it holds that $\mathbf{w}^{(k)} + \alpha \delta \mathbf{w}^{(k)} \in \Omega$ for any sufficiently small $\alpha > 0$. In other words, small perturbations of the current solution $\mathbf{w}^{(k)}$ along direction $\delta \mathbf{w}^{(k)}$ do not lead outside the feasible region Ω . This fact is illustrated in Fig. 2. Let us

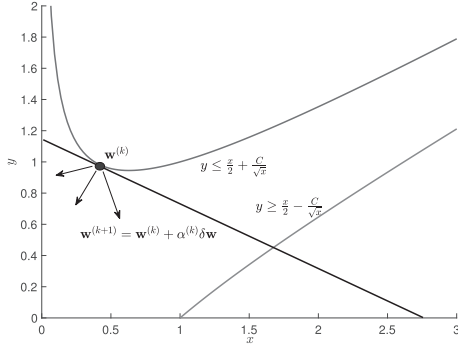


Fig. 2. Constraints (13) and (14) and their linearization ($C = 4h^2J$).

477 rewrite constraints (13) and (14) as follows:

$$478 \quad |(x - 2y)\sqrt{x}| \leq C \quad (23)$$

479 where $x = \ell_i(\mathbf{w})$, $y = 2w_i$, and $C = 4h^2J$ is a constant. The
 480 feasible region associated with constraint (23) is reported in
 481 Fig. 2. In particular, it is the region between the blue and red
 482 curves. Suppose that constraint $y \leq (x/2) + (C/2\sqrt{x})$ is active
 483 at $\mathbf{w}^{(k)}$ (the case when $y \geq (x/2) - (C/2\sqrt{x})$ is active can
 484 be dealt with in a completely analogous way). If we linearize
 485 such constraint around $\mathbf{w}^{(k)}$, then we obtain a linear constraint
 486 (black line in Fig. 2), which defines a region completely
 487 contained into the one defined by the nonlinear constraint
 488 $y \leq (x/2) + (C/2\sqrt{x})$. Hence, for each direction $\delta\mathbf{w}^{(k)}$ feasible
 489 with respect to the linearized constraint, we are always able to
 490 perform sufficiently small steps, without violating the original
 491 nonlinear constraints, i.e., for $\alpha > 0$ small enough, it holds
 492 that $\mathbf{w}^{(k)} + \alpha\delta\mathbf{w}^{(k)} \in \Omega$.

493 Constraints (13) and (14) can also be rewritten as follows:

$$494 \quad w_{i-1} + w_{i+1} - 2w_i - 4h^2J(\ell_i(\mathbf{w}))^{-\frac{1}{2}} \leq 0 \quad (24)$$

$$495 \quad 2w_i - w_{i-1} - w_{i+1} - 4h^2J(\ell_i(\mathbf{w}))^{-\frac{1}{2}} \leq 0. \quad (25)$$

496 Note that the functions on the left-hand side of these
 497 constraints are concave. Now, we can define a variant of
 498 Problem 3 where constraints (20) and (21) are replaced by
 499 the following linearizations of constraints (24) and (25):

$$500 \quad -\beta_i\delta w_{i-1} - \beta_i\delta w_{i+1} + \delta w_i \leq b'_{N_i} \quad (26)$$

$$501 \quad \theta_i\delta w_{i-1} + \theta_i\delta w_{i+1} - \delta w_i \leq b'_{P_i} \quad (27)$$

502 where

$$503 \quad \theta_i = \frac{1 + 2h^2J(\ell_i(\mathbf{w}))^{-\frac{3}{2}}}{2 - 4h^2J(\ell_i(\mathbf{w}))^{-\frac{3}{2}}}$$

$$504 \quad \beta_i = \frac{1 - 2h^2J(\ell_i(\mathbf{w}))^{-\frac{3}{2}}}{2 + 4h^2J(\ell_i(\mathbf{w}))^{-\frac{3}{2}}}$$

$$505 \quad b'_{N_i} = \frac{6h^2J(\ell_i(\mathbf{w}))^{-\frac{1}{2}}}{2 + 4h^2J(\ell_i(\mathbf{w}))^{-\frac{3}{2}}}$$

$$506 \quad b'_{P_i} = \frac{6h^2J(\ell_i(\mathbf{w}))^{-\frac{1}{2}}}{2 - 4h^2J(\ell_i(\mathbf{w}))^{-\frac{3}{2}}}. \quad (28)$$

507 The following proposition states that constraints (26)
 508 and (27) are tighter than constraints (20) and (21).

Proposition 2: For all $i = 2, \dots, n - 1$, it holds that $\beta_i \leq$ 509
 $\eta_i \leq \theta_i$. Equality $\eta_i = \theta_i$ holds if the corresponding nonlinear 510
 constraint (24) is active at the current point \mathbf{w} . Similarly, $\eta_i =$ 511
 β_i holds if the corresponding nonlinear constraint (25) is active 512
 at the current point \mathbf{w} . 513

Proof: We only prove the results about θ_i and η_i . Those 514
 about β_i and η_i are proved in a completely analogous way. 515
 By definition of η_i and θ_i , we need to prove that 516

$$517 \quad \frac{3w_{i+1} + 3w_{i-1} + 2w_i}{w_{i+1} + 6w_i + w_{i-1}} \leq \frac{1 + 2h^2J(\ell_i(\mathbf{w}))^{-\frac{3}{2}}}{2 - 4h^2J(\ell_i(\mathbf{w}))^{-\frac{3}{2}}}.$$

After few simple computations, this inequality can be 518
 rewritten as 519

$$520 \quad 4h^2J(\ell_i(\mathbf{w}))^{-\frac{1}{2}} \geq (w_{i-1} - 2w_i + w_{i+1})$$

521 which holds in view of feasibility of \mathbf{w} and, moreover, holds
 522 as an equality if constraint (24) is active at the current point
 \mathbf{w} , as we wanted to prove. 523

In view of this result, by replacing constraints (20) and (21) 524
 with (26) and (27), we reduce the search space of the new 525
 displacement $\delta\mathbf{w}$. On the other hand, the following proposition 526
 states that, with constraints (26) and (27), no line search is 527
 needed along the direction $\delta\mathbf{w}$, i.e., we can always choose the 528
 step length $\alpha = 1$. 529

Proposition 3: If constraints (26) and (27) are employed as 530
 a replacement of constraints (20) and (21) in the definition of 531
 Problem 3, then, for each feasible solution $\delta\mathbf{w}$ of this problem, 532
 it holds that $\mathbf{w} + \delta\mathbf{w} \in \Omega$. 533

Proof: For the sake of convenience, let us rewrite 534
 Problem 2 in the following more compact form: 535

$$536 \quad \min f(\mathbf{w} + \delta\mathbf{w})$$

$$537 \quad \mathbf{c}(\mathbf{w} + \delta\mathbf{w}) \leq 0 \quad (29)$$

538 where the vector function \mathbf{c} contains all constraints
 539 of Problem 2 and the nonlinear ones are given as
 540 in (24) and (25) (recall that, in that case, vector \mathbf{c} is a vector of
 541 concave functions). Then, Problem 3 can be written as follows:

$$542 \quad \min f(\mathbf{w} + \delta\mathbf{w}) \quad \mathbf{c}(\mathbf{w}) + \nabla\mathbf{c}(\mathbf{w})\delta\mathbf{w} \leq 0. \quad (30)$$

543 Now, it is enough to observe that, by concavity,

$$544 \quad \mathbf{c}(\mathbf{w} + \delta\mathbf{w}) \leq \mathbf{c}(\mathbf{w}) + \nabla\mathbf{c}(\mathbf{w})\delta\mathbf{w}$$

545 so that each feasible solution of (30) is also feasible for (29). 546

547 The above proposition states that the feasible region of
 548 Problem 3, when constraints (26) and (27) are employed
 549 in its definition, is a subset of the feasible region Ω of
 550 the original Problem 2. As a final result of this section,
 551 we state the following theorem, which establishes convergence
 552 of algorithm SCA to a stationary (KKT) point of Problem 2.

Theorem 1: If algorithm SCA is run for an infinite number 553
 of iterations and there exists some positive integer value K 554
 such that for all iterations $k \geq K$, constraints (26) and (27) are 555
 always employed in the definition of Problem 3, and then, the 556
 sequence of points $\{\mathbf{w}^{(k)}\}$ generated by the algorithm converges 557
 to a KKT point of Problem 2. 558

In order to prove the theorem, we first need to prove some lemmas.

Lemma 1: The sequence $\{f(\mathbf{w}^{(k)})\}$ of the function values at points generated by algorithm SCA converges to a finite value.

Proof: The sequence is nonincreasing and bounded from below, e.g., by the value $f(\mathbf{u}_B)$, in view of the fact that the objective function f is monotonic decreasing. Thus, it converges to a finite value. \square

Next, we need the following result based on strict convexity of the objective function f .

Lemma 2: For each $\delta > 0$ sufficiently small, it holds that

$$\min \left\{ \max\{f(\mathbf{x}), f(\mathbf{y})\} - f\left(\frac{\mathbf{x} + \mathbf{y}}{2}\right) : \mathbf{x}, \mathbf{y} \in \Omega, \|\mathbf{x} - \mathbf{y}\| \geq \delta \right\} \geq \varepsilon_\delta > 0. \quad (31)$$

Proof: Due to strict convexity, it holds that, $\forall \mathbf{x} \neq \mathbf{y}$,

$$\max\{f(\mathbf{x}), f(\mathbf{y})\} - f\left(\frac{\mathbf{x} + \mathbf{y}}{2}\right) > 0.$$

Moreover, the function is a continuous one. Next, we observe that the region

$$\{\mathbf{x}, \mathbf{y} \in \Omega : \|\mathbf{x} - \mathbf{y}\| \geq \delta\}$$

is a compact set. Thus, by the Weierstrass theorem, the minimum in (31) is attained, and it must be strictly positive, as we wanted to prove. \square

Finally, we prove that also the sequence of points generated by algorithm SCA converges to some point, feasible for Problem 2.

Lemma 3: It holds that

$$\|\delta \mathbf{w}^{(k)}\| \rightarrow 0.$$

Proof: Let us assume, by contradiction, that, over some infinite subsequence with index set \mathcal{K} , it holds that $\|\delta \mathbf{w}^{(k)}\| \geq 2\rho > 0$ for all $k \in \mathcal{K}$, i.e.,

$$\|\mathbf{w}^{(k+1)} - \mathbf{w}^{(k)}\| \geq 2\rho > 0 \quad (32)$$

where $\mathbf{w}^{(k+1)} = \mathbf{w}^{(k)} + \delta \mathbf{w}^{(k)}$. Over this subsequence, it holds, by strict convexity, that

$$f(\mathbf{w}^{(k+1)}) \leq f(\mathbf{w}^{(k)}) - \zeta \quad \forall k \in \mathcal{K} \quad (33)$$

for some $\zeta > 0$. Indeed, it follows by optimality of $\mathbf{w}^{(k)} + \delta \mathbf{w}^{(k)}$ for Problem 3 and convexity of f that

$$f(\mathbf{w}^{(k+1)}) \leq f\left(\frac{\mathbf{w}^{(k+1)} + \mathbf{w}^{(k)}}{2}\right) \leq f(\mathbf{w}^{(k)})$$

so that

$$\max\{f(\mathbf{w}^{(k)}), f(\mathbf{w}^{(k+1)})\} = f(\mathbf{w}^{(k)}).$$

Then, it follows from (32) and Lemma 2 that we can choose $\zeta = \varepsilon_\rho > 0$. Thus, since (33) holds infinitely often, we should have $f(\mathbf{w}^{(k)}) \rightarrow -\infty$, which, however, is not possible in view of Lemma 1. \square

Now, we are ready to prove Theorem 1.

Proof: As a consequence of Lemma 3, it also holds that

$$\mathbf{w}^{(k)} \rightarrow \bar{\mathbf{w}} \in \Omega. \quad (34)$$

Indeed, all points $\mathbf{w}^{(k)}$ belong to the compact feasible region Ω so that the sequence $\{\mathbf{w}^{(k)}\}$ admits accumulation points. However, due to Lemma 3, the sequence cannot have distinct accumulation points.

Now, let us consider the compact reformulation (29) of Problem 2 and the related linearization (30), equivalent to Problem 3 with the linearized constraints (26) and (27). Since the latter is a convex problem with linear constraints, its local minimizer $\delta \mathbf{w}^{(k)}$ (unique in view of strict convexity of the objective function) fulfills the following KKT conditions:

$$\begin{aligned} \nabla f(\mathbf{w}^{(k)} + \delta \mathbf{w}^{(k)}) + \boldsymbol{\mu}_k^\top \nabla \mathbf{c}(\mathbf{w}^{(k)}) &= \mathbf{0} \\ \mathbf{c}(\mathbf{w}^{(k)}) + \nabla \mathbf{c}(\mathbf{w}^{(k)}) \delta \mathbf{w}^{(k)} &\leq \mathbf{0} \\ \boldsymbol{\mu}_k^\top (\mathbf{c}(\mathbf{w}^{(k)}) + \nabla \mathbf{c}(\mathbf{w}^{(k)}) \delta \mathbf{w}^{(k)}) &= 0 \\ \boldsymbol{\mu}_k &\geq \mathbf{0} \end{aligned} \quad (35)$$

where $\boldsymbol{\mu}_k$ is the vector of Lagrange multipliers. Now, by taking the limit of system (35), possibly over a subsequence, in order to guarantee convergence of the multiplier vectors $\boldsymbol{\mu}_k$ to a vector $\bar{\boldsymbol{\mu}}$, in view of Lemma 3 and (34), we have that

$$\begin{aligned} \nabla f(\bar{\mathbf{w}}) + \bar{\boldsymbol{\mu}}^\top \nabla \mathbf{c}(\bar{\mathbf{w}}) &= \mathbf{0} \\ \mathbf{c}(\bar{\mathbf{w}}) &\leq \mathbf{0} \\ \bar{\boldsymbol{\mu}}^\top \mathbf{c}(\bar{\mathbf{w}}) &= 0 \\ \bar{\boldsymbol{\mu}} &\geq \mathbf{0} \end{aligned}$$

or, equivalently, the limit point $\bar{\mathbf{w}}$ is a KKT point of Problem 2, as we wanted to prove. \square

Remark 2: In algorithm SCA at each iteration, we solve to optimality Problem 3. This is indeed necessary for the final iterations to prove the convergence result stated in Theorem 1. However, during the first iterations, it is not necessary to solve the problem to optimality: finding a feasible descent direction is enough. This does not alter the theoretical properties of the algorithm and allows to reduce the computing times.

In the rest of this article, we refer to constraints (18) and (19) as acceleration constraints, while constraints (20) and (21) [or (26) and (27)] are called (linearized) negative acceleration rate (NAR) and positive acceleration rate (PAR) constraints, respectively. Also, note that, in the different subproblems discussed in the following, we always refer to the linearization with constraints (20) and (21) and, thus, with parameters η_i , but the same results also hold for the linearization with constraints (26) and (27) and, thus, with parameters θ_i and β_i .

III. SUBPROBLEM WITH ACCELERATION AND NAR CONSTRAINTS

In this section, we propose an efficient method to solve Problem 3 when PAR constraints are removed. The solution of this subproblem becomes part of an approach to solve a suitable relaxation of Problem 3 and, in fact, under very mild assumptions, to solve Problem 3 itself. This is clarified in Section IV. We discuss: 1) the subproblem including only (17) and the acceleration constraints (18) and (19); 2) the subproblem including only (17) and the NAR constraints (20);

and 2) the subproblem including all constraints (17)–(20). Throughout the section, we need the results stated in the following two propositions. Let us consider problems with the following form, where $N = \{1, \dots, n\}$ and $M_j = \{1, \dots, m_j\}$, $j \in N$:

$$\begin{aligned} \min \quad & g(x_1, \dots, x_n) \\ & x_j \leq a_{i,j}x_{j-1} + b_{i,j}x_{j+1} + c_{i,j}, \quad i \in M_j, \quad j \in N \\ & \ell_j \leq x_j \leq u_j, \quad j \in N \end{aligned} \quad (36)$$

where g is a monotonic decreasing function; $a_{i,j}, b_{i,j}, c_{i,j} \geq 0$, for $i \in M_j$ and $j \in N$; $a_{i,1} = 0$ for $i \in M_1$; and $b_{i,n} = 0$ for $i \in M_n$. The following result is proven in [28]. Here, we report the proof in order to make this article self-contained. We denote by P the feasible polytope of problem (36). Moreover, we denote by \mathbf{z} the componentwise maximum of all feasible solutions in P , i.e., for each $j \in N$, $z_j = \max_{\mathbf{x} \in P} x_j$ (note that the above maximum value is attained since P is a polytope).

Proposition 4: The unique optimal solution of (36) is the componentwise maximum \mathbf{z} of all its feasible solutions.

Proof: If we are able to prove that the componentwise maximum \mathbf{z} of all feasible solutions is itself a feasible solution, by monotonicity of g , it must also be the unique optimal solution. In order to prove that \mathbf{z} is feasible, we proceed as follows. For $j \in N$, let \mathbf{x}^{*j} be the optimal solution of $\max_{\mathbf{x} \in P} x_j$ so that $z_j = x_j^{*j}$. Since $\mathbf{x}^{*j} \in P$, then it must hold that $\ell_j \leq z_j \leq u_j$. Moreover, let us consider the generic constraint

$$x_j \leq a_{i,j}x_{j-1} + b_{i,j}x_{j+1} + c_{i,j}$$

for $i \in M_j$. It holds that

$$\begin{aligned} z_j = x_j^{*j} &\leq a_{i,j}x_{j-1}^{*j} + b_{i,j}x_{j+1}^{*j} + c_{i,j} \\ &\leq a_{i,j}z_{j-1} + b_{i,j}z_{j+1} + c_{i,j} \end{aligned}$$

where the first inequality follows from feasibility of \mathbf{x}^{*j} , while the second follows from nonnegativity of a_{ij} and b_{ij} and the definition of \mathbf{z} . Since this holds for all $j \in N$, the result is proven. \square

Now, consider the problem obtained from (36) by removing some constraints, i.e., by taking $M'_j \subseteq M_j$ for each $j \in N$

$$\begin{aligned} \min \quad & g(x_1, \dots, x_n) \\ & x_j \leq a_{i,j}x_{j-1} + b_{i,j}x_{j+1} + c_{i,j}, \quad i \in M'_j, \quad j \in N \\ & \ell_j \leq x_j \leq u_j, \quad j \in N. \end{aligned} \quad (37)$$

Later, we also need the result stated in the following proposition.

Proposition 5: The optimal solution $\bar{\mathbf{x}}^*$ of problem (37) is an upper bound for the optimal solution \mathbf{x}^* of problem (36), i.e., $\bar{\mathbf{x}}^* \geq \mathbf{x}^*$.

Proof: It holds that \mathbf{x}^* is a feasible solution of problem (37) so that, in view of Proposition 4, $\bar{\mathbf{x}}^* \geq \mathbf{x}^*$ holds. \square

A. Acceleration Constraints

The simplest case is the one where we only consider the acceleration constraints (18) and (19), besides constraints (17)

with a generic upper bound vector $\mathbf{y} \geq \mathbf{0}$. The problem to be solved is

Problem 4:

$$\begin{aligned} \min_{\delta \mathbf{w} \in \mathbb{R}^n} \quad & \sum_{i=1}^{n-1} \frac{2h}{\sqrt{w_{i+1} + \delta w_{i+1}} + \sqrt{w_i + \delta w_i}} \\ & \mathbf{l}_B \leq \delta \mathbf{w} \leq \mathbf{y} \\ & \delta w_{i+1} - \delta w_i \leq b_{A_i}, \quad i = 1, \dots, n-1 \\ & \delta w_i - \delta w_{i+1} \leq b_{D_i}, \quad i = 1, \dots, n-1. \end{aligned}$$

It can be seen that such a problem belongs to the class of problems (36). Therefore, in view of Proposition 4, the optimal solution of Problem 4 is the componentwise maximum of its feasible region. Moreover, in [3], it has been proven that Algorithm 1, based on a forward and a backward iteration and with $O(n)$ computational complexity, returns an optimal solution of Problem 4.

Algorithm 1 Routine SOLVEACC for the Solution of the Problem With Acceleration Constraints

input : Upper bound \mathbf{y}
output: $\delta \mathbf{w}$
1 $\delta w_1 = 0, \delta w_n = 0$;
2 **for** $i = 1$ **to** $n - 1$ **do**
3 $\lfloor \delta w_{i+1} = \min\{\delta w_i + b_{A_i}, y_{i+1}\}$
4 **for** $i = n - 1$ **to** 1 **do**
5 $\lfloor \delta w_i = \min\{\delta w_{i+1} + b_{A_i}, y_i\}$
6 **return** $\delta \mathbf{w}$

B. NAR Constraints

Now, we consider the problem only including NAR constraints (20) and constraints (17) with upper bound vector \mathbf{y}

Problem 5:

$$\begin{aligned} \min_{\delta \mathbf{w} \in \mathbb{R}^n} \quad & \sum_{i=1}^{n-1} \frac{2h}{\sqrt{w_{i+1} + \delta w_{i+1}} + \sqrt{w_i + \delta w_i}} \\ & \mathbf{0} \leq \delta \mathbf{w} \leq \mathbf{y} \\ & \delta w_i \leq \eta_i(\delta w_{i-1} + \delta w_{i+1}) + b_{N_i}, \quad i = 2, \dots, n-1 \end{aligned} \quad (38)$$

$$(39)$$

where $y_1 = y_n = 0$ because of the boundary conditions. Also, this problem belongs to the class of problems (36) so that Proposition 4 states that its optimal solution is the componentwise maximum of its feasible region. Problem 5 can be solved by using the graph-based approach presented in [4] and [28]. However, Cabassi *et al.* [4] show that, by exploiting the structure of a simpler version of the NAR constraints, it is possible to develop an algorithm more efficient than the graph-based one. Our purpose is to extend the results presented in [4] to a case with different and more challenging NAR constraints in order to develop an efficient algorithm outperforming the graph-based one.

Now, let us consider the restriction of Problem 5 between two generic indexes s and t such that $1 \leq s < t \leq n$, obtained by fixing $\delta w_s = y_s$ and $\delta w_t = y_t$ and by considering only the

NAR and upper bound constraints at $s + 1, \dots, t - 1$. Let $\delta \mathbf{w}^*$ be the optimal solution of the restriction. We first prove the following lemma.

Lemma 4: The optimal solution $\delta \mathbf{w}^*$ of the restriction of Problem 5 between two indexes s and t , $1 \leq s < t \leq n$, is such that, for each $j \in \{s + 1, \dots, t - 1\}$, either $\delta w_j^* \leq y_j$ or $\delta w_j^* \leq \eta_j(\delta w_{j+1}^* + \delta w_{j-1}^*) + b_{N_j}$ holds as an equality.

Proof: It is enough to observe that, in case both inequalities were strict for some j , then, in view of the monotonicity of the objective function, we could decrease the objective function value by increasing the value of δw_j^* , thus contradicting optimality of $\delta \mathbf{w}^*$. \square

Note that the above result also applies to the full Problem 5, which corresponds to the special case $s = 1, t = n$ with $y_1 = y_n = 0$. In view of Lemma 4, we have that there exists an index j , with $s < j \leq t$, such that: 1) $\delta w_j^* = y_j$; 2) the upper bound constraint is not active at $s + 1, \dots, j - 1$; and 3) all NAR constraints $s + 1, \dots, j - 1$ are active. Then, j is the lowest index in $\{s + 1, \dots, t - 1\}$ where the upper bound constraint is active. If index j were known, then the following observation allows returning the components of the optimal solution between s and j . Let us first introduce the following definitions of matrix \mathbf{A} and vector \mathbf{q} :

$$\mathbf{A} = \begin{bmatrix} 1 & -\eta_{s+1} & 0 & \cdots & 0 \\ -\eta_{s+2} & 1 & -\eta_{s+2} & \ddots & \vdots \\ 0 & \ddots & \ddots & \ddots & 0 \\ 0 & \cdots & 0 & -\eta_{j-1} & 1 \end{bmatrix}$$

$$\mathbf{q} = \begin{bmatrix} b_{N_{s+1}} + \eta_{s+1}y_s \\ b_{N_{s+2}} \\ \vdots \\ b_{N_{j-2}} \\ b_{N_{j-1}} + \eta_{j-1}y_j \end{bmatrix}. \quad (40)$$

Note that \mathbf{A} is the square submatrix of the NAR constraints restricted to rows $s + 1$ up to $j - 1$ and the related columns.

Observation 1: Let $\delta \mathbf{w}^*$ be the optimal solution of the restriction of Problem 5 between s and t and let $s < j$. If constraints $\delta w_s^* \leq y_s$, $\delta w_j^* \leq y_j$, and $\delta w_i^* \leq \eta_i(\delta w_{i+1}^* + \delta w_{i-1}^*) + b_{N_i}$, for $i = s + 1, \dots, j - 1$, are all active, then $\delta w_{s+1}^*, \dots, \delta w_{j-1}^*$ are obtained by the solution of the following tridiagonal system:

$$\begin{aligned} \delta w_s &= y_s \\ \delta w_r - \eta_r \delta w_{r+1} - \eta_r \delta w_{r-1} &= b_{N_r}, \quad r = s + 1, \dots, j - 1 \\ \delta w_j &= y_j \end{aligned}$$

or, equivalently, as

$$\begin{aligned} \delta w_{s+1} - \eta_{s+1} \bar{x}_{s+2} &= b_{N_{s+1}} + \eta_{s+1} y_s \\ \delta w_r - \eta_r \delta w_{r+1} - \eta_r \delta w_{r-1} &= b_{N_r}, \quad r = s + 2, \dots, j - 2 \\ \delta w_{s+1} - \eta_{s+1} \bar{x}_{s+2} &= b_{N_{s+1}} + \eta_{s+1} y_s. \end{aligned} \quad (41)$$

In the matrix form, the above tridiagonal linear system can be written as

$$\mathbf{A} \delta \mathbf{w}_{s+1, j-1}^* = \mathbf{q} \quad (42)$$

where matrix \mathbf{A} and vector \mathbf{q} are defined in (40) and $\delta \mathbf{w}_{s+1, j-1}^*$ is the restriction of vector $\delta \mathbf{w}$ to its components between $s + 1$ and $j - 1$.

Tridiagonal systems

$$a_i x_{i-1} + b_i x_i + c_i x_{i+1} = d_i, \quad i = 1, \dots, m$$

with $a_1 = c_m = 0$ can be solved through so-called Thomas algorithm [29] with $O(m)$ operations. In order to detect the lowest index $j \in \{s + 1, \dots, t - 1\}$ such that the upper bound constraint is active at j , we propose Algorithm 2, also called `SolveNAR` and described in what follows. We initially set $j = t$. Then, at each iteration, we solve the linear system (42). Let $\bar{\mathbf{x}} = (\bar{x}_{s+1}, \dots, \bar{x}_{j-1})$ be its solution. We check whether it is feasible and optimal or not. Namely, if there exists $k \in \{s + 1, \dots, j - 1\}$ such that either $\bar{x}_k < 0$ or $\bar{x}_k > y_k$, then $\bar{\mathbf{x}}$ is unfeasible, and consequently, we need to reduce j by 1. If $\bar{x}_k = y_k$ for some $k \in \{s + 1, \dots, j - 1\}$, then we also reduce j by 1 since j is not in any case the lowest index of the optimal solution where the upper bound constraint is active. Finally, if $0 \leq \bar{x}_k < y_k$, for $k = s + 1, \dots, j - 1$, then we need to verify if $\bar{\mathbf{x}}$ is the best possible solution over the interval $\{s + 1, \dots, j - 1\}$. We are able to check that after proving the following result.

Proposition 6: Let matrix \mathbf{A} and vector \mathbf{q} be defined as in (40). The optimal solution $\delta \mathbf{w}^*$ of the restriction of Problem 5 between s and t satisfies

$$\delta w_s^* = y_s, \quad \delta w_r^* = \bar{x}_r, \quad r = s + 1, \dots, j - 1, \quad \delta w_j^* = y_j \quad (43)$$

if and only if the optimal value of the LP problem

$$\begin{aligned} \max_{\boldsymbol{\epsilon}} \quad & \mathbf{1}^T \boldsymbol{\epsilon} \\ \boldsymbol{\epsilon} \mathbf{A} & \leq \mathbf{0} \\ \boldsymbol{\epsilon} & \leq \bar{\mathbf{y}} - \bar{\mathbf{x}} \end{aligned} \quad (44)$$

is strictly positive or, equivalently, if the following system admits no solution:

$$\mathbf{A}^T \boldsymbol{\lambda} = \mathbf{1}, \quad \boldsymbol{\lambda} \geq \mathbf{0}. \quad (45)$$

Proof: Let us first assume that $\delta \mathbf{w}^*$ does not fulfill (43). Then, in view of Lemma 4, j is not the lowest index such that the upper bound is active at the optimal solution, and consequently, $\delta w_k^* = y_k > \bar{x}_k$ for some $k \in \{s + 1, \dots, j - 1\}$. Such optimal solution must be feasible, and in particular, it must satisfy all NAR constraints between $s + 1$ and $j - 1$ and the upper bound constraints between $s + 1$ and j , i.e.,

$$\begin{aligned} \delta w_{s+1}^* - \eta_{s+1} \delta w_{s+2}^* &\leq b_{N_{s+1}} + \eta_{s+1} y_s \\ \delta w_r^* - \eta_r \delta w_{r+1}^* - \eta_r \delta w_{r-1}^* &\leq b_{N_r}, \quad r = s + 2, \dots, j - 2 \\ \delta w_{j-1}^* - \eta_{j-1} \delta w_{j-2}^* - \eta_{j-1} \delta w_j^* &\leq b_{N_{j-1}} \\ \delta w_r^* &\leq y_r, \quad r = s + 1, \dots, j. \end{aligned}$$

In view of $\delta w_j^* \leq y_j$ and $\eta_{j-1} \geq 0$, $\delta \mathbf{w}^*$ also satisfies the following system of inequalities:

$$\begin{aligned} \delta w_{s+1}^* - \eta_{s+1} \delta w_{s+2}^* &\leq b_{N_{s+1}} + \eta_{s+1} y_s \\ \delta w_r^* - \eta_r \delta w_{r+1}^* - \eta_r \delta w_{r-1}^* &\leq b_{N_r}, \quad r = s + 2, \dots, j - 2 \end{aligned}$$

$$\begin{aligned} \delta w_{j-1}^* - \eta_{j-1} \delta w_{j-2}^* &\leq b_{Nj-1} + \eta_{j-1} y_j \\ \delta w_r^* &\leq y_r, \quad r = s+1, \dots, j-1. \end{aligned}$$

After making the change of variables $\delta w_r^* = \bar{x}_r + \epsilon_r$ for $r = s+1, \dots, j-1$, and recalling that $\bar{\mathbf{x}}$ solves system (41), the system of inequalities can be further rewritten as

$$\begin{aligned} \epsilon_{s+1} - \eta_{s+1} \epsilon_{s+2} &\leq 0 \\ \epsilon_r - \eta_r \epsilon_{r+1} - \eta_r \epsilon_{r-1} &\leq 0, \quad r = s+2, \dots, j-2 \\ \epsilon_{j-1} - \eta_{j-1} \epsilon_{j-2} &\leq 0 \\ \epsilon_r &\leq y_r - \bar{x}_r, \quad r = s+1, \dots, j-1. \end{aligned}$$

Finally, recalling the definition of matrix \mathbf{A} and vector \mathbf{q} given in (40), this can also be written in a more compact form as

$$\begin{aligned} \mathbf{A}\boldsymbol{\epsilon} &\leq \mathbf{0} \\ \boldsymbol{\epsilon} &\leq \bar{\mathbf{y}} - \bar{\mathbf{x}}. \end{aligned}$$

If $\delta w_k^* = y_k > \bar{x}_k$ for some $k \in \{s+1, \dots, j-1\}$, then the system must admit a solution with $\epsilon_k > 0$. This is equivalent to prove that problem (44) has an optimal solution with at least one strictly positive component, and the optimal value is strictly positive. Indeed, in view of the definition of matrix \mathbf{A} , problem (44) has the structure of the problems discussed in Proposition 4. More precisely, to see that, we need to remark that maximizing $\mathbf{1}^T \boldsymbol{\epsilon}$ is equivalent to minimizing the decreasing function $-\mathbf{1}^T \boldsymbol{\epsilon}$. Then, observing that $\boldsymbol{\epsilon} = \mathbf{0}$ is a feasible solution of problem (44), by Proposition 4, the optimal solution $\boldsymbol{\epsilon}^*$ must be a nonnegative vector, and since at least one component, namely, component k , is strictly positive, then the optimal value must also be strictly positive.

Conversely, let us assume that the optimal value is strictly positive, and $\boldsymbol{\epsilon}^*$ is an optimal solution with at least one strictly positive component. Then, there are two possible alternatives. Either the optimal solution $\delta \mathbf{w}^*$ of the restriction of Problem 5 between s and t is such that $\delta w_j^* < y_j$, in which case (43) obviously does not hold, or $\delta w_j^* = y_j$. In the latter case, let us assume by contradiction that (43) holds. We observe that the solution that is defined as follows:

$$\begin{aligned} x'_s &= y_s \\ x'_r &= \bar{x}_r + \epsilon_r^* = \delta w_r^* + \epsilon_r^*, \quad r = s+1, \dots, j-1 \\ x'_j &= y_j = \delta w_j^* \\ x'_r &= \delta w_r^*, \quad r = j+1, \dots, t \end{aligned}$$

is feasible for the restriction of Problem 5 between s and t . Indeed, by feasibility of $\boldsymbol{\epsilon}^*$ in problem (44), all upper bound and NAR constraints between s and $j-1$ are fulfilled. Those between, $j+1$ and t , are also fulfilled by the feasibility of $\delta \mathbf{w}^*$. Then, we only need to prove that the NAR constraint at j is satisfied. By feasibility of $\delta \mathbf{w}^*$ and in view of $\epsilon_{j-1}^*, \eta_j \geq 0$, we have that

$$\begin{aligned} x'_j &= \delta w_j^* \leq \eta_j \delta w_{j-1}^* + \eta_j \delta w_{j+1}^* + b_{Nj} \\ &\leq \eta_j (\delta w_{j-1}^* + \epsilon_{j-1}^*) + \eta_j \delta w_{j+1}^* + b_{Nj} \\ &= \eta_j x'_{j-1} + \eta_j x'_{j+1} + b_{Nj}. \end{aligned}$$

Thus, \mathbf{x}' is feasible such that $\mathbf{x}' \geq \delta \mathbf{w}^*$ with at least one strict inequality (recall that at least one component of $\boldsymbol{\epsilon}^*$ is strictly positive), which contradicts the optimality of $\delta \mathbf{w}^*$ (recall that the optimal solution must be the componentwise maximum of all feasible solutions).

In order to prove the last part, i.e., problem (44) has a positive optimal value if and only if (45) admits no solution, and we notice that the optimal value is positive if and only if the feasible point $\boldsymbol{\epsilon} = \mathbf{0}$ is not an optimal solution, or equivalently, the null vector is not a KKT point. Since, at $\boldsymbol{\epsilon} = \mathbf{0}$, constraints $\boldsymbol{\epsilon} \leq \bar{\mathbf{y}} - \bar{\mathbf{x}}$ cannot be active, then the KKT conditions for problem (44) at this point are exactly those established in (45), where vector $\boldsymbol{\lambda}$ is the vector of Lagrange multipliers for constraints $\mathbf{A}\boldsymbol{\epsilon} \leq \mathbf{0}$. This concludes the proof. \square

Then, if (45) admits no solution, (43) does not hold, and again, we need to reduce j by 1. Otherwise, we can fix the optimal solution between s and j according to (43). After that, we recursively call the routine `SolveNAR` on the remaining subinterval $\{j, \dots, t\}$ in order to obtain the solution over the full interval.

Remark 3: In Algorithm 2, routine `isFeasible` is the routine used to verify if, for $k = s+1, \dots, j-1$, $0 \leq \bar{x}_k < y_k$, while `isOptimal` is the procedure to check optimality of $\bar{\mathbf{x}}$ over the interval $\{s+1, \dots, j-1\}$, i.e., (43) holds.

Now, we are ready to prove that Algorithm 2 solves Problem 5.

Proposition 7: The call `solveNAR(y, 1, n)` of Algorithm 2 returns the optimal solution of Problem 5.

Proof: After the call `solveNAR(y, 1, n)`, we are able to identify the portion of the optimal solution between 1 and some index j_1 , $1 < j_1 \leq n$. If $j_1 = n$, then we are done. Otherwise, we make the recursive call `solveNAR(y, j_1, n)`, which enables to identify also the portion of the optimal solution between j_1 and some index j_2 , $j_1 < j_2 \leq n$. If $j_2 = n$, then we are done. Otherwise, we make the recursive call `solveNAR(y, j_2, n)` and so on. After at most n recursive calls, we are able to return the full optimal solution. \square

Algorithm 2 `SolveNAR(y, s, t)`

input : Upper bound \mathbf{y} and two indices s and t with $1 \leq s < t \leq n$
output: $\delta \mathbf{w}^*$

- 1 Set $j = t$;
- 2 $\delta \mathbf{w}^* = \mathbf{y}$;
- 3 **while** $j \geq s+1$ **do**
- 4 Compute the solution $\bar{\mathbf{x}}$ of the linear system (42);
- 5 **if** `isFeasible`($\bar{\mathbf{x}}$) and `isOptimal`($\bar{\mathbf{x}}$) **then**
- 6 **Break**;
- 7 **else**
- 8 Set $j = j-1$;
- 9 **for** $i = s+1, \dots, j-1$ **do**
- 10 Set $\delta w_i^* = \bar{x}_i$;
- 11 **return** $\delta \mathbf{w}^* = \min\{\delta \mathbf{w}^*, \text{SolveNAR}(\delta \mathbf{w}^*, j, t)\}$;

Remark 4: Note that Algorithm 2 involves solving a significant amount of linear systems, both to compute $\bar{\mathbf{x}}$ and verify its optimality [see (42) and (45)]. Some tricks can be employed to reduce the number of operations. Some of these are discussed in [30].

The following proposition states the worst case complexity of `solveNAR`($\mathbf{y}, 1, n$).

Proposition 8: Problem 5 can be solved with $O(n^3)$ operations by running the procedure `SolveNAR`($\mathbf{y}, 1, n$) and by using the Thomas algorithm for the solution of each linear system.

Proof: In the worst case, at the first call, we have $j_1 = 2$ since we need to go all the way from $j = n$ down to $j = 2$. Since, for each j , we need to solve a tridiagonal system, which requires at most $O(n)$ operations, the first call of `SolveNAR` requires $O(n^2)$ operations. This is similar for all successive calls, and since the number of recursive calls is at most $O(n)$, the overall effort is at most of $O(n^3)$ operations. \square

In fact, what we observed is that the practical complexity of the algorithm is much better, namely, $\Theta(n^2)$.

C. Acceleration and NAR Constraints

Now, we discuss the problem with acceleration and NAR constraints, with upper bound vector \mathbf{y} , i.e.,

Problem 6:

$$\min_{\delta \mathbf{w} \in \mathbb{R}^n} \sum_{i=1}^{n-1} \frac{2h}{\sqrt{w_{i+1} + \delta w_{i+1}} + \sqrt{w_i + \delta w_i}}$$

$$\mathbf{l}_B \leq \delta \mathbf{w} \leq \mathbf{y}$$

$$\delta w_{i+1} - \delta w_i \leq b_{A_i}, \quad i = 1, \dots, n-1$$

$$\delta w_i - \delta w_{i+1} \leq b_{D_i}, \quad i = 1, \dots, n-1$$

$$\delta w_i - \eta_i \delta w_{i-1} - \eta_i \delta w_{i+1} \leq b_{N_i}, \quad i = 2, \dots, n-1.$$

We first remark that Problem 6 has the structure of problem (36) so that, by Proposition 4, its unique optimal solution is the componentwise maximum of its feasible region. As for Problem 5, we can solve Problem 6 by using the graph-based approach proposed in [28]. However, Cabassi *et al.* [4] show that, if we adopt a very efficient procedure to solve Problems 4 and 5, then it is worth splitting the full problem into two separated ones and use an iterative approach (see Algorithm 3). Indeed, Problems 4–6 share the common property that their optimal solution is also the componentwise maximum of the corresponding feasible region. Moreover, according to Proposition 5, the optimal solutions of Problems 4 and 5 are valid upper bounds for the optimal solution (actually, also for any feasible solution) of the full Problem 6. In Algorithm 3, we first call the procedure `SolveACC` with input the upper bound vector \mathbf{y} . Then, the output of this procedure, which, according to what we have just stated, is an upper bound for the solution of the full Problem 6, satisfies $\delta \mathbf{w}_{\text{Acc}} \leq \mathbf{y}$, and becomes the input for a call of the procedure `SolveNAR`. The output $\delta \mathbf{w}_{\text{NAR}}$ of this call is again an upper bound for the solution of the full Problem 6, and it satisfies $\delta \mathbf{w}_{\text{NAR}} \leq \delta \mathbf{w}_{\text{Acc}}$. This output becomes the input of a further call to the procedure `SolveACC`, and we proceed in this way until the distance between two consecutive output vectors falls below a

prescribed tolerance value ε . The following proposition states that the sequence of output vectors generated by the alternate calls to the procedures `SolveACC` and `SolveNAR` converges to the optimal solution of the full Problem 6.

Proposition 9: Algorithm 3 converges to the the optimal solution of Problem 6 when $\varepsilon = 0$ and stops after a finite number of iterations if $\varepsilon > 0$.

Proof: We have observed that the sequence of alternate solutions of Problems 4 and 5, here denoted by $\{\mathbf{y}_i\}$, is: 1) a sequence of valid upper bounds for the optimal solution of Problem 6; 2) componentwise monotonic nonincreasing; and 3) componentwise bounded from below by the null vector. Thus, if $\varepsilon = 0$, an infinite sequence is generated, which converges to some point $\bar{\mathbf{y}}$, which is also an upper bound for the optimal solution of Problem 6 but, more precisely, by continuity, is also a feasible point of the problem and, is thus, also the optimal solution of the problem. If $\varepsilon > 0$, due to the convergence to some point $\bar{\mathbf{y}}$, at some finite iteration, the exit condition of the while loop must be satisfied. \square

Algorithm 3 Algorithm `SolveACCNAR` for the Solution of Problem 6

input : The upper bound \mathbf{y} and the tolerance ε

output: The optimal solution $\delta \mathbf{w}^*$ and the optimal value f^*

```

1  $\delta \mathbf{w}_{\text{Acc}} = \text{SolveACC}(\mathbf{y});$ 
2  $\delta \mathbf{w}_{\text{NAR}} = \text{SolveNAR}(\delta \mathbf{w}_{\text{Acc}}, 1, n);$ 
3 while  $\|\delta \mathbf{w}_{\text{NAR}} - \delta \mathbf{w}_{\text{Acc}}\| > \varepsilon$  do
4    $\delta \mathbf{w}_{\text{Acc}} = \text{SolveACC}(\delta \mathbf{w}_{\text{NAR}});$ 
5    $\delta \mathbf{w}_{\text{NAR}} = \text{SolveNAR}(\delta \mathbf{w}_{\text{Acc}}, 1, n);$ 
6  $\delta \mathbf{w}^* = \delta \mathbf{w}_{\text{NAR}};$ 
7 return  $\delta \mathbf{w}^*$ , evaluateObj( $\delta \mathbf{w}^*$ )
```

IV. DESCENT METHOD FOR THE CASE OF ACCELERATION, PAR, AND NAR CONSTRAINTS

Unfortunately, PAR constraints (21) do not satisfy the assumptions requested in Proposition 4 in order to guarantee that the componentwise maximum of the feasible region is the optimal solution of Problem 3. However, in Section III, we have shown that Problem 6, i.e., Problem 3 without the PAR constraints, can be efficiently solved by Algorithm 3. Our purpose then is to separate the acceleration and NAR constraints from the PAR constraints.

Definition 1: Let $f: \mathbb{R}^n \rightarrow \mathbb{R}$ be the objective function of Problem 3, and let \mathcal{D} be the region defined by the acceleration and NAR constraints (the feasible region of Problem 6). We define the function $F: \mathbb{R}^n \rightarrow \mathbb{R}$ as follows:

$$F(\mathbf{y}) = \min\{f(\mathbf{x}) \mid \mathbf{x} \in \mathcal{D}, \mathbf{x} \leq \mathbf{y}\}.$$

Namely, F is the optimal value function of Problem 6 when the upper bound vector is \mathbf{y} .

Proposition 10: Function F is a convex function.

Proof: Since Problem 6 is convex, then the optimal value function F is convex (see [31, Sec. 5.6.1]). \square

Now, let us introduce the following problem:

1017 *Problem 7:*

$$1018 \quad \min_{\mathbf{y} \in \mathbb{R}^n} F(\mathbf{y}) \quad (46)$$

$$1019 \quad \eta_i(y_{i-1} + y_{i+1}) - y_i \leq b_{P_i}, \quad i = 2, \dots, n-1 \quad (47)$$

$$1020 \quad \mathbf{l}_B \leq \mathbf{y} \leq \mathbf{u}_B. \quad (48)$$

1021 Such a problem is a relaxation of Problem 3. Indeed, each
1022 feasible solution of Problem 3 is also feasible for Problem 7,
1023 and the value of F at such solution is equal to the value
1024 of the objective function of Problem 3 at the same solution.
1025 We solve Problem 7 rather than Problem 3 to compute the
1026 new displacement $\delta \mathbf{w}$. More precisely, if \mathbf{y}^* is the optimal
1027 solution of Problem 7, then we set

$$1028 \quad \delta \mathbf{w} = \arg \min_{\mathbf{x} \in \mathcal{D}, \mathbf{x} \leq \mathbf{y}^*} f(\mathbf{x}). \quad (49)$$

1029 In the following proposition, we prove that, under a very
1030 mild condition, the optimal solution of Problem 7 computed
1031 in (49) is feasible and, thus, optimal for Problem 3 so that,
1032 although we solve a relaxation of the latter problem, we return
1033 an optimal solution for it.

1034 *Proposition 11:* Let $\mathbf{w}^{(k)}$ be the current point. If

$$1035 \quad \ell_j(\delta \mathbf{w}) \leq \ell_j(\mathbf{w}^{(k)})(3 + \min\{0, \zeta(\mathbf{w}^{(k)})\}), \quad j = 2, \dots, n-1 \quad (50)$$

1037 where $\delta \mathbf{w}$ is computed through (49) and

$$1038 \quad \zeta(\mathbf{w}^{(k)}) = \frac{\sqrt{\ell_j(\mathbf{w}^{(k)})} (w_{j-1}^{(k)} + w_{j+1}^{(k)} - 2w_j^{(k)})}{2h^2 J} \geq -2$$

1039 (the inequality follows from feasibility of $\mathbf{w}^{(k)}$), then $\delta \mathbf{w}$ is
1040 feasible for Problem 3, both if the nonlinear constraints are
1041 linearized as in (20) and (21), and if they are linearized as
1042 in (26) and (27).

1043 *Proof:* First, we notice that, if we prove the result for
1044 the tighter constraints (26) and (27), then it must also hold
1045 for constraints (20) and (21). Thus, we prove the result only
1046 for the former. By definition (49), $\delta \mathbf{w}$ satisfies the acceleration
1047 and NAR constraints so that

$$1048 \quad \delta w_j \leq \delta w_{j+1} + b_{D_j}$$

$$1049 \quad \delta w_j \leq \delta w_{j-1} + b_{A_{j-1}}$$

$$1050 \quad \delta w_j \leq \beta_j(\delta w_{j+1} + \delta w_{j-1}) + b'_{N_j}$$

$$1051 \quad \delta w_j \leq y_j^*.$$

1052 At least one of these constraints must be active; otherwise,
1053 δw_j could be increased, thus contradicting optimality. If the
1054 active constraint is $\delta w_j \leq \beta_j(\delta w_{j+1} + \delta w_{j-1}) + b'_{N_j}$, then
1055 constraint (27) can be rewritten as follows:

$$1056 \quad 4h^2 J (\ell_j(\mathbf{w}^{(k)}))^{-\frac{3}{2}} (\delta w_{j+1} + 2\delta w_j + \delta w_{j-1}) \\ 1057 \quad \leq 12h^2 J (\ell_j(\mathbf{w}^{(k)}))^{-\frac{1}{2}}$$

1058 or, equivalently,

$$1059 \quad \ell_j(\delta \mathbf{w}) \leq 3\ell_j(\mathbf{w}^{(k)})$$

1060 implied by (50), and thus, the constraint is satisfied under the
1061 given assumption. If $\delta w_j = y_j^*$, then

$$1062 \quad \theta_j(\delta w_{j-1} + \delta w_{j+1}) \leq \theta_j(y_{j-1}^* + y_{j+1}^*) \leq y_j^* + b'_{P_j} = \delta w_j + b'_{P_j}$$

1063 where the second inequality follows from the fact that \mathbf{y}^*
1064 satisfies the PAR constraints. Now, let $\delta w_j = \delta w_{j+1} + b_{D_j}$
1065 (the case when $\delta w_j \leq \delta w_{j-1} + b_{A_{j-1}}$ is active can be dealt
1066 with in a completely analogous way). First, we observe that
1067 $\delta w_j \geq \delta w_{j-1} - b_{D_{j-1}}$. Then,

$$1068 \quad 2\delta w_j \geq \delta w_{j+1} + \delta w_{j-1} + b_{D_j} - b_{D_{j-1}}.$$

1069 In view of the definitions of b_{D_j} and $b_{D_{j-1}}$, this can also be
1070 written as

$$1071 \quad 2\delta w_j \geq \delta w_{j+1} + \delta w_{j-1} + w_{j+1}^{(k)} - 2w_j^{(k)} + w_{j-1}^{(k)}. \quad (51)$$

1072 Now, after recalling the definitions of θ_j and b'_{P_j} given
1073 in (28), and setting $\Delta = h^2 J$, (27) can be rewritten as

$$1074 \quad 2\delta w_j \geq \delta w_{j+1} + \delta w_{j-1} + 2\Delta (\ell_j(\mathbf{w}^{(k)}))^{-\frac{3}{2}} \ell_j(\delta \mathbf{w}) \\ 1075 \quad - 6\Delta (\ell_j(\mathbf{w}^{(k)}))^{-\frac{1}{2}}.$$

1076 Taking into account (51), such inequality certainly holds if

$$1077 \quad w_{j+1}^{(k)} - 2w_j^{(k)} + w_{j-1}^{(k)} \geq 2\Delta (\ell_j(\mathbf{w}^{(k)}))^{-\frac{3}{2}} \ell_j(\delta \mathbf{w}) \\ 1078 \quad - 6\Delta (\ell_j(\mathbf{w}^{(k)}))^{-\frac{1}{2}}$$

1079 which is equivalent to

$$1080 \quad \ell_j(\delta \mathbf{w}) \leq \ell_j(\mathbf{w}^{(k)})(3 + \zeta(\mathbf{w}^{(k)})).$$

1081 This is also implied by (50). \square

1082 Assumption (50) is mild. In order to fulfill it, one can
1083 impose restrictions on δw_{j-1} , δw_j and δw_{j+1} . In fact, in the
1084 computational experiments, we did not impose such restric-
1085 tions unless a positive step-length along the computed direc-
1086 tion $\delta \mathbf{w}$ could not be taken (which, however, never occurred
1087 in our experiments).

1088 Now, let us turn our attention toward the solution of
1089 Problem 7. In order to solve it, we propose a descent method.
1090 We can exploit the information provided by the dual optimal
1091 solution $\mathbf{v} \in \mathbb{R}_+^n$ associated with the upper bound constraints
1092 of Problem 6. Indeed, from the sensitivity theory, we know
1093 that the dual solution is related to the gradient of the optimal
1094 value function F (see Definition 1) and provides information
1095 about how it changes its value for small perturbations of the
1096 upper bound values (for further details, see [31, Secs. 5.6.2 and
1097 5.6.5]). Let $\mathbf{y}^{(t)}$ be a feasible solution of Problem 7 and $\mathbf{v} \in \mathbb{R}_+^n$
1098 be the Lagrange multipliers of the upper bound constraints of
1099 Problem 6 when the upper bound is $\mathbf{y}^{(t)}$. Let

$$1100 \quad \varphi_i = b_{P_i} - \eta_i(y_{i-1}^{(t)} + y_{i+1}^{(t)}) + y_i^{(t)}, \quad i = 2, \dots, n-1.$$

1101 Then, a feasible descent direction $\mathbf{d}^{(t)}$ can be obtained by
1102 solving the following LP problem:

1103 *Problem 8:*

$$1104 \quad \min_{\mathbf{d} \in \mathbb{R}^n} -\mathbf{v}^T \mathbf{d} \quad (52)$$

$$1105 \quad \eta_i(d_{i-1} + d_{i+1}) - d_i \leq \varphi_i, \quad i = 2, \dots, n-1 \quad (53)$$

$$1106 \quad \mathbf{l}_B \leq \mathbf{y}^{(t)} + \mathbf{d} \leq \mathbf{u}_B \quad (54)$$

1107 where the objective function (52) imposes that $\mathbf{d}^{(t)}$ is a
1108 descent direction, while constraints (53) and (54) guarantee
1109 feasibility with respect to Problem 7. Problem 8 is an LP
1110

1110 problem, and consequently, it can easily be solved through a
 1111 standard LP solver. In particular, we employed GUROBI [32].
 1112 Unfortunately, since the information provided by the dual
 1113 optimal solution \mathbf{v} is local and related to small perturbations of
 1114 the upper bounds, it might happen that $F(\mathbf{y}^{(t)} + \mathbf{d}^{(t)}) \geq F(\mathbf{y}^{(t)})$.
 1115 To overcome this issue, we introduce a trust-region constraint
 1116 in Problem 8. Thus, let $\sigma^{(t)} \in \mathbb{R}_+$ be the radius of the trust
 1117 region at iteration t ; then, we have

1118 *Problem 9:*

$$1119 \quad \min_{\mathbf{d} \in \mathbb{R}^n} -\mathbf{v}^T \mathbf{d} \quad (55)$$

$$1120 \quad \eta_i (d_{i-1} + d_{i+1}) - d_i \leq \varphi_i, \quad i = 2, \dots, n-1 \quad (56)$$

$$1121 \quad \bar{\mathbf{l}}_{\mathbf{B}} \leq \mathbf{d} \leq \bar{\mathbf{u}}_{\mathbf{B}} \quad (57)$$

1122 where $\bar{l}_{B_i} = \max\{l_{B_i} - y_i^{(t)}, -\sigma^{(t)}\}$ and $\bar{u}_{B_i} = \min\{u_{B_i} -$
 1123 $y_i^{(t)}, \sigma^{(t)}\}$ for $i = 1, \dots, n$. After each iteration of the descent
 1124 algorithm, we change the radius $\sigma^{(t)}$ according to the following
 1125 rules.

- 1126 1) If $F(\mathbf{y}^{(t)} + \mathbf{d}^{(t)}) \geq F(\mathbf{y}^{(t)})$, then we set $\mathbf{y}^{(t+1)} = \mathbf{y}^{(t)}$, and
 1127 we tight the trust region by decreasing $\sigma^{(t)}$ by a factor
 1128 $\tau \in (0, 1)$.
- 1129 2) If $F(\mathbf{y}^{(t)} + \mathbf{d}^{(t)}) < F(\mathbf{y}^{(t)})$, then we set $\mathbf{y}^{(t+1)} = \mathbf{y}^{(t)} + \mathbf{d}^{(t)}$
 1130 and enlarge the radius $\sigma^{(t)}$ by a factor $\rho > 1$.

1131 The proposed descent algorithm is sketched in Fig. 3, which
 1132 reports the flowchart of the procedure `ComputeUpdate` used
 1133 in algorithm SCA. We initially set $\mathbf{y}^{(0)} = \mathbf{0}$. At each iteration t ,
 1134 we evaluate the objective function $F(\mathbf{y}^t)$ by solving Problem 6
 1135 with upper bound vector $\mathbf{y}^{(t)}$ through a call of the routine
 1136 `solveACCNAR` (see Algorithm 3). Then, we compute the
 1137 Lagrange multipliers $\mathbf{v}^{(t)}$ associated with the upper bound con-
 1138 straints. After that, we compute a candidate descent direction
 1139 $\mathbf{d}^{(t)}$ by solving Problem 9. If $\mathbf{d}^{(t)}$ is a descent step, then we set
 1140 $\mathbf{y}^{(t+1)} = \mathbf{y}^{(t)} + \mathbf{d}^{(t)}$ and enlarge the radius of the trust region;
 1141 otherwise, we do not move to a new point, and we tight the
 1142 trust region and solve again Problem 9. The descent algorithm
 1143 stops as soon as the radius of the trust region becomes smaller
 1144 than a fixed tolerance ε_1 .

1145 *Remark 5:* Note that we initially set $\mathbf{y}^{(0)} = \mathbf{0}$. However, any
 1146 feasible solution of Problem 9 does the job, and actually, start-
 1147 ing with a good initial solution may enhance the performance
 1148 of the algorithm.

1149 *Remark 6:* Problem 9 is an LP and can be solved by
 1150 any existing LP solver. However, a suboptimal solution to
 1151 Problem 9, obtained by a heuristic approach, is also accept-
 1152 able. Indeed, we observe that: 1) an *optimal* descent direction
 1153 is not strictly required and 2) a heuristic approach allows to
 1154 reduce the time needed to get a descent direction. In this
 1155 article, we employed a possible heuristic, whose description
 1156 can be found in [30], but the development of further heuristic
 1157 approaches is a possible topic for future research.

1158 V. COMPUTATIONAL EXPERIMENTS

1159 In this section, we present various computational experi-
 1160 ments performed in order to evaluate the approaches proposed
 1161 in Sections III and IV.

1162 In particular, we compared solutions of Problem 2 computed
 1163 by algorithm SCA to solutions obtained with commercial NLP

solvers. Note that, with a single exception, we did not carry out
 a direct comparison with other methods specifically tailored to
 Problem 2 for the following reasons.

- 1164 1) Some algorithms (such as [22] and [23]) use heuristics to
 1165 quickly find suboptimal solutions of acceptable quality
 1166 but do not achieve local optimality. Hence, comparing
 1167 their solution times with SCA would not be fair. How-
 1168 ever, in one of our experiments (see Experiment 4),
 1169 we made a comparison between the most recent heuristic
 1170 proposed in [23] and algorithm SCA, both in terms
 1171 of computing times and in terms of the quality of the
 1172 returned solution.
- 1173 2) The method presented in [26] does not consider the
 1174 (nonconvex) jerk constraint but solves a convex problem
 1175 whose objective function has a penalization term that
 1176 includes pseudojerk. Due to this difference, a direct
 1177 comparison with SCA is not possible.
- 1178 3) The method presented in [24] is based on the numerical
 1179 solution of a large number of nonlinear and nonconvex
 1180 subproblems and is, therefore, structurally slower than
 1181 SCA, whose main iteration is based on the efficient
 1182 solution of the convex Problem 3.

1183 In the first two experiments, we compare the computational
 1184 time of IPOPT, a general-purpose NLP solver [33], with that
 1185 of algorithm SCA over some randomly generated instances of
 1186 Problem 2. In particular, we tested two different versions of
 1187 the algorithm SCA. The first version, called SCA-H in what
 1188 follows, employs the heuristic mentioned in Remark 6. Since
 1189 the heuristic procedure may fail in some cases, in such cases,
 1190 we also need an LP solver. In particular, in our experiments,
 1191 we used GUROBI whenever the heuristic did not produce
 1192 either a feasible solution to Problem 9 or a descent direc-
 1193 tion. In the second version, called SCA-G in what follows,
 1194 we always employed GUROBI to solve Problem 9. For what
 1195 concerns the choice of the NLP solver IPOPT, we remark
 1196 that we chose it after a comparison with two further general-
 1197 purpose NLP solvers, SNOPT and MINOS, which, however,
 1198 turned out to perform worse than IPOPT on this class of
 1199 problems.

1200 In the third experiment, we compare the performance of
 1201 the two implemented versions of algorithm SCA applied to
 1202 two specific paths and see their behavior as the number n of
 1203 discretized points increases.

1204 In the fourth experiment, we compare the solutions returned
 1205 by algorithm SCA with those returned by the heuristic recently
 1206 proposed in [23].

1207 Finally, in the fifth experiment, we present a real-life speed
 1208 planning task for an LGV operating in an industrial setting,
 1209 using real problem bounds and paths layouts, provided by an
 1210 automation company based in Parma, Italy.

1211 We remark that, according to our experiments, the spe-
 1212 cial purpose routine `solveACCNAR` (Algorithm 3) strongly
 1213 outperforms general-purpose approaches, such as the graph-
 1214 based approach proposed in [28], and GUROBI, when solving
 1215 Problem 6 (which can be converted into an LP as discussed
 1216 in [28]).

1217 Finally, we remark that we also tried to solve the con-
 1218 vex Problem 3 arising at each iteration of the proposed
 1219

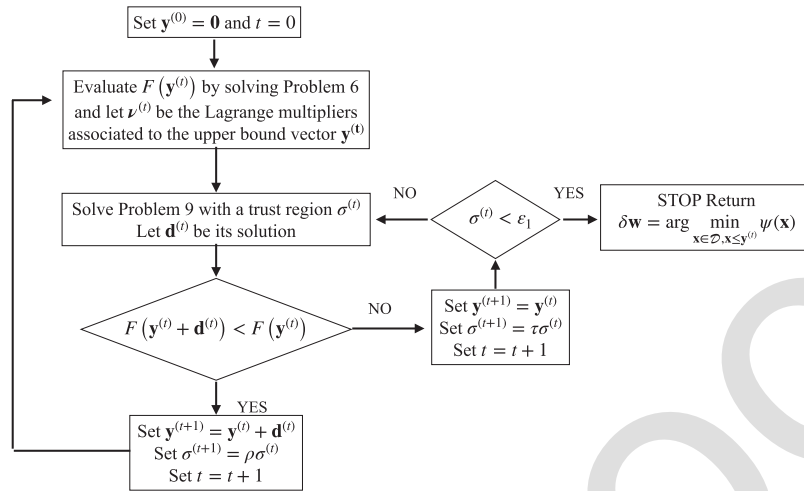


Fig. 3. Flowchart of the routine ComputeUpdate.

1222 method with an NLP solver in place of the procedure
1223 ComputeUpdate, presented in this article. However, the
1224 experiments revealed that, in doing this, the computing times
1225 become much larger even with respect to the single call to the
1226 NLP solver for solving the nonconvex Problem 2.

1227 All tests have been performed on an IntelCore i7-8550U
1228 CPU at 1.8 GHz. Both for IPOPT and algorithm SCA, the
1229 null vector was chosen as a starting point. The parameters
1230 used within algorithm SCA were $\varepsilon = 1e^{-8}$, $\varepsilon_1 = 1e^{-6}$
1231 (tolerance parameters), $\rho = 4$, and $\tau = 0.25$ (trust-region
1232 update parameters). The initial trust region radius $\sigma^{(0)}$ was
1233 initialized to 1 in the first iteration $k = 0$ but adaptively
1234 set equal to the size of the last update $\|w^{(k)} - w^{(k-1)}\|_\infty$
1235 in all subsequent iterations (this adaptive choice allowed to
1236 reduce computing times by more than a half). We remark that
1237 algorithm SCA has been implemented in MATLAB, so we
1238 expect better performance after a C/C++ implementation.

1239 A. Experiments 1 and 2

1240 In Experiment 1, we generated a set of 50 different paths,
1241 each of which was discretized setting $n = 100$, $n = 500$,
1242 and $n = 1000$ sample points. The instances were generated
1243 by assuming that the traversed path was divided into seven
1244 intervals over which the curvature of the path was assumed
1245 to be constant. Thus, the n -dimensional upper bound vector
1246 \mathbf{u} was generated as follows. First, we fixed $u_1 = u_n = 0$,
1247 i.e., the initial and final speeds must be equal to 0. Next,
1248 we partitioned the set $\{2, \dots, n-1\}$ into seven subintervals
1249 I_j , $j \in \{1, \dots, 7\}$, which corresponds to intervals with
1250 constant curvature. Then, for each subinterval, we randomly
1251 generated a value $u_j \in (0, \tilde{u}]$, where \tilde{u} is the maximum upper
1252 bound (which was set equal to $100 \text{ m}^2\text{s}^{-2}$). Finally, for each
1253 $j \in \{1, \dots, 7\}$, we set $u_k = \tilde{u}_j \forall k \in I_j$. The maximum
1254 acceleration parameter A is set equal to 2.78 ms^{-2} and the
1255 maximum jerk J to 0.5 ms^{-3} , while the path length is $s_f =$
1256 60 m . The values for A and J allow a comfortable motion for
1257 a ground transportation vehicle (see [34]).

1258 In Experiment 2, we generated a further set of 50 different
1259 paths, each of which was discretized using $n = 100$, $n = 500$,
1260 and $n = 1000$ variables. These new instances were randomly
1261 generated such that the traversed path was divided into up to
1262 five intervals over which the curvature could be zero, linear
1263 with respect to the arc length or constant. We chose this kind
1264 of path since they are able to represent the curvature of a
1265 road trip (see [35]). The maximum squared speed along the
1266 path was fixed equal to $192.93 \text{ m}^2\text{s}^{-2}$ (corresponding to a
1267 maximum speed of 50 kmh^{-1} , a typical value for an urban
1268 driving scenario). The total length of the paths was fixed to
1269 $s_f = 1000 \text{ m}$, while parameter A was set equal to 0.25 ms^{-2} ,
1270 J to 0.025 ms^{-3} , and A_N to 4.9 ms^{-2} .

1271 The results are reported in Table I, in which we show
1272 the average (minimum and maximum) computational times
1273 for SCA-H, SCA-G, and IPOPT. They show that algorithm
1274 SCA-H is the fastest one, while SCA-G is slightly faster than
1275 IPOPT at $n = 100$ but clearly faster for a larger number of
1276 sample points n . In general, we observe that both SCA-H and
1277 SCA-G tend to outperform IPOPT as n increases. Moreover,
1278 while the computing times for IPOPT at $n = 100$ are not much
1279 worse than those of SCA-H and SCA-G, we should point out
1280 that, at this dimension, IPOPT is sometimes unable to converge
1281 and return solutions whose objective function value differs
1282 from the best one by more than 100%. Also, the objective
1283 function values returned by SCA-H and SCA-G are sometimes
1284 slightly different, due to numerical issues related to the choice
1285 of the tolerance parameters, but such differences are mild ones
1286 and never exceed 1%. Therefore, these approaches appear to
1287 be fast and robust. It is also worthwhile to remark that SCA
1288 approaches are compatible with online planning requirements
1289 within the context of the LGV application. According to
1290 Haschke *et al.* [18] (see also [36]), in “highly unstructured,
1291 unpredictable, and dynamic environments,” there is a need to
1292 replan in order to adapt the motion in reaction to unforeseen
1293 events or obstacles. How often to replan depends strictly on the
1294 application. Within the context of the LGV application (where
1295 the environment is structured), replanning every 100–150 ms

TABLE I

AVERAGE (MINIMUM AND MAXIMUM) COMPUTING TIMES (IN SECONDS) FOR SCA-H, SCA-G, AND IPOPT OVER EXPERIMENTS 1 AND 2

| Exp. | n | | SCA-H | SCA-G | IPOPT |
|------|------|------|-------|-------|-------|
| 1 | 100 | min | 0.012 | 0.042 | 0.03 |
| | | mean | 0.016 | 0.072 | 0.132 |
| | | max | 0.026 | 0.138 | 0.305 |
| 1 | 500 | min | 0.042 | 0.21 | 0.352 |
| | | mean | 0.064 | 0.276 | 1.01 |
| | | max | 0.104 | 0.456 | 1.828 |
| 1 | 1000 | min | 0.1 | 0.426 | 1.432 |
| | | mean | 0.149 | 0.626 | 3.289 |
| | | max | 0.237 | 0.828 | 7.137 |
| 2 | 100 | min | 0.012 | 0.036 | 0.052 |
| | | mean | 0.02 | 0.047 | 0.113 |
| | | max | 0.038 | 0.073 | 0.263 |
| 2 | 500 | min | 0.049 | 0.102 | 0.534 |
| | | mean | 0.093 | 0.172 | 0.886 |
| | | max | 0.212 | 0.237 | 1.457 |
| 2 | 1000 | min | 0.083 | 0.228 | 1.733 |
| | | mean | 0.242 | 0.386 | 2.487 |
| | | max | 0.709 | 0.539 | 3.74 |

is acceptable, and thus, the computing times of the SCA approaches at $n = 100$ are suitable. Of course, computing times increase with n , but we notice that the computing times of SCA-H still meet the requirement at $n = 500$. Moreover, a relevant feature of SCA-H and SCA-G is that, at each iteration, a feasible solution is available. Thus, we could stop them as soon as a time limit is reached. At $n = 500$, if we impose a time limit of 150 ms, which is still quite reasonable for the application, SCA-G returns slightly worse feasible solutions, but these do not differ from the best ones by more than 2%.

B. Experiment 3

In our third experiment, we compared the performance of the two proposed approaches (SCA-H and SCA-G), over two possible automated driving scenarios, as the number n of samples increases. As a first example, we considered a continuous curvature path composed of a line segment, a clothoid, a circle arc, a clothoid, and a final line segment (see Fig. 4). The minimum-time velocity planning on this path, whose total length is $s_f = 90$ m, is addressed with the following data. The problem constants are compatible with a typical urban driving scenario. The maximum squared velocity is $225 \text{ m}^2\text{s}^{-2}$ (corresponding to 54 km h^{-1}), the longitudinal acceleration limit is $A = 1.5 \text{ ms}^{-2}$, and the maximal normal acceleration is $A_N = 1 \text{ ms}^{-2}$, while, for the jerk constraints, we set $J = 1 \text{ ms}^{-3}$. Next, we considered a path of length $s_f = 60$ m (see Fig. 5) whose curvature was defined according to the following function:

$$k(s) = \frac{1}{5} \sin\left(\frac{s}{10}\right), \quad s \in [0, s_f]$$

and parameter A , A_N , and J were set equal to 1.39 ms^{-2} , 4.9 ms^{-2} , and 0.5 ms^{-3} , respectively. The maximum squared velocity is still equal to $225 \text{ m}^2\text{s}^{-2}$. The computational results are reported in Figs. 6 and 7 for values of n that grows from 100 to 1000. They show that the performance of SCA-H and SCA-G depends on the path. In particular, it seems that the heuristic performs in a poorer way when the number of

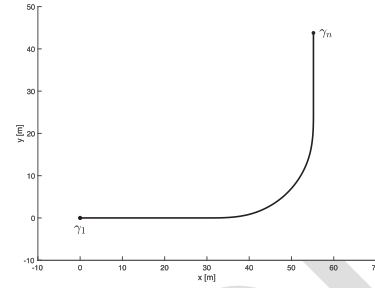


Fig. 4. Experiment 3—first path.

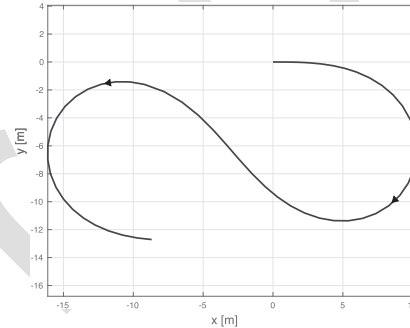


Fig. 5. Experiment 3—second path.

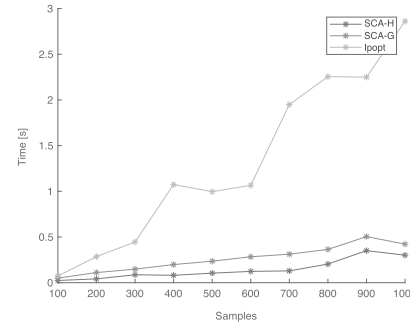


Fig. 6. Computing times (in seconds) for the path in Fig. 4.

points of the upper bound vector at which PAR constraints are violated tends to be large, which is the case for the second instance. We can give two possible motivations: 1) the directions computed by the heuristic procedure are not necessarily good descent directions, so routine `computeUpdate` slowly converges to a solution and 2) the heuristic procedure often fails, and it is in any case necessary to call `GUROBI`. Note that the computing times of IPOPT on these two paths are larger than those of SCA-H and SCA-G, and, as usual, the gap increases with n . Moreover, for the second path, IPOPT was unable to converge for $n = 100$ and returned a solution, which differed by more than 35% with respect to those returned by SCA-H and SCA-G.

As a final remark, we notice that the computed traveling times along the paths only slightly vary with n . For the first path, they vary between 14.44 and 14.45 s while, for the second path, between 20.65 and 20.66 s. The differences are very mild, but we should point out that this is not always

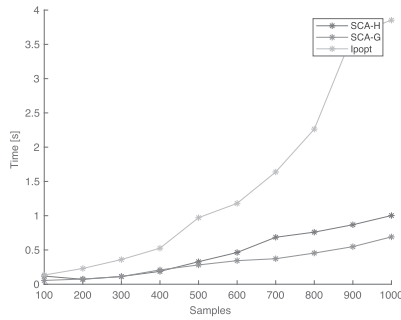


Fig. 7. Computing times (in seconds) for the path in Fig. 5.

TABLE II

MINIMUM, AVERAGE, AND MAXIMUM COMPUTING TIMES (IN SECONDS) AND RELATIVE PERCENTAGE DIFFERENCE BETWEEN THE TRAVELING TIMES COMPUTED BY THE HEURISTIC PRESENTED IN [23] AND THE SCA APPROACHES WITH $n = 100$ FOR THE INSTANCES OF EXPERIMENT 1

| Heuristic from [23] | min | mean | max |
|--------------------------------|-------|-------|--------|
| Time | 0.016 | 0.048 | 0.2049 |
| Relative percentage difference | 5.5% | 12.1% | 31.2% |

1350 the case. We further comment on this point when presenting
1351 Experiment 5.

1352 C. Experiment 4

1353 In this experiment, we compared the performance of our
1354 approach with the heuristic procedure recently proposed
1355 in [23]. In Table II, we report the computing times and the
1356 relative percentage difference $[(f_{\text{HEUR}} - f_{\text{SCA}})/f_{\text{SCA}}] * 100\%$
1357 between the traveling times computed by the heuristic and
1358 the SCA approaches for the instances of Experiment 1 with
1359 $n = 100$. Algorithms SCA-H and SCA-G have comparable
1360 computing times (actually, better for what concerns SCA-H)
1361 with respect to that heuristic, and the quality of the final
1362 solutions is, on average, larger than 10% (these observations
1363 also extend to other experiments). Such difference between
1364 the quality of the solutions returned by algorithm SCA and
1365 those returned by the heuristic is best explained through the
1366 discussion of a representative instance, taken from Experiment
1367 1 with $n = 100$. In this instance, we set $A = 2.78 \text{ ms}^{-2}$,
1368 while, for the jerk constraints, we set $J = 2 \text{ ms}^{-3}$. The total
1369 length of the path is $s_f = 60 \text{ m}$. The maximum velocity
1370 profile is the piecewise constant black line in Fig. 8. In the
1371 same figure, we report in red the velocity profile returned
1372 by the heuristic and in blue the one returned by algorithm
1373 SCA. The computing time for the heuristic is 45 ms, while,
1374 for algorithm SCA-H, it is 39 ms. The final objective function
1375 value (i.e., the traveling time along the given path) is 15.4 s
1376 for the velocity profile returned by the heuristic and 14.02 s
1377 for the velocity profile returned by algorithm SCA. From the
1378 qualitative point of view, it can be observed in this instance
1379 (and similar observations hold for the other instances that we
1380 tested) that the heuristic produces velocity profiles whose local
1381 minima coincide with those of the maximum velocity profile.
1382 For instance, in the interval between 10 and 20 m, we notice
1383 that the velocity profile returned by the heuristic coincides

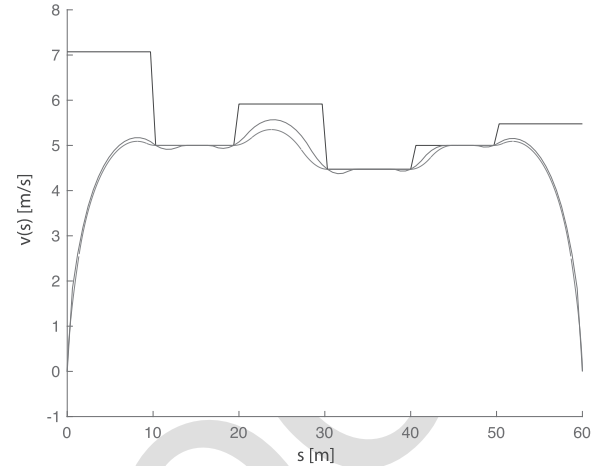


Fig. 8. Velocity profile returned by the heuristic proposed in [23] (red line) and by algorithm SCA (blue line). The black line is the maximum velocity profile.

1384 with the maximum velocity profile in that interval. Instead, the
1385 velocity profile generated by algorithm SCA generates velocity
1386 profiles that fall below the local minima of the maximum
1387 velocity profile, but, this way, they are able to keep the
1388 velocity higher in the regions preceding and following the local
1389 minima of the maximum velocity profile. Again, referring to
1390 the interval between 10 and 20 m, we notice that the velocity
1391 profile computed by algorithm SCA falls below the maximum
1392 velocity profile in that region and, thus, below the velocities
1393 returned by the heuristic, but, this way, velocities in the region
1394 before 10 m and in the one after 20 m are larger with respect
1395 to those computed by the heuristic.

1396 D. Experiment 5

1397 As a final experiment, we planned the speed law of an
1398 autonomous guided vehicle operating in a real-life auto-
1399 mated warehouse. Paths and problem data have been provided
1400 by packaging company Ocme S.r.l., based in Parma, Italy.
1401 We generated 50 random paths from a general layout. Fig. 9
1402 shows the warehouse layout and a possible path. In all paths,
1403 we set maximum velocity to 2 m s^{-1} , maximum longitudinal
1404 acceleration to $A = 0.28 \text{ m/s}^2$, maximum normal acceleration
1405 to 0.2 m/s^2 , and maximum jerk to $J = 0.025 \text{ m/s}^3$. Table III
1406 shows computation times for algorithms SCA-H, SCA-G, and
1407 IPOPT for a number of sampling points $n \in \{100, 500, 1000\}$.
1408 SCA-H is quite fast although it sometimes returns slightly
1409 worse solutions (the largest percentage error, at a single
1410 instance with $n = 1000$, is 8%). IPOPT is clearly slower than
1411 SCA-H and SCA-G for $n = 500$ and 1000, while, for $n = 100$,
1412 it is slower than SCA-H but quite similar to SCA-G. However,
1413 for these paths, the difference in terms of traveling times as
1414 n increases is much more significant with respect to the other
1415 experiments (see also the discussion at the end of Experiment
1416 3). More precisely, the percentage difference between the
1417 traveling times of solutions at $n = 100$ and $n = 1000$ is
1418 0.5% on average for Experiment 1 with a maximum of 2.1%,
1419 while, for Experiment 2, the average difference is 0.3% with
1420 a maximum of 0.4%. Instead, for the current experiment,

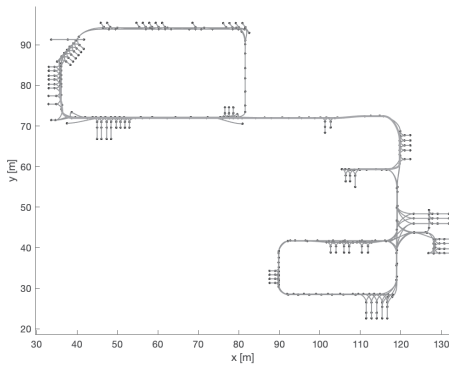


Fig. 9. Warehouse layout considered in Example 5 and a possible path.

TABLE III

AVERAGE, MINIMUM, AND MAXIMUM COMPUTING TIMES (IN SECONDS) FOR SCA-H, SCA-G, AND IPOPT OVER EXPERIMENT 5

| n | | SCA-H | SCA-G | IPOPT |
|------|------|-------|-------|-------|
| 100 | min | 0.009 | 0.033 | 0.029 |
| | mean | 0.013 | 0.043 | 0.037 |
| | max | 0.026 | 0.062 | 0.052 |
| 500 | min | 0.032 | 0.104 | 0.222 |
| | mean | 0.068 | 0.146 | 0.289 |
| | max | 0.174 | 0.224 | 0.423 |
| 1000 | min | 0.078 | 0.249 | 0.744 |
| | mean | 0.201 | 0.385 | 1.25 |
| | max | 0.501 | 0.65 | 3.359 |

1421 the average difference is 2.7% with a maximum of 7.9%.
 1422 However, the average falls to 0.2% and the maximum to 0.6%
 1423 if we consider the percentage difference between the traveling
 1424 times of solutions at $n = 500$ and $n = 1000$. Thus, for this
 1425 experiment, it is advisable to use a finer discretization or,
 1426 equivalently, a larger number of sampling points. A tentative
 1427 explanation for such different behavior is related to the lower
 1428 velocity limits of Experiment 5 with respect to the other
 1429 experiments. Indeed, the objective function is much more
 1430 sensitive to small changes at low speeds so that a finer grid of
 1431 sampling points is able to reduce the impact of approximation
 1432 errors. However, this is just a possible explanation. A further
 1433 possible explanation is that, in Experiments 1–4, curves are
 1434 composed of segments with constant and linear curvature,
 1435 whereas curves on industrial LGV layouts typically have
 1436 curvatures that are highly nonlinear with respect to arc length.

1437 VI. CONCLUSION

1438 In this article, we considered a speed planning problem
 1439 under jerk constraints. The problem is a nonconvex one,
 1440 and we proposed a sequential convex approach, where we
 1441 exploited the special structure of the convex subproblems
 1442 to solve them very efficiently. The approach is fast and is
 1443 theoretically guaranteed to converge to a stationary point of the
 1444 nonconvex problem. As a possible topic for future research, we
 1445 would like to investigate ways to solve Problem 9, currently
 1446 the bottleneck of the proposed approach, alternative to the
 1447 solver GUROBI, and the heuristic mentioned in Remark 6.
 1448 Moreover, we suspect that the stationary point to which the
 1449 proposed approach converges is, in fact, a global minimizer

of the nonconvex problem, and proving this fact is a further
 interesting topic for future research.

ACKNOWLEDGMENT

The authors are really grateful to the Associate Editor and
 the three anonymous reviewers for their careful reading and
 very useful suggestions.

REFERENCES

[1] P. Pharpatara, B. Hérisse, and Y. Bestaoui, “3-D trajectory planning of aerial vehicles using RRT*,” *IEEE Trans. Control Syst. Technol.*, vol. 25, no. 3, pp. 1116–1123, May 2017.

[2] K. Kant and S. W. Zucker, “Toward efficient trajectory planning: The path-velocity decomposition,” *Int. J. Robot. Res.*, vol. 5, no. 3, pp. 72–89, Sep. 1986.

[3] L. Consolini, M. Locatelli, A. Minari, and A. Piazzi, “An optimal complexity algorithm for minimum-time velocity planning,” *Syst. Control Lett.*, vol. 103, pp. 50–57, May 2017.

[4] F. Cabassi, L. Consolini, and M. Locatelli, “Time-optimal velocity planning by a bound-tightening technique,” *Comput. Optim. Appl.*, vol. 70, no. 1, pp. 61–90, May 2018.

[5] F. Pfeiffer and R. Johanni, “A concept for manipulator trajectory planning,” *IEEE J. Robot. Autom.*, vol. RA-3, no. 2, pp. 115–123, Apr. 1987.

[6] D. Verscheure, B. Demeulenaere, J. Swevers, J. De Schutter, and M. Diehl, “Time-optimal path tracking for robots: A convex optimization approach,” *IEEE Trans. Autom. Control*, vol. 54, no. 10, pp. 2318–2327, Oct. 2009.

[7] M. Yuan, Z. Chen, B. Yao, and X. Zhu, “Time optimal contouring control of industrial biaxial gantry: A highly efficient analytical solution of trajectory planning,” *IEEE/ASME Trans. Mechatronics*, vol. 22, no. 1, pp. 247–257, Feb. 2017.

[8] E. Velenis and P. Tsotras, “Minimum-time travel for a vehicle with acceleration limits: Theoretical analysis and receding-horizon implementation,” *J. Optim. Theory Appl.*, vol. 138, no. 2, pp. 275–296, 2008.

[9] M. Frego, E. Bertolazzi, F. Biral, D. Fontanelli, and L. Palopoli, “Semi-analytical minimum time solutions with velocity constraints for trajectory following of vehicles,” *Automatica*, vol. 86, pp. 18–28, Dec. 2017.

[10] K. Hauser, “Fast interpolation and time-optimization with contact,” *Int. J. Robot. Res.*, vol. 33, no. 9, pp. 1231–1250, 2014.

[11] H. Pham and Q.-C. Pham, “A new approach to time-optimal path parameterization based on reachability analysis,” *IEEE Trans. Robot.*, vol. 34, no. 3, pp. 645–659, Jun. 2018.

[12] L. Consolini, M. Locatelli, A. Minari, A. Nagy, and I. Vajk, “Optimal time-complexity speed planning for robot manipulators,” *IEEE Trans. Robot.*, vol. 35, no. 3, pp. 790–797, Jun. 2019.

[13] T. Lipp and S. Boyd, “Minimum-time speed optimisation over a fixed path,” *Int. J. Control*, vol. 87, no. 6, pp. 1297–1311, 2014.

[14] F. Debrouwere *et al.*, “Time-optimal path following for robots with convex constraints using sequential convex programming,” *IEEE Trans. Robot.*, vol. 29, no. 6, pp. 1485–1495, Dec. 2013.

[15] A. K. Singh and K. M. Krishna, “A class of non-linear time scaling functions for smooth time optimal control along specified paths,” in *Proc. IEEE/RSJ Int. Conf. Intell. Robots Syst. (IROS)*, Sep. 2015, pp. 5809–5816.

[16] A. Palleschi, M. Garabini, D. Caporale, and L. Pallottino, “Time-optimal path tracking for jerk controlled robots,” *IEEE Robot. Autom. Lett.*, vol. 4, no. 4, pp. 3932–3939, Oct. 2019.

[17] S. Macfarlane and E. A. Croft, “Jerk-bounded manipulator trajectory planning: Design for real-time applications,” *IEEE Trans. Robotics Autom.*, vol. 19, no. 1, pp. 42–52, Feb. 2003.

[18] R. Haschke, E. Weitnauer, and H. Ritter, “On-line planning of time-optimal, jerk-limited trajectories,” in *Proc. IEEE/RSJ Int. Conf. Intell. Robots Syst.*, Sep. 2008, pp. 3248–3253.

[19] H. Pham and Q.-C. Pham, “On the structure of the time-optimal path parameterization problem with third-order constraints,” in *Proc. IEEE Int. Conf. Robot. Automat. (ICRA)*, May 2017, pp. 679–686.

[20] J. E. Bobrow, S. Dubowsky, and J. S. Gibson, “Time-optimal control of robotic manipulators along specified paths,” *Int. J. Robot. Res.*, vol. 4, no. 3, pp. 3–17, Sep. 1985.

[21] K. G. Shin and N. D. McKay, “Minimum-time control of robotic manipulators with geometric path constraints,” *IEEE Trans. Autom. Control*, vol. AC-30, no. 6, pp. 531–541, Jun. 1985.

- 1520 [22] J. Villagra, V. Milanés, J. Pérez, and J. Godoy, "Smooth path and speed
1521 planning for an automated public transport vehicle," *Robot. Auton. Syst.*,
1522 vol. 60, no. 2, pp. 252–265, 2012.
- 1523 [23] M. Raineri and C. G. L. Bianco, "Jerk limited planner for real-time
1524 applications requiring variable velocity bounds," in *Proc. IEEE Int. Conf.*
1525 *Automat. Sci. Eng. (CASE)*, Aug. 2019, pp. 1611–1617.
- 1526 [24] J. Dong, P. M. Ferreira, and J. A. Stori, "Feed-rate optimization with
1527 jerk constraints for generating minimum-time trajectories," *Int. J. Mach.*
1528 *Tools Manuf.*, vol. 47, nos. 12–13, pp. 1941–1955, Oct. 2007.
- 1529 [25] K. Zhang, X. S. Gao, H. B. Li, and C. M. Yuan, "A greedy algorithm for
1530 feedrate planning of CNC machines along curved tool paths with con-
1531 fined jerk," *Robot. Comput.-Integr. Manuf.*, vol. 28, no. 4, pp. 472–483,
1532 Aug. 2012.
- 1533 [26] Y. Zhang *et al.*, "Speed planning for autonomous driving via convex
1534 optimization," in *Proc. 21st Int. Conf. Intell. Transp. Syst. (ITSC)*,
1535 Nov. 2018, pp. 1089–1094.
- 1536 [27] R. Fletcher, *Practical Methods of Optimization*, 2nd ed. Singapore:
1537 Wiley, 2000.
- 1538 [28] L. Consolini, M. Laurini, and M. Locatelli, "Graph-based algorithms for
1539 the efficient solution of optimization problems involving monotone func-
1540 tions," *Comput. Optim. Appl.*, vol. 73, no. 1, pp. 101–128, May 2019.
- 1541 [29] N. J. Higham, *Accuracy and Stability of Numerical Algorithms*, vol. 80.
1542 Philadelphia, PA, USA: SIAM, 2002.
- 1543 [30] L. Consolini, M. Locatelli, and A. Minari, "A sequential approach
1544 for speed planning under jerk constraints," 2021, *arXiv:2105.15095*.
1545 [Online]. Available: <http://arxiv.org/abs/2105.15095>
- 1546 [31] S. Boyd and L. Vandenberghe, *Convex Optimization*. Cambridge, U.K.:
1547 Cambridge Univ. Press, 2004.
- 1548 [32] Gurobi Optimization Inc. (2016). *Gurobi Optimizer Reference Manual*.
1549 [Online]. Available: <http://www.gurobi.com>
- 1550 [33] A. Wächter and L. T. Biegler, "On the implementation of an interior-
1551 point filter line-search algorithm for large-scale nonlinear programming,"
1552 *Math. Program.*, vol. 106, no. 1, pp. 25–57, May 2006.
- 1553 [34] L. L. Hoberock, "A survey of longitudinal acceleration comfort studies
1554 in ground transportation vehicles," *J. Dyn. Syst., Meas., Control*, vol. 99,
1555 no. 2, pp. 76–84, Jun. 1977.
- 1556 [35] T. Fraichard and A. Scheuer, "From Reeds and Shepp's to continuous-
1557 curvature paths," *IEEE Trans. Robot.*, vol. 20, no. 6, pp. 1025–1035,
1558 Dec. 2004.
- 1559 [36] D. Verscheure, M. Diehl, J. De Schutter, and J. Swevers, "Recursive log-
1560 barrier method for on-line time-optimal robot path tracking," in *Proc.*
1561 *Amer. Control Conf.*, St. Louis, MO, USA, Apr. 2009, pp. 4134–4140.



Luca Consolini (Member, IEEE) received the Lau-
rea degree (*cum laude*) in electronic engineering
and the Ph.D. degree from the University of Parma,
Parma, Italy, in 2000 and 2005, respectively.

From 2005 to 2009, he held a post-doctoral posi-
tion at the University of Parma, where he was an
Assistant Professor from 2009 to 2014. Since 2014,
he has been an Associate Professor with the Univer-
sity of Parma. His main current research interests
are nonlinear control, motion planning, and control
of mechanical systems.



Marco Locatelli is currently a Full Professor of
Operations Research with the University of Parma,
Parma, Italy. He published more than 90 arti-
cles in international journals and coauthored, with
F. Schoen, the book *Global Optimization: Theory,*
Algorithms, and Applications [Society for Indus-
trial and Applied Mathematics (SIAM)]. His main
research interests are the theoretical, practical, and
applicative aspects of optimization.

Dr. Locatelli has been nominated as a EUROPT
Fellow in 2018. He is also on the Editorial Board of
the journals *Computational Optimization and Applications*, *Journal of Global*
Optimization, and *Operations Research Forum*.



Andrea Minari received the B.S. and M.S. degrees
(*cum laude*) in computer engineering and the Ph.D.
degree from the University of Parma, Parma, Italy,
in 2013, 2016, and 2020, respectively. He presented
a dissertation about optimization-based algorithms
applied to the speed planning problem for mobile
robots and industrial manipulators.